Composite Higgs at high transverse momentum

Wissarut Ketaiam

Submitted for the degree of Doctor of Philosophy

Department of Physics and Astronomy,
University of Sussex

September 2018

Declaration

I hereby declare that this thesis has not been and will not be submitted in whole or in part to another University for the award of any other degree.

The work in this thesis has been completed in collaboration with Andrea Banfi, Sandra Kvedaraitė, Barry Dillon, and is the core of the paper arXiv:1905.12747, that is to be submitted for publication.

Signature:

Wissarut Ketaiam

UNIVERSITY OF SUSSEX

WISSARUT KETAIAM, Doctor of Philosophy

Composite Higgs at high transverse momentum

Abstract

The Standard Model (SM) of particle physics provides no explanation of the lightness of the Higgs particle found at the Large Hardron Collider (LHC) in 2012 compared to the natural scale of its mass, the Planck scale. This problem leads to the study of the class of physics models known as composite Higgs models, where the Higgs boson is considered to be a bound state of a new strongly interacting gauge theory. In this type of models, elementary particles have to couple with this composite state in order to gain masses. The dependence on the composite partners of the top quark, known as the top-partners, of Higgs production through gluon fusion has been studied. There it was found that, due to a subtle cancellation between the contribution of the top and that of the top partners, it is not possible to infer the top-partner mass from that process. However, there has been a study on the Higgs plus jet production from gluon fusion in a model with a top and an additional top partner. In that case, the transverse momentum distribution of the Higgs boson showed a depenence on the top-partner mass and coupling.

In this thesis we extend that study by considering Higgs production with a jet in explicit composite Higgs models, which has never been considered before in the literature. In particular, we consider composite Higgs models where the right handed top quark t_R was considered to be a composite state of a strong interacting sector containing either one or two top-partner multiplets. We then study Higgs production in association with a jet in these models, and in particular we examine thoroughly the impact of increasing number of the top partner multiplets.

The models studied in our work were categorised according to the representation of the top partners and the way the standard model left-handed doublet is embedded in the representations of the symmetry of the strong sector. In the case where there is only one top partner multiplet in the models, we derived the explicit forms of the Yukawa couplings of the top quark and the top partners, and the CP-odd couplings that are present as a result of having a bound state t_R. In the case where there are two top partners multiplets, we discussed the behaviour of the Yukawas and the masses

of the top partners as a function of the input parameters of the models. Numerical values of the masses, Yukawa couplings, and CP-odd couplings were calculated for both cases, and these values were input in a numerical programme to calculate the transverse momentum distribution of the Higgs. Various deviations from the Standard Model behaviour appear. They are typically model dependent, and have been studied on a case-by-case basis. In particular, we have discussed the difference between models with one and two top-partners.

Acknowledgements

I wish to thank my supervisor Dr. Andrea Banfi for his help, patient and support during the course of my PhD. Even though I am a slow learner, he has been patient, and gave me support throughout this 3 years and 4 months. I really appreciate this.

I would like to thank Barry Dillon and Sandra Kvedaraitė for their help during my PhD work.

I would like to thank Development and Promotion of Science and Technology Talents Project (DPST), and the Office of Educational Affairs for your help, support and funding for my study.

I wish to thank all of my primary school friends. Even though I have not been in touch with them for a long time, I can still remember the good time I spent with them.

I would like to thank Warangkana Monmuang, Phaochon Suksang, Tananun Suwanwiwat, Warakorn Kaewsaiha, Chan and other friends during my lower secondary school. Because of all of you, I managed to push myself through any difficulties that came to my life during this surprisingly hard time.

I would like to thank Suchinda Raungdech and Khwunchai Sukma for your help and support during the time that I competed for the DPST scholarship. Without both of you, I might not be able to achieve this scholarship.

I would like to thank all of my upper secondary school friends known collectively as the DOGS 01. Since, we have 57 members in total, I could not name all of you here. However, I want you to know that the time we spent together, either in the class rooms, restaurants and other places, still remain one of the most precious time in my life.

I would like to thank Piyamaporn Wipa for your friendship and kindness that you have been given to me, despite my bad behaviour toward you.

I would also like to thank all other friends that I made during my time in the upper secondary school.

I would also like to thank Piyatida Tungkitisub for your friendship and kindness and for sharing the common interest in gunpla and animation.

I would also like to thank Supee Trideth for being a teacher who stays beside your student irrespective of their behaviour.

I would like to thank all of my friends I met at Durham university including Nonthiwat Taesuk, Chulachat Kanjana-oransiri, Tum Nuttapol, Joyce Uerpairojkit, Chaiyakorn Srisakvarakul, Kiara Kijburana, Duangduan Chaiyaveij, Monsit Tanasit-

tikosol, Pichet Vanichchapongjaroen, Suphakorn Chunlen, Pimpunyawat Tummuangpak, Supachai Ritjareonwattu, Chinli Gwee, Sol Ee Lim, Pacharawan Viseshasumana, Waiwiwat Prangthawat, Pong Praditvorakhun, Makhala Atcharawongchai and many more that I do not mention here for your help, friendship and support. Even though, at that time, I hardly ever came out of my place to meet with people, I still cherish the many memories I had with all of the people there until the present day.

I would like to thank all of my office mates Jack Setford, Luke Arpino, Alba Carrillo, Sonali Mohapatra, Charlie Cresswell-Hogg, Chloe Gowling, Mike Soughton. I felt really grateful that we have a chance to share the time in that office. I would feel very please if you will always remember all of the jokes and all of the catchphrase I have said.

I would like to thank all of the people I met at the Department of Physics including Christopher Fritz, Niall Fealty, Christopher Harman, Tugba Buyukbese, Felipe Ferreira de Freitas, Agamemnon Sfondilis, Andrew Bond, Gustavo Medina, Jonathan Manuel, Daniel Cutting, Basem El-Menoufi, Boris Latosh, Luiz Vale Silva, Charanjit Khosa, Yannick Kluth, Folkert Kuipers, Lucia Fonseca de la Bella, Ridwan Barbhuiyan, Scott Clay, Dniel Molnr, Jos Pedro Vieira, Benot Fournier, Azizah Hosein for bringing fun and great times to this tough PhD journey.

I would also like to thank my disciples Ratima Satheanvaree and Tanyaluk Ruangket for giving me a change to be someone tutor.

I would like to thank all friends that I made during the time I spent in Brighton including Anusara Permmaneerat, Piyarat Panlee, Supojjanee Sansook, Sarote Boonseng, Kiattisak Thepsuriya, Jose Gascon, Chaichalit Srisawat, Siska Riefelyna, Xyla. I would also like to thank Khemmanat Konmungkorn for being a wonderful person to share the house with during the time I was writing this thesis.

I would also like to thank University of Sussex ITS service staff members for giving me the opportunity to learn new skills during the time I work with them.

Most importantly, I would like to thank all of my family members, especially my dad, my mom, my cousins, my younger sister and my younger brother who always believe in my potential. It is actually quite a phenomenon of my life to be born in a family with members who believe I can almost always reach a higher point in live, while, in fact, I might just fall, with styles.

Contents

Chapter 1

Introduction

After the discovery, and the experimental tests, of the electro-magnetic and weak forces, two of the four fundamental forces, attempts has been made in order to describe these two forces by one theory, namely, the electroweak theory. In the Standard Model (SM) of particle physics, the electroweak theory is described by the symmetry of the $SU(2)_L \times U(1)_Y$ gauge group [1–3]. This symmetry is spontaneously broken to give rise to the $U(1)_{QED}$ electromagnetic gauge interaction at low energy. The structure of the Higgs Lagrangian in the SM is similar to case where, in the theory, we consider the $U(1)$ gauge theory which is spontaneously broken to give mass to a massive gauge boson, namely the Abelian Higgs model [4]. In both models there exist a multiplet of scalar fields ϕ (the Higgs field) with a Lagrangian

$$\mathcal{L} \supset \left(D_\mu \phi\right)^\dagger \left(D^\mu \phi\right) - V\left(\phi^\dagger \phi\right) , \tag{1.1}$$

where the Higgs potential $V(\phi^\dagger \phi)$ is given by

$$V(\phi^\dagger \phi) = \mu^2 \phi^\dagger \phi + \lambda \left(\phi^\dagger \phi\right)^2 , \tag{1.2}$$

with $\lambda > 0$. For the Abelian Higgs model, ϕ is a complex scalar field, i.e.

$$\phi = \frac{1}{\sqrt{2}} \left(\phi_1 + i\phi_2\right) , \tag{1.3}$$

and

$$D_\mu = \partial_\mu + iqA_\mu \, , \tag{1.4}$$

where A_μ is used to denote the gauge field associated with the $U(1)$ symmetry. From Eq (1.2), if $\mu^2 > 0$, the vacuum expectation value (VEV) of the field, which corresponds to the location of the minimum of the potential, is given by $\langle 0 \left|\phi\right| 0 \rangle = \langle \phi \rangle_0 = 0$. In

this case, the VEV of ϕ will be invariant under the symmetry of the model. In the case $\mu^2 < 0$, however, the potential in Eq. (1.2) has a continuous set of degenerate minima corresponding to the VEVs satisfying

$$\sqrt{\langle \phi^\dagger \phi \rangle_0} = \sqrt{\frac{-\mu^2}{2\lambda}} \equiv \frac{v}{\sqrt{2}} \,. \tag{1.5}$$

Any of such VEVs is not invariant under the symmetry in the theory, i.e. $U(1)$ for the Abelian Higgs model. On the other hand, the Lagrangian of the Abelian Higgs model is invariant under the $U(1)$ symmetry. This situation is known as spontaneous breaking of the symmetry ($U(1)$ in this case). An important idea, closely related to the spontaneous symmetry breaking, is incorporated in the SM, and the Abelian Higgs model. This is the Higgs mechanism, whose purpose is to describe how gauge bosons are given masses after the spontaneous breaking of the symmetries in the theory. If we multiply the $U(1)$ generator, which can be taken as an identity matrix, on any of the VEVs in Eq. (1.5), the result is not zero. The group generators of the theory that cannot annihilate the VEV, such as this case, are referred to as broken generators. Let us know choose a particular VEV, for instance $v/\sqrt{2}$. Fluctuations around this VEV that can be expressed as

$$\phi(x) = \frac{1}{\sqrt{2}} \left[v + \rho(x) \right] e^{i\theta(x)/v} \,, \tag{1.6}$$

where $\theta(x)$ would be a massless scalar field, known as the Nambu-Goldstone boson (NGB) or Goldstone boson [5, 6]. Now consider the Goldstone theorem which states that for each of broken group generators of a spontaneously broken continuous global symmetry, there exist a massless Goldstone boson in the theory [7]. If $U(1)$ were a global symmetry, $\theta(x)$ would be a physical Goldstone boson. However, in the Abelian Higgs model, the $U(1)$ is a gauge symmetry, and this is not a physical symmetry, but can then be removed from the theory by applying to $\phi(x)$ a gauge transformation of the form [4]

$$\begin{aligned} \phi(x) \to e^{-i\theta(x)/v} \phi(x) &= \frac{1}{\sqrt{2}} \left[v + \rho(x) \right] \,, \\ A_\mu(x) \to A_\mu(x) + \frac{1}{qv} \partial_\mu \theta(x) &= A'_\mu \,. \end{aligned} \tag{1.7}$$

Substituting the $\phi(x)$ given in Eq. (1.7) into Eq. (1.1), the $A_\mu(x)$ obtains a mass given by

$$m_A = qv \,. \tag{1.8}$$

The last equation is the core of the Higgs mechanism: the gauge fields associated to each of the spontaneously broken gauge group generators become massive.

While the Abelian Higgs model is regarded as a model where the important features of a particle physics model can be studied, it cannot be considered as a physical theory that can be used to describe electroweak interactions, since the group structure is not large enough to give masses to all of the known electromagnetic and weak gauge fields. Then, in the SM, the group structure is enlarged to $SU(2)_L \times U(1)_Y$ as described above.

In the SM, ϕ is an $SU(2)_L$ doublet of scalar fields, i.e.

$$\phi = \frac{1}{\sqrt{2}} \begin{pmatrix} \phi_1 + i\phi_2 \\ \phi_3 + i\phi_4 \end{pmatrix} \tag{1.9}$$

and

$$D_\mu = \partial_\mu - i\frac{g_0'}{2} B_\mu y - i\frac{g_0}{2} W_\mu^a \sigma^a \tag{1.10}$$

where B_μ and W_μ^a are the gauge fields associated with the $U(1)_Y$ generator y and $SU(2)_L$ generators, which is taken to be the Pauli matrices σ^a, respectively. The doublet in Eq. (1.9) has an infinite number of degenerate VEV. For concreteness, we can consider one particular VEV given by

$$\langle\phi\rangle_0 = \begin{pmatrix} 0 \\ \frac{v}{\sqrt{2}} \end{pmatrix} . \tag{1.11}$$

Similar to the VEV given in Eq. (1.5), the VEV in Eq. (1.11) is not invariant under $SU(2)_L \times U(1)_Y$ symmetry of the SM models, while the Lagrangian of the model is still invariant under these symmetries. The symmetry of the SM model is then said to be spontaneously broken. The generators of the SM, σ_a and y, can be traded to the new set of the generators $(\sigma_1, \sigma_2, K, Q)$, where

$$K = \frac{\sigma_3 - y}{2} = \begin{pmatrix} 0 & 0 \\ 0 & -1 \end{pmatrix}, \quad Q = \frac{\sigma_3 + y}{2} = \begin{pmatrix} 1 & 0 \\ 0 & 0 \end{pmatrix} . \tag{1.12}$$

Applying this set of the generators to the SM VEV in Eq. (1.11), one would obtain that

$$\begin{aligned}
\sigma_1\langle\phi\rangle_0 &= \begin{pmatrix} 0 & 1 \\ 1 & 0 \end{pmatrix}\begin{pmatrix} 0 \\ \frac{v}{\sqrt{2}} \end{pmatrix} = \begin{pmatrix} \frac{v}{\sqrt{2}} \\ 0 \end{pmatrix} \neq 0 \\
\sigma_2\langle\phi\rangle_0 &= \begin{pmatrix} 0 & -i \\ i & 0 \end{pmatrix}\begin{pmatrix} 0 \\ \frac{v}{\sqrt{2}} \end{pmatrix} = \begin{pmatrix} \frac{-iv}{\sqrt{2}} \\ 0 \end{pmatrix} \neq 0 \\
K\langle\phi\rangle_0 &= \begin{pmatrix} 0 & 0 \\ 0 & -1 \end{pmatrix}\begin{pmatrix} 0 \\ \frac{v}{\sqrt{2}} \end{pmatrix} = \begin{pmatrix} -\frac{v}{\sqrt{2}} \\ 0 \end{pmatrix} \neq 0 \\
Q\langle\phi\rangle_0 &= \begin{pmatrix} 1 & 0 \\ 0 & 0 \end{pmatrix}\begin{pmatrix} 0 \\ \frac{v}{\sqrt{2}} \end{pmatrix} = \begin{pmatrix} 0 \\ 0 \end{pmatrix}.
\end{aligned} \tag{1.13}$$

Among the new set of generators, three of them do not annihilate the vacuum. The generators of a symmetry that possess this property are known as broken generators. From Eq. (1.13), the broken generators can be defined by T^α, for $\alpha = 1, 2, 3$, where

$$T^1 = \frac{\sigma_1}{2}, \quad T^2 = \frac{\sigma_2}{2}, \quad T^3 = \frac{K}{2}. \tag{1.14}$$

For each of the broken generators, those that do not annihilate the vacuum, there exists an associated massless scalar Goldstone field. These fields, denoted as $\theta^\alpha(x)$, can be parametrised as fluctuation around the VEV as follows

$$\phi(x) = \exp\left(\frac{i\theta^\alpha(x)\,T^\alpha}{v}\right)\begin{pmatrix} 0 \\ \frac{v+\rho(x)}{\sqrt{2}} \end{pmatrix} \tag{1.15}$$

where $\rho(x)$ is used here to denote the SM Higgs field, and σ^α denotes the broken generators in Eq. (1.13). If the $SU(2)_L \times U(1)_Y$ were a global symmetry, instead of being a gauge symmetry as appears in the SM, $\theta^\alpha(x)$ would have been physical Goldstone fields. In the SM, however, they can be removed from theory by applying to $\phi(x)$ given in Eq. (1.15) a gauge transformation, known as the unitary gauge [8, 9], with the action

$$\phi(x) \to \exp\left(\frac{-i\theta^\alpha(x)\,T^\alpha}{v}\right)\phi(x) = \begin{pmatrix} 0 \\ \frac{v+\rho(x)}{\sqrt{2}} \end{pmatrix}. \tag{1.16}$$

Substituting Eq. (1.16) into Eq. (1.1), we find that the SM gauge fields are given by

$$\begin{aligned}
W_\mu^- &\equiv \frac{W_\mu^1 + iW_\mu^2}{\sqrt{2}}, \qquad & W_\mu^- &\equiv \frac{W_\mu^1 - iW_\mu^2}{\sqrt{2}} \\
Z_\mu &\equiv \frac{-g_0' B_\mu + g_0 W_\mu^3}{\sqrt{g_0^2 + {g_0'}^2}}, \qquad & A_\mu &\equiv \frac{g_0 B_\mu + g_0' W_\mu^3}{\sqrt{g_0^2 + {g_0'}^2}}
\end{aligned} \tag{1.17}$$

and the masses of the fields are

$$m_\rho = \sqrt{-2\mu^2}, \quad m_W = \frac{g_0 v}{2}, \quad m_Z = \frac{g_0 v}{2}\sqrt{1+\left(\frac{g_0'}{g_0}\right)^2}. \tag{1.18}$$

The Standard Model (SM) of particle physics has been successful in describing the particle with 125 GeV mass found at the Large Hadron Collider (LHC) in 2012. The LHC performed proton-proton collisions with centre-of-mass energies of 7 and 8 TeV, and a resonance with a mass of about 125 GeV was declared [10, 11]. This particle provided an excellent candidate for the SM Higgs particle. The properties of this particle have been tested and, so far, significant deviations from the SM properties of this Higgs particle have not been found. Despite this success, the SM does not seem to be able to provide sensible answers to many questions that our observations propose. One example is the so-called hierarchy problem, whose solution is the main topic of this thesis. The main issue is that the SM does not provide an explanation why the SM Higgs has a light mass compared to its natural scale, which is the Planck mass (of the order of 10^{19} GeV). Solutions to this problem lead to new models for particle physics.

It is inevitable that theory with fundamental scalar fields, such as the SM, is affected by quadratic divergences associated with the scalar fields. These divergences could eventually lead to fine-tuning problems when some parameters of the model have to be adjusted. In order to see where difficulties arise, suppose in a theory there exists a fundamental energy scale κ and a dimensionsless bare coupling g_0. The quantity κ is considered to be of the same order as the Planck mass. Suppose further that in the theory, for a scalar field, there exist a dimensionless bare mass μ_0, defined as the ratio of the bare mass m_0 of the scalar field and κ [12]

$$\mu_0 = \frac{m_0}{\kappa}\,. \tag{1.19}$$

If this scalar field receives a self-energy correction, arising from e.g. loops of fermions, then it is possible to write its renormalised mass m^2 as [12]

$$m^2 = m_0^2 + \Delta m^2 = m_0^2 + \kappa^2 g_0^2\,, \tag{1.20}$$

where Δm^2 denotes the self-energy correction. From Eq. (1.19), it is then easy to solve for μ_0^2 from Eq. (1.20), and we obtain [12]

$$\mu_0^2 = \frac{m_0^2}{\kappa^2} = \frac{m^2}{\kappa^2} - g_0^2. \tag{1.21}$$

As m is one of the physical properties of the theory, it is expected to be stale against variations of g^0 and μ^0 for a theory to occur naturally as described above. With κ of order 10^{19} GeV, if m is a light mass of order 1 GeV, then it is required that

$$\mu_0^2 = -g_0^2 \left(1 - 10^{-38}\right). \tag{1.22}$$

The equation above means that μ_0^2 must be adjusted to the 38^{th} decimal place, otherwise m will be of order 10^{19} GeV. Hence, quadratic divergences in the scalar particle masses can lead to unnatural adjustment of the parameters in the theory. In natural theories, the dimensionless ratios between the free parameters should appear with values of order 1, and the free parameters should not be fine-tuned. Moreover, in natural theories, the observable properties should be stable under the variation of the fundamental parameters [12]. One of the main issues of the hierarchy problem is the natuaralness of the model considered to describe the force in nature.

Two particularly interesting scenarios were proposed for solving the problems above. One of them is supersymmetry, on which a huge amount of work has been carried out in terms of its search strategies and implications [13–15]. In this model, supersymmetric partners with a different spin are introduced for any SM particle. Supersymmetry is in fact the symmetry that constrains the couplings in such a way that cancellation of quadratic divergences occurring in the calculation of the Higgs mass occurs between loops of a SM particle and that of its supersymmetric partner.

The other is the composite Higgs [16–18] which instead of being an elementary particle as the Higgs in the SM, the Higgs particle is now a composite state arising from the strongly interacting sector in the theory. The composite Higgs model is the kind of model we have studied in this thesis. The composite Higgs models are based on two aspects. One is that the Higgs is a pseudo Nambu-Goldstone boson arising from the spontaneous breaking of a global symmetry [19]. Because of this nature, the Higgs has no potential at tree level. As a result, the Higgs potential, and hence the EWSB, must occur via loops of particles. The other is partial compositeness, where quarks and leptons acquire their masses via a linear mixing with a composite sector. This type of mixing results in the breaking of the global symmetry of the strong sector, since the mixings will be invariant under the SM electroweak group, but not under the global symmetry of the composite sector. The Higgs potential can then arise from loops of both SM particles, and composite fermions emerging from the strong sector. Since the top coupling to the Higgs is the strongest among the couplings of SM particles with the Higgs, the top quark and its composite states, known as the top partners, give the

most significant contribution to the Higgs potential. The existence of top partners is expected to have influences on the properties of the top quark, and can therefore be a viable way to probe the compositeness of the Higgs particle.

However, searching for top-partners is a difficult task. Direct searches for top partners can be carried out via pair production $pp \to T\bar{T}$ and single production $pp \to T+X$. However, this type of searches will be highly model dependent since the search strategy and limits rely heavily on the knowledge of the decay modes of the top partners. For top partner searches focusing on some decay channels such as $T \to W^+b$, $T \to Zt$ and $T \to ht$, some experimental bounds can be applied. However, these bounds will weaken if other decay channels are proved to be possible [20, 21]. Moreover, this type of searches suffers from the presence of background processes with large cross sections. Indirect searches, on the other hand, lead to a complementary approach since they do not depend on how the top-partner decay modes. Some dependency on top partner masses is expected in some physical processes. For instance, top partners contribute through loops to the Higgs total cross section. Unfortunately, due to a very stingent low energy theorem [22], their contribution cannot be disentangled from that of the top quark. It has been pointed out recently that [23], in Higgs plus one jet, on the other hand, the transverse momentum p_T distribution of the Higgs (or the associated jet) can depend on the top partner masses and therefore can be used as a tool to search for top partners.

In this thesis, we will deal with composite scenarios where the right-handed top quark is assumed to be a totally composite state rather than an elementary particle as in the SM. In these models the top partners are also categorised in different representations of the group symmetry. We concentrate on two models and in each of the models, we will study the case where we have either one or two top-partner multiplets.

In chapter 2, we will give an overview of the basic principles behind the construction of composite Higgs models, and explore some important features. Also, we will discuss a simple model where the basic properties of a composite Higgs model can be learned and then discuss the procedure for extending the group structure of the model to the one we studied in the rest of the thesis.

In chapter 3 we describe the models arising from top partner multiplets transforming in the fourplet and singlet representations of the group $SO(4)$, which were developed in Ref. [24]. Instead of dealing with only one top partner case as generally done in previous works, in this thesis we will explain how to deal both with scenarios with one

top-partner multiplet and two top-partner multiplets. We will also explore the effect of a term emerging as a result of having a totally composite right-handed top partner and explain how it eventually leads to CP-odd Yukawa couplings [24, 25]. As a novel result, we have computed the analytical form of the Yukawa couplings in the case of one top partner, in both models. In the cases where we have two top partner multiplets, these formulae cannot be derived, and instead, we show how the mass spectrum and couplings change when we vary the parameters in the models. All these analyses are presented in chapter 3

In chapter 4, we provide numerical predictions for Higgs plus one additional jet at the LHC. First, we discuss about previous studies showing that, due to low energy cancelation the single Higgs production $pp \to h$ is not a possible choice for probing the mass of the top partner. We then discuss how the p_T distribution computed from the production $pp \to$ Higgs plus a high-p_T jet can show sensitivity to the mass of the top partner, following the strategy of [23]. With this knowledge, we introduce the variable, closely related to the p_T distribution, that we will use as a tool to probe the dependence on the mass of the top partner, and hence on the compositeness of the Higgs boson. We then present numerical results for both the cases where, in the theory, there are one and two top partner multiplets. The chapter ends with a discussion on the significance of the results.

In the final chapter, we present some conclusion, and some considerations for further studies.

Chapter 2

Background Knowledge

2.1 Composite Higgs Models

Since the Higgs field plays such an important role in the breaking of electroweak symmetry, understanding the origin of this particle is an essential task. A strong motivation for the study of theories where the Higgs boson is a composite state comes from the lack of explanation for the lightness of the Higgs in the SM, where the Higgs field is an elementary particle. In fact, it is known that a very effective way to have a light scalar boson in a theory is to identify it as a pseudo Nambu Goldstone boson (pNGB) of a broken global symmetry. Such mechanism, for instance, explains the smallness of the masses of the pions compared to the characteristic confinement scale of QCD $\Lambda_{\mathrm{QCD}} \sim 200\,\mathrm{MeV}$. Similarly, if we want to allow the Higgs to be formed this way, a new strongly interacting sector, i.e. a new strong force needs to be included in the theory [26]. The very same strong sector is responsible, through the Higgs mechanism, for the masses of the vector bosons. QCD cannot be a good candidate for such a theory, because it will lead to masses of the vector bosons of the order of Λ_{QCD}, hence too small compared to what we observe in nature. It was pointed out that if the composite Higgs boson emerges as pNGB resulting from the breaking of a global symmetry of the strong sector, its mass can be naturally light [17, 27]. This is the main benefit of composite Higgs models. Since the Higgs behaves effectively as an elementary particle at the EW scale, such theories automatically satisfy the electroweak precision tests.

As stated in the Introduction, a theory which is invariant under a symmetry, but whose vacuum state, or equivalently the vacuum expectation value of a scalar field, is not invariant is referred to as being spontaneously broken. It is known from the Goldstone

theorem that if a continuous global symmetry is spontaneously broken so as to leave a smaller symmetry group, there exits a massless Goldstone boson for each broken generator. Under the larger symmetry group, the corresponding scalar Goldstone fields transform non-linearly and, as a result, have no potential.

Let us consider the field $\theta(x)$ corresponding to a NGB. This field transforms non-linearly as follows [29]

$$\theta \to \theta + \chi, \tag{2.1}$$

where θ is used to denote a NGB and χ represents the parameter of this "shift" transformation. If we want to introduce a potential $V(\theta)$ to the theory, this potential needs to be symmetric under the field shift in Eq. (2.1). Polynomial terms θ^n, e.g. a mass or a self coupling of θ are forbidden. Also, an interaction term between NGB and gauge fields θAA, where A_μ denotes the gauge fields, cannot be written down. The transformation in Eq. (2.1) only allows the derivative interactions in the form of $\partial_\mu\theta$ attached to other conserved current [29]. Hence, at tree-level we cannot construct a potential for NGBs.

Nambu Goldstone bosons can become pNGBs if the symmetry in the model is broken explicitly as well as spontaneously [4,29,30]. For a pNGB, a potential can be developed, and having the Higgs boson as a pNGB can lead to many interesting features, some of which will be discussed in this section.

There are three main parts required to construct a composite Higgs model. The first main part is the strong sector which, as briefly described above, will give rise to the Higgs as its bound state. The strong sector must be constructed from a fundamental theory with a confinement scale $\Lambda_{UV} \gg$ TeV, so EW physics is insensitive to it. The other is an extra elementary sector containing all particles that are not composite states of the strong sector at the TeV scale. These fields that do not possess the composite nature that the fields from the strong sector have are referred to as elementary fields. Actually, these fields are SM fields appearing in the composite Higgs models with one exception, the right handed top quark, which, in the models we studied, can be considered a totally composite state of the strong sector. These will also be referred to as external fields as they are external to the strong sector. This weakly-coupled sector contains the SM gauge group and its particle content, apart from the Higgs. However, interaction terms between those particles and the Higgs, which give rise to the Yukawa couplings, are not included at this stage since there is no Higgs yet. Note that the SM vector bosons are required to be described by elementary gauge fields only. This requirement

means that the whole theory, including the strong sector, must respect the SM gauge symmetry, i.e. the strong sector symmetry group $\mathcal{G}$ must contain, apart from an $SU(3)_c$, one $SU(2)_L \times U(1)_Y$ subgroup. The W_μ and B_μ fields from the elementary sector can be gauged with the latter subgroup resulting in one communication channel between the elementary and the composite sector. This communication channel is the last part required to construct a composite Higgs models.

The introduction of a composite Higgs boson could be understood from the following arguments. We first assume that there exists a strongly interacting sector with a global symmetry group $\mathcal{G}$ broken to a subgroup $\mathcal{H}_1$ at a scale f. This implies that there are $n = \dim(\mathcal{G}) - \dim(\mathcal{H}_1)$ Goldstone bosons, one for each broken generator of the group. Then, if the subgroup $\mathcal{H}_0 \subset \mathcal{G}$ is gauged by external vectors bosons, and $n_0 = \dim(\mathcal{H}_0) - \dim(\mathcal{H})$ of all the Goldstone bosons are eaten to give mass to n_0 vector bosons, then the remaining $n - n_0$ are pNGBs, and the unbroken gauge group is $\mathcal{H} = \mathcal{H}_0 \cap \mathcal{H}_1$. Among the vector bosons associated with the gauge group $\mathcal{H}_0$ are the SM electroweak gauge fields, and, for simplicity, it is possible to consider $\mathcal{H}_0$ as the SM electroweak group [17].

Then, there are two basic requirements for the Higgs boson to be a pNGB, living on the coset $\mathcal{G}/\mathcal{H}_1$, in a composite Higgs model [17]. First, it must be possible to embed the SM electroweak group $G_{SM} = SU(2)_L \times U(1)_Y$ in $\mathcal{H}_1$, $\mathcal{G} \to \mathcal{H}_1 \supset G_{SM}$ [17, 26]. Second, at least one $SU(2)_L$ doublet must be contained in the coset $\mathcal{G}/\mathcal{H}_1$, so that it is possible to identify this with the Higgs doublet [17, 26]. If these requirements are met, a composite pNGB Higgs can then develop its mass and potential from loop of SM fermions and gauge bosons. At tree level, it cannot develop its potential as result of the non-linear Goldstone symmetry acting on it, and G_{SM} is broken radiatively rather than at tree level.

One interesting feature that arises when the Higgs is a pNGB is the vacuum misalignment which explains how the Higgs can behave effectively as an elementary particle in this type of models [16, 26–28]. This mechanism can be understood as follows. The field $\vec{\Phi}(x)$ corresponding to the pNGBs is a member of the coset $\mathcal{G}/\mathcal{H}_1$, and as such can be represented in terms of the transformation in the direction of the broken generators T^k as

$$\vec{\Phi}(x) = e^{i\theta^k(x)T^k}\vec{F}\,, \tag{2.2}$$

where the pNGB fields are denoted by $\theta^k(x)$, $\vec{\Phi}(x)$ denotes the field operators of the theory and $\vec{F}$ is known as the reference vacuum field configuration. For a global symmetry

$\mathcal{G}$ with the generators

$$\{T^A\} = \{T^\alpha, T^k\}\,, \tag{2.3}$$

where T^α and T^k denotes the unbroken and broken generators respectively, the reference vacuum field must be selected so that it can satisfy the conditions

$$T^\alpha \vec{F} = 0, \quad T^k \vec{F} \neq 0. \tag{2.4}$$

We can identify, among $\theta^k(x)$, the four real components of the Higgs doublet. The non-vanishing VEV of this Higgs field, arising from the loop-induced potential, can then break G_{SM} as in the SM. The VEV $\langle\theta^k\rangle$ can be considered as the "angle" by which the vacuum is misaligned with respect to $\vec{F}$. The projection of $\vec{F}$ on the G_{SM} controls all the effects of EWSB, such as the masses of SM particles. This projection is equivalent to set the EWSB scale to $v = f \sin\langle\theta^k\rangle$. The actual value of $\langle\theta^k\rangle$ is different in each of the models, depending on the details of the composite sector, but it can be determined by minimising the potential of the pNGBs in the model. For a composite Higgs model, we can define the ξ parameter as [26]

$$\xi = \frac{v^2}{f^2} = \sin^2\langle\theta^k\rangle\ . \tag{2.5}$$

For a fixed value of v, the composite sector can be decoupled from the low-energy physics by sending the global symmetry breaking scale f to infinity. This is corresponding to the limit $\xi \to 0$, in which all the other bound states decouple from the theory except the Goldstone boson Higgs. For $\xi \to 0$, the theory reduces to SM, and the composite Higgs that remains in the theory becomes effectively elementary. The quantity ξ is the only adjustable parameter in composite Higgs models that controls all the departure from the standard Higgs model, and all the experimental confirmations of the SM can be recovered by setting ξ to a very small value. This could happen at the cost of fine-tuning.

We note here that in the case where the global symmetry is spontaneously broken without explicit breaking in the theory, the Higgs VEV cannot be the source of EWSB. In this case, when the global symmetry is only spontaneously broken, the $\theta^k(x)$ are exact NGB. In this case, their potential cannot be formed and $\langle\theta^k\rangle$ are arbitrary [26]. The $\langle\theta^k\rangle$ can technically be removed from the theory by a suitable field redefinition that induces the transformation $\vec{\Phi} \to \exp\left[-i\langle\theta^k\rangle T^k\right]\vec{\Phi}$. This is equivalent to setting $\langle\theta^k\rangle = 0$. Hence, the VEV cannot be responsible for the EWSB.

On the other hand, when there is a small explicit breaking of the global symmetry in the theory, the $\theta^k(x)$ are now pNGB, and their VEVs are not arbitrary. In fact,

their VEVs are now observable, since it is no longer possible to set them to zero by an exact symmetry transformation. As as upshot, this approximate global symmetry, i.e. the symmetry which is spontaneously broken as well as explicitly broken, is said to be "non-linearly realised", in the sense that the transformations related to the broken generators act non-linearly on the Goldstone fields [26]. This is the point which we will illustrate later when we talk about models related to our study.

Having mentioned that the global symmetry can be spontaneously broken by the vacuum state, we note here that if the global symmetry $\mathcal{G}$ is to be broken explicitly, this must occur via other methods. One is by gauging the SM electroweak group, and the other is the mixing between the SM fermion fields and the fields of strong sector. The latter is known as partial compositeness, and results in the masses of the fermion fields. These mechanisms responsible for global symmetry breaking will be mentioned throughout the rest of this thesis.

The composite Higgs models can be classified according to the symmetries involved in each model. In our work, we will consider only models where the strongly interacting sector has a global symmetry $\mathcal{G} = SO(5) \times U(1)_X$ broken down to $\mathcal{H}_1 = SO(4) \times U(1)_X$ [17]. For illustrative purpose on how these models work, we will start discussing a very simple model known as the Abelian Higgs model. This model is not a physical one in a sense that we cannot embed G_{SM} in the subgroup $\mathcal{H}_1$, but it is a model in which the basic aspects of a composite Higgs model can be studied. Then, we will proceed to study the model with a global symmetry $SO(5)$ broken to $SO(4)$. The structure of the models studied in our work shares similar features with the Callan-Coleman-Wess-Zumino (CCWZ) model [31, 32].

The Abelian Higgs model

In this simple model, we consider a Lagrangian for a triplet $\vec{\Phi}$ of real scalar fields [26]

$$\mathcal{L}_{\mathcal{S}} = \frac{1}{2}\partial_\mu \vec{\Phi}^T \partial^\mu \vec{\Phi} - \frac{g_*^2}{8}\left(\vec{\Phi}^T\vec{\Phi} - f^2\right)^2 . \tag{2.6}$$

This Lagrangian is an example of a strongly-interacting composite sector. In this model, the Lagrangian is invariant under $SO(3)$ transformations, which act on the triplet $\vec{\Phi}$ as follows [26]

$$\vec{\Phi} \to g \cdot \vec{\Phi}, \quad g = e^{i\alpha^A T^A} \in SO(3) \tag{2.7}$$

where $SO(3)$ generators obey the relation $\mathrm{Tr}[T^A T^B] = \delta^{AB}$. These operators can be chosen to be $T^A = \{T^\alpha, T^k\}$

$$T^\alpha = \frac{1}{\sqrt{2}} \begin{pmatrix} 0 & -i & 0 \\ i & 0 & 0 \\ 0 & 0 & 0 \end{pmatrix}, \quad T^k = \{ \frac{1}{\sqrt{2}} \begin{pmatrix} 0 & 0 & i \\ 0 & 0 & 0 \\ i & 0 & 0 \end{pmatrix}, \frac{1}{\sqrt{2}} \begin{pmatrix} 0 & 0 & 0 \\ 0 & 0 & -i \\ 0 & i & 0 \end{pmatrix} \} \tag{2.8}$$

where $k = 1, 2$. A non vanishing VEV of the field $\vec{\Phi}$ spontaneously break $SO(3)$ to $SO(2)$ subgroup of rotations around $\left\langle \vec{\Phi} \right\rangle$. From the conditions in Eq. (2.4) and the basis given in (2.8), the representative vacuum $\vec{F}$ is selected for this model as

$$\vec{F} = \begin{pmatrix} 0 \\ 0 \\ f \end{pmatrix} \tag{2.9}$$

where f is derived from $\left\langle \vec{\Phi}^T \right\rangle \left\langle \vec{\Phi} \right\rangle = f^2$. In order to study the fluctuations around the vacuum, a field redefinition must be performed on the three components of $\vec{\Phi}$ to trade them for one radial coordinate σ and two Goldstone boson field h^k that describe the fluctuation around the broken generators. This is in analogy with Eq. (2.2), and we obtain

$$\vec{\Phi} = e^{i \frac{\sqrt{2}}{f} h^k(x) T^k} \begin{bmatrix} 0 \\ 0 \\ f + \sigma(x) \end{bmatrix} \tag{2.10}$$

where the normalisation factor has been selected to obtain a canonical kinetic term for h^k. The exponential matrix $\exp\left(i \frac{\sqrt{2}}{f} h^k(x) T^k \right)$ in the expression above is space-time dependent and known in general as the σ-Goldstone matrix U. For any $\mathcal{G} \to \mathcal{H}_1$ symmetry breaking ($\mathcal{G} = SO(3)$ and $\mathcal{H}_1 = SO(2)$ for the case at hand), this matrix U can be defined, and it will be present very often in composite Higgs models. The Goldstone matrix, computed in this $SO(3) \to SO(2)$ case and in general, is given by

$$U = e^{i \frac{\sqrt{2}}{f} h^k T^k} = \begin{bmatrix} I - (1 - \cos\frac{h}{f}) \frac{\vec{h}\vec{h}^T}{h^2} & \sin\frac{h}{f} \frac{\vec{h}}{h} \\ -\sin\frac{h}{f} \frac{\vec{h}^T}{h} & \cos\frac{h}{f} \end{bmatrix}. \tag{2.11}$$

where

$$\vec{h} = \begin{bmatrix} h_1 \\ h_2 \end{bmatrix}, \tag{2.12}$$

$h = \sqrt{\vec{h}^T \vec{h}}$, and I denotes 2×2 unit matrix. We can define U in this form for any $SO(N) \to SO(N-1)$ symmetry breaking as long as the broken $N - 1$ generators are

chosen to have one non-vanishing entry in the last line and column. With Eq. (2.11), the field redefinition can be written as

$$\vec{\Phi} = (f+\sigma)\begin{bmatrix}\sin\frac{h}{f}\frac{\vec{h}}{h}\\ \cos\frac{h}{f}.\end{bmatrix} \tag{2.13}$$

Substituting this expression back into the Lagrangian Eq. (2.6), we find

$$\begin{aligned}\mathcal{L} = \frac{1}{2}\partial_\mu\sigma\partial^\mu\sigma - \frac{(g_* f)^2}{2}\sigma^2 - \frac{g_*^2 f}{2}\sigma^3 - \frac{g_*^2}{8}\sigma^4\\ +\frac{1}{2}\left(1+\frac{\sigma}{f}\right)^2\left[\frac{f^2}{h^2}\sin^2\frac{h}{f}\partial_\mu\vec{h}^T\partial^\mu\vec{h} + \frac{f^2}{4h^4}\left(\frac{h^2}{f^2}-\sin^2\frac{h}{f}\right)\partial_\mu h^2\partial^\mu h^2\right].\end{aligned} \tag{2.14}$$

From this equation, we find that the field σ has a mass

$$m_* = g_* f. \tag{2.15}$$

The σ particle is generally referred to as a resonance, as is any particle that emerges from the composite sector aside from the Goldstone bosons. The mass m_* is effectively the confinement scale of the strong sector. Also from Eq. (2.14), after inspecting the symmetry of this Lagrangian, we can recognise the presence of an $SO(2)$ group, since $\vec{h}$ forms a doublet and transforms as [26]

$$\vec{h} \to e^{i\alpha\sigma_2}\vec{h}. \tag{2.16}$$

The example of $SO(2)$ symmetry is referred to as linearly realised, since it acts in a linear and homogenous way on the field variables. From $\vec{h}$, we can define a complex field H given by

$$H = \frac{h_1 - ih_2}{\sqrt{2}}\,. \tag{2.17}$$

This is identified with the Higgs field with unit charge under the group $SO(2) = U(1)$. The linearly realised $SO(2)$ group induces an $SO(3)$ rotation along the unbroken generator T^α, as follows:

$$\vec{h} \to e^{i\alpha\sigma_2}\vec{h} \Leftrightarrow \vec{\Phi} \to e^{i\sqrt{2}\alpha T^\alpha}\vec{\Phi}\,, \tag{2.18}$$

since the $SO(2)$ invariance follows from one of the symmetries of the original Lagrangian. From Eq. (2.14), one would expect an identical symmetry involving the broken generators T^k. In fact, there also exist the Goldstone field transformations that induce rotations of $\vec{\Phi}$ along the broken generators

$$\begin{aligned}\vec{h} \to \vec{h} + h\cot\frac{h}{f}\vec{\alpha} + \left(\frac{f}{h} - \cot\frac{h}{f}\right)\left(\vec{\alpha}^T\vec{h}\right)\frac{\vec{h}}{f}\,,\\ \Updownarrow\\ \vec{\Phi} \to i\alpha_k T^k\vec{\Phi}\,.\end{aligned} \tag{2.19}$$

The correspondence between these transformations arises in the same way as in the unbroken $SO(2)$ case. This correspondence ensures that they are symmetries of the Lagrangian in Eq. (2.14), which we can also verify with a direct calculation. The broken transformations above act non-linearly on the Goldstone field variable h. This is different from those associated with the unbroken subgroup. Hence, they are referred to as "non-linearly realised". According to the form of the transformations, one would also find that the zero field configuration is transformed into one with constant $\vec{h}$ field, i.e. $\vec{0} \to f\vec{\alpha}$. This means that for any field configuration, e.g. the one defining the generic vacuum $\left\langle \vec{h} \right\rangle$, there exists a transformation that changes it into the trivial vacuum $\left\langle \vec{h} \right\rangle = 0$. This implies, as explained above, that the VEV of the composite Higgs has no physical effect unless an explicit breaking of the symmetry is introduced into the theory.

The last part that we need in order to fully construct the Abelian Higgs model is the $U(1)$ gauge field. This field can be introduced into the model by simply gauging the unbroken $U(1)$ subgroup, namely by promoting ordinary derivatives into covariant derivative in the Lagrangian with

$$\partial_\mu \vec{\Phi} \to D_\mu \vec{\Phi} = \left(\partial_\mu - i\sqrt{2}eA_\mu T^\alpha\right) \vec{\Phi}\,, \tag{2.20}$$

where A_μ is a $U(1)$ gauge field with canonical kinetic term. A_μ is a field residing in the elementary sector, so its couplings with $\vec{\Phi}$ are the elementary/composite interactions we discussed previously. The gauging of A_μ leads to the explicit breaking of $SO(3)$ to $SO(2)$, since it selects only one generator out of three. As a result, the composite Higgs becomes a pNGB. Having introduced the gauging of $U(1)$, it is now possible to write down the Abelian composite Higgs theory. We must first replace in Eq. (2.14)

$$\partial_\mu \vec{h} \to D_\mu \vec{h} = \left(\partial_\mu - ieA_\mu \sigma_2\right) \vec{h}\,. \tag{2.21}$$

In term of the complex field notation defined in Eq. (2.17), we can define the covariant derivative for H [26]

$$D_\mu H = \partial_\mu H - ieA_\mu H \tag{2.22}$$

and the term involving the Higgs in the Lagrangian Eq. (2.14) becomes

$$\frac{1}{2}\left(1+\frac{\sigma}{f}\right)^2 \left[\frac{f^2}{|H|^2}\sin^2\frac{\sqrt{2}|H|}{f} D_\mu H^\dagger D^\mu H + \frac{f^2}{4|H|^4}\left(2\frac{|H|^2}{f^2} - \sin^2\frac{\sqrt{2}|H|}{f}\right)\left(\partial_\mu |H|^2\right)^2\right], \tag{2.23}$$

where the part involving σ field in the Lagrangian remains unchanged. In Eq. (2.23), $|H|$ is defined by

$$|H| = \sqrt{H^\dagger H}\,. \tag{2.24}$$

Now as the global symmetry is broken explicitly, the Higgs potential can be formed. It still vanishes in the tree level Lagrangian, but it can be radiatively constructed from the loops of the gauge bosons. We note that the loops of the fermions can similarly lead to formation of the Higgs potential. Eventually, this potential gives the composite Higgs field a VEV, which is now an observable and can be responsible for the breaking of the $U(1)$ symmetry. Setting the Higgs to its VEV,

$$H \to \langle H \rangle \equiv \frac{V}{\sqrt{2}}, \tag{2.25}$$

we obtain from the first term in the square bracket of Eq. (2.23), a mass for the gauge field given by [26]

$$m_A = ef \sin\frac{V}{f} \equiv ev\,. \tag{2.26}$$

In this expression, the scale v of the $U(1)$ symmetry would have been defined as simply the Higgs VEV in the elementary Abelian Higgs model. In this model, however, the symmetry breaking scale is provided by the projection of the vacuum configuration, the feature of the model described as vacuum misalignment above. So, the relation between v and the Higgs VEV in this Abelian Higgs model is

$$v = f \sin\frac{V}{f} \implies \xi = \frac{v^2}{f^2} = \sin^2\frac{V}{f}\,. \tag{2.27}$$

The minimal composite Higgs model

We now discuss the model where the $SO(5)$ global symmetry group is broken to $SO(4)$. In this case, the group structure can be enlarged, so that G_{SM} is contained in the unbroken group. In addition, the structure of symmetry breaking implies there exist four real NGBs that transform as a **4** of $SO(4)$. Under $SU(2)_L$, which is embedded in $SO(4)$, these bosons will transform as a complex doublet H, and can be identified as the composite Higgs.

$SO(4)$ can be shown to be isomorphic to $SU(2)_L \times SU(2)_R$ [17]. This can be seen as follow. Suppose there exist a real vector $\vec{\Pi}$ in the **4** of $SO(4)$, whose components are in one-to-one correspondence with a 2×2 pseudo-real matrix Σ elements, i.e.

$$\Sigma = \frac{1}{\sqrt{2}}\left(i\sigma_\beta \Pi^\beta + I_2 \Pi^4\right) = \frac{1}{\sqrt{2}}\bar{\sigma}_j \Pi^j\,. \tag{2.28}$$

In this expression, $\beta = 1, 2, 3$, σ_β are Pauli matrices and

$$\bar{\sigma}_j = \{i\sigma_\beta, I_2\} \ . \tag{2.29}$$

with the following normalisation, completeness, and reality condition

$$\begin{gathered} \mathrm{Tr}\left[\bar{\sigma}_j^\dagger \bar{\sigma}_k\right] = 2\delta_{jk} \, , \quad \sum_{j=1}^{4} \left(\bar{\sigma}_j^\dagger\right)_a{}^b (\bar{\sigma}_j)_c{}^d = 2\delta_a^d \delta_c^b \, , \\ (\bar{\sigma}_j)^* = \sigma_2 \bar{\sigma}_j \sigma_2 \, , \quad \bar{\sigma}_j \bar{\sigma}_k^\dagger - \bar{\sigma}_k \bar{\sigma}_j^\dagger = 2\bar{\sigma}_j \bar{\sigma}_k^\dagger - 2\delta_{jk} I_2 \, . \end{gathered} \tag{2.30}$$

From the relations in Eq. (2.30), Σ is seen to be pseudo-real, i.e. it obeys [26]

$$\Sigma^* = \sigma_2 \Sigma \sigma_2. \tag{2.31}$$

The action of the chiral group $SU(2)_L \times SU(2)_R$ on Σ is a matrix multiplication of the form [26]

$$\Sigma \to g_L \Sigma g_R^\dagger, \tag{2.32}$$

which preserves the pseudo-reality condition in Eq. (2.31). So, it can be said that a matrix Σ offers a consistent representation of $SU(2)_L \times SU(2)_R$. This matrix is then noticed as a pseudo real bidoublet $(\mathbf{2}, \mathbf{2})$. If the local isomorphism between $SO(4)$ and $SU(2)_L \times SU(2)_R$ exists, an infinitesimal chiral transformation on Σ will have the same effect as an $SO(4)$ rotation has on the $\vec{\Pi}$. This follows since

$$\mathrm{Tr}\left[\Sigma^\dagger \Sigma\right] = |\vec{\Pi}|^2. \tag{2.33}$$

The trace is invariant under the matrix transformation in Eq. (2.32), and this means that the norm of $\vec{\Pi}$ is not changed by the chiral transformations. The arguments above demonstrate that any chiral transformation must be an element of $SO(4)$ since it contains the most general norm-preserving infinitesimal transformation of a four-component vector. So, the $SO(4)$ algebra contains the $SU(2)_L \times SU(2)_R$ one. But, aside from the full $SO(4)$ algebra, no sub-algebra with the same dimensionality of the original one is found. Thus, it is proven that the isomorphism among the two groups exits. We can then take $SU(2)_L$ part as the SM left-handed gauge group.

Having mentioned the isomorphism of $SO(4)$ and $SU(2)_L \times SU(2)_R$, it is worth mentioning that $SU(2)_L \times SU(2)_R$ is an approximate symmetry of the SM. The SM model Higgs potential $V(H^\dagger H)$ is invariant under this symmetry which can be seen if we write the Higgs doublet H as

$$H = \begin{bmatrix} h_1 + ih_2 \\ h_3 + ih_4 \, , \end{bmatrix} , \tag{2.34}$$

where h_i, with $i = 1, \ldots, 4$, are real fields. However, the Higgs VEV

$$H = \begin{pmatrix} 0 \\ \frac{v}{\sqrt{2}} \end{pmatrix} \tag{2.35}$$

breaks $SU(2)_L \times SU(2)_R \to SU(2)_V \simeq SO(3)$. This symmetry breaking can also be appreciated by considering the SM Higgs in the sigma-model scenario. More details about this particular scenario can be found in Ref. [29]. In this scenario, the Higgs doublet is parametrised in term of the matrix

$$\Sigma = \frac{\sqrt{2}}{v}(\tilde{H}H)\,, \tag{2.36}$$

where

$$\tilde{H} = -i\sigma_2 H^*. \tag{2.37}$$

The SM model Higgs potential is invariant under $SU(2)_L \times SU(2)_R$ if the matrix Σ transforms under this symmetry as $\Sigma \to U_L \Sigma U_R^\dagger$, where $U_{L,R}$ denotes the transformation under $SU(2)_{L,R}$. In the unitary gauge, i.e. in Eq. (2.35), the vacuum expectation value of $\Sigma = I_2$. Under $SU(2)_L \times SU(2)_R$, it transforms as [29]

$$\langle \Sigma \rangle = \left\langle U_L \Sigma U_R^\dagger \right\rangle = \left\langle U_L I_2 U_R^\dagger \right\rangle = U_L U_R^\dagger\,. \tag{2.38}$$

The $\langle \Sigma \rangle$ will correspond to I_2 if $U_L = U_R$, i.e. $SU(2)_L \times SU(2)_R$ is broken to $SU(2)_V$. Furthermore, if the Yukawa coupling is written as

$$\mathcal{L}_{\text{Yuk}} = \begin{pmatrix} \bar{t}_L & \bar{b}_L \end{pmatrix} y \Sigma \begin{pmatrix} t_R \\ b_R \end{pmatrix}\,, \tag{2.39}$$

where y is the Yukawa coupling between the SM particles and the Higgs, then this term transforms under $SU(2)_L \times SU(2)_R$ as

$$\begin{pmatrix} \bar{t}_L & \bar{b}_L \end{pmatrix} U_L^\dagger y U_L \Sigma U_R^\dagger U_R \begin{pmatrix} t_R \\ b_R \end{pmatrix} = \begin{pmatrix} \bar{t}_L & \bar{b}_L \end{pmatrix} U_L^\dagger y U_L \Sigma \begin{pmatrix} t_R \\ b_R \end{pmatrix}\,, \tag{2.40}$$

where y is the matrix of top-bottom Yukawa couplings. This term will be invariant under $SU(2)_L \times SU(2)_R$ under the assumption that the top quark Yukawa coupling is the same as the bottom Yukawa coupling, so that y is now proportional to the identity. However, it is known that this is not the case in the SM.

In the fundamental representation, $SO(5)$ generators acting on **5** are given by

$$\begin{aligned} (T^a_{L,R})_{IJ} &= -\frac{i}{2}\left[\frac{1}{2}\epsilon^{abc}\left(\delta^b_I\delta^c_J - \delta^b_J\delta^c_I\right) \pm \delta^a_I\delta^4_J - \delta^a_J\delta^4_I\right]\,, \\ T^k_{IJ} &= -\frac{i}{\sqrt{2}}\left(\delta^k_I\delta^5_J - \delta^k_J\delta^5_I\right)\,, \end{aligned} \tag{2.41}$$

where $T^a_{L,R}$, $a = 1, 2, 3$, are the $SO(4) \simeq SU(2)_L \times SU(2)_R$ unbroken generators, T^k_{IJ}, $k = 1, \ldots, 4$, are the broken generators of the coset $SO(5)/SO(4)$ [24]. The indices I and J run from 1 to 5. Note that it is also possible to use the notation T^α for the unbroken generators, where $\alpha = 1, \ldots, 6$. The unbroken generators T^a_L and T^a_R can be identified as those of the $SU(2)_L$ and $SU(2)_R$ subgroups respectively. They thus satisfy the commutation relation

$$[T^a_{L,R}, T^b_{L,R}] = i\epsilon^{abc} T^c_{L,R}. \tag{2.42}$$

When we consider fermions in the theory, we can extend the structure of the group to $\mathcal{G} = SO(5) \times U(1)_X$ broken down to $\mathcal{H}_1 = SO(4) \times U(1)_X$. The $U(1)_X$ was included, so that the correct hypercharge can be reproduced for these fermions. It is then possible to embed the SM electroweak group $SU(2)_L \times U(1)_Y$ into $\mathcal{H}_1 = SO(4) \times U(1)_X$, hence satisfying one of the requirements above. The hypercharge is then given by $Y = T^{3R} + X$, where T^{3R} is the third $SU(2)_R$ generator [17, 24]. Notice that if we do not extend the group structure, the hypercharge would have been given by $Y = T^{3R}$.

The Lagrangian describing the composite sector in this model is again given in Eq. (2.6), where $\vec{\Phi}$ is now a **5** of $SO(5)$. Similar to the Abelian Higgs model, one can parametrise the components of $\vec{\Phi}$ as fluctuation along the broken generators as

$$\vec{\Phi} = e^{i\frac{\sqrt{2}}{f}h^k(x)T^k} \begin{bmatrix} \vec{0} \\ f + \sigma \end{bmatrix} = (f + \sigma) \begin{bmatrix} \sin\frac{h}{f}\frac{\vec{h}}{h} \\ \cos\frac{h}{f} \end{bmatrix} \tag{2.43}$$

where σ is again a resonance field and $\vec{h}$ represents the four NGBs associated to each of the broken generators. Writing the generators in the form given in Eq. (2.41), we can describe the four pNGBs using the σ-Goldstone matrix defined in Eq. (2.11), which is applicable in general to $SO(N) \to SO(N-1)$. The expression in Eq. (2.43) was in fact derived from this definition of U. Under $\mathbf{g} \in SO(5)$, the transformation of this matrix U is given by [24]

$$U \to \mathbf{g} \cdot U \cdot \mathbf{h}^\dagger\big(\mathbf{g}, h^k(x)\big) \ , \tag{2.44}$$

where

$$\mathbf{h}^\dagger\big(\mathbf{g}, h^k(x)\big) = \mathbf{h} = \begin{pmatrix} h_4 & 0 \\ 0 & 1 \end{pmatrix} \tag{2.45}$$

with $h_4 \in SO(4)$. This means that the matrix U transforms non-linearly under $SO(5)$ rotations.

Substituting Eq. (2.43) in the full composite sector Lagrangian, we again obtain Eq. (2.14). The symmetry involved in the resulting is very similar to the Abelian Higgs

model. The $SO(4)$ group is now linearly realised as a rotation of $\vec{h}$. This corresponds to the rotation of $\vec{\Phi}$ along the unbroken generators of $SO(4)$, i.e.

$$\vec{h} \to e^{i\alpha_\alpha t^\alpha} \Leftrightarrow \vec{\Phi} \to e^{i\alpha_\alpha T^\alpha}\,, \tag{2.46}$$

which is immediately verified by noticing that the rotation of $\vec{h}$ in Eq. (2.43) induced the rotation of $\vec{\Phi}$ under $SO(4)$ of the first 4×4 block. The pNGB fourplet can be written as

$$\vec{h} = \begin{pmatrix} h^1 \\ h^2 \\ h^3 \\ h^4 \end{pmatrix} = \frac{1}{\sqrt{2}} \begin{pmatrix} -i\left(h_u - h_u^\dagger\right) \\ h_u + h_u^\dagger \\ i\left(h_d - h_d^\dagger\right) \\ h_d + h_d^\dagger \end{pmatrix}. \tag{2.47}$$

From Eq. (2.47), the composite Higgs doublet in this model is given by

$$H = \begin{pmatrix} h_u \\ h_d \end{pmatrix}. \tag{2.48}$$

The full Lagrangian in this model also has the other symmetry involving the four non-linearly realised unbroken generators T^k, and their infinitesimal action on $\vec{h}$ is the same as in the Eq. (2.19).

Under an $SU(2)_R$ rotation, the Higgs doublet mixes with its conjugate $H^c = i\sigma_2 H^*$, and (H, H^c) is a bidoublet under $SU(2)_L \times SU(2)_R$.

If we now consider the unitary gauge where the components of the Higgs doublet are given by

$$h_u = 0, \quad h_d \equiv \frac{h}{\sqrt{2}} = \frac{\langle h \rangle + \rho}{\sqrt{2}}\,, \tag{2.49}$$

where ρ is the canonically normalised physical Higgs field and $\langle h \rangle$ is the VEV of the Higgs field, the matrix U is simplified, and can be written as [24, 33]

$$U = \begin{pmatrix} 1 & 0 & 0 & 0 & 0 \\ 0 & 1 & 0 & 0 & 0 \\ 0 & 0 & 1 & 0 & 0 \\ 0 & 0 & 0 & \cos\frac{h}{f} & \sin\frac{h}{f} \\ 0 & 0 & 0 & -\sin\frac{h}{f} & \cos\frac{h}{f} \end{pmatrix}. \tag{2.50}$$

This form of U will be used in the construction of the models we studied.

As an example, we now discuss the case in which also the fermions transform according to the **4** of $SO(4)$. The complex components of the fermionic field fourplet ψ^i

can be related to the elements of a generic 2×2 matrix via

$$\Psi = \frac{1}{\sqrt{2}} \left(\psi^4 + i\sigma_\beta \psi^\beta \right) = \frac{1}{\sqrt{2}} \bar{\sigma}_j \psi^j \,. \tag{2.51}$$

This matrix Ψ transform in the $(\mathbf{2}, \mathbf{2})$ representation shown in Eq. (2.32). It can be referred as a complex bidoublet $(\mathbf{2}, \mathbf{2})_\mathbf{c}$ since it does not obey the pseudo-reality condition. The two columns of Ψ form two doublets with opposite T^{3R} charge $\pm 1/2$ under the $SU(2)_L \times U(1)_Y$ subgroup

$$\Psi = \frac{1}{\sqrt{2}} \begin{bmatrix} \psi^4 + i\psi^3 & \psi^2 + i\psi^1 \\ -\psi^2 + i\psi^1 & \psi^4 - i\psi^3 \end{bmatrix} \equiv (\Psi_-, \Psi_+) \,. \tag{2.52}$$

The fourplet components can be written in terms of the up and down components of the two doublets $\Psi_\pm^{u,d}$ as [26]

$$\vec{\psi} = \frac{1}{\sqrt{2}} \left\{ -i\Psi_+^u - i\Psi_-^d, \Psi_+^u - \Psi_-^d, i\Psi_+^d - i\Psi_-^u, \Psi_+^d + \Psi_-^u \right\}^T \,. \tag{2.53}$$

We now discuss the kinetic Lagrangian of the pNGB and the SM gauge fields, introducing parameters that will be used later. The $SO(5)$-invariant kinetic Lagrangian for the pNGBs is given by

$$\mathcal{L}_\sigma = \frac{f^2}{4} \hat{d}_\mu^k \hat{d}^{k\mu} \,, \tag{2.54}$$

where $iU^\dagger \partial_\mu U = \hat{d}_\mu^k T^k + \hat{E}_\mu^\alpha T^\alpha$, where T^k are given in Eq. (2.41), and T^α are again the unbroken $SO(4)$ generators. Similar to the Abelian Higgs model, the electroweak gauge group can be introduced into the theory by a gauging procedure. The electroweak group of the SM can be gauged via promotion of the ordinary derivatives to covariant ones, $\partial_\mu \to D_\mu = \partial_\mu - ig_0 W_\mu^a T_L^a - ig_0' B_\mu T_R^3$, and addition of the kinetic terms for the gauge fields. Here, $T_{L/R}^a$ denote the generators of $SU(2)_{L/R}$, and g_0 and g_0' are approximate SM gauge couplings. The SM gauge fields' and pNGBs' kinetic terms are given by

$$\mathcal{L}_\sigma = -\frac{1}{4} W_{\mu\nu}^{aL} W^{aL\mu\nu} - \frac{1}{4} B_{\mu\nu} B^{\mu\nu} + \frac{f^2}{4} d_\mu^k d^{k\mu} \,, \tag{2.55}$$

where $\bar{A}_\mu = iU^\dagger D_\mu U = d_\mu^k T^k + E_\mu^\alpha T^\alpha$ are the gauged versions of the relation given in terms of $\hat{d}_\mu^k$ and $\hat{E}_\mu^\alpha$, and $W_{\mu\nu}^{aL}$ and $B_{\mu\nu}$ are the field strength tensors for the $SU(2)_L$ and $U(1)_Y$ gauge fields respectively. Under $SO(5)$, $\bar{A}_\mu$ transforms as

$$\bar{A}_\mu \to \bar{A}_\mu^{(h)} = \mathbf{h} \left(\bar{A}_\mu + i\partial_\mu \right) \mathbf{h}^\dagger \,, \tag{2.56}$$

which gives rise to a shift term $i\mathbf{h}\partial_\mu \mathbf{h}^\dagger$ living in the $SO(4)$ subalgebra. If we now introduce the notation $d_\mu = d_\mu^k T^k$ and $E_\mu = E_\mu^\alpha T^\alpha$, and consider their transformation

properties under $SO(5)$

$$\begin{aligned} d_\mu &\to \mathbf{h} d_\mu \mathbf{h}^\dagger, \\ E_\mu &\to \mathbf{h}\left(E_\mu + i\partial_\mu\right)\mathbf{h}^\dagger, \end{aligned} \tag{2.57}$$

it can be seen that the shift term is carried only by E_μ. Since the dynamical gauge fields belong to the $SO(4)$ subalgebra, as can be seen when we defined the $\bar{A}_\mu$, we consider the **4** representation of $SO(4)$ instead of the **5** of $SO(5)$, and the full form of the d_μ^k and E_μ^α are given, in this representation, by

$$\begin{aligned} d_\mu^k &= \sqrt{2}\left(\frac{\sin h/f}{h} - \frac{1}{f}\right)\frac{\vec{h}.\nabla_\mu\vec{h}}{h^2}h^k - \sqrt{2}\frac{\sin h/f}{h}\nabla_\mu h^k, \\ E_\mu^{La} &= A_\mu^{La} - 4i\frac{\sin^2(h/2f)}{h^2}\vec{h}^T t_L^a \nabla_\mu \vec{h}, \\ E_\mu^{Ra} &= A_\mu^{Ra} - 4i\frac{\sin^2(h/2f)}{h^2}\vec{h}^T t_R^a \nabla_\mu \vec{h}, \end{aligned} \tag{2.58}$$

where $\nabla_\mu\vec{h}$ is the covariant derivative of the h field

$$\nabla_\mu\vec{h} = \left(\partial_\mu - iA_{\mu,a}^L t_L^a + iA_{\mu,a}^R t_R^a\right)\vec{h}, \tag{2.59}$$

and

$$\begin{aligned} A_{\mu,a}^L &= \{g_0 W_\mu^1, g_0 W_\mu^2, g_0 W_\mu^3\}, \\ A_{\mu,a}^R &= \{0, 0, g_0' B_\mu\}. \end{aligned} \tag{2.60}$$

In this definition, we used the 4×4 form of $SU(2)_L \times SU(2)_R$ generators $t_{L,R}^a$ given by

$$T_L^a = \begin{bmatrix} t_L^a & 0 \\ 0 & 0 \end{bmatrix}, \quad T_R^a = \begin{bmatrix} t_R^a & 0 \\ 0 & 0 \end{bmatrix}. \tag{2.61}$$

In this **4** representation, we obtain the transformations

$$\begin{aligned} d_\mu^k &\to (h_4)_l^k\, d_\mu^l, \\ E_\mu \equiv E_\mu^\alpha t^\alpha &\to h_4\left(E_\mu + i\partial_\mu\right)h_4^\dagger, \end{aligned} \tag{2.62}$$

in which d_μ^k transforms linearly and E_μ takes into account the shift. In these transformations, the 4×4 form of the $SO(4)$ generators t^α, defined in the same way as $t_{L,R}^a$ in Eq. (2.61), is used.

Gauging the SM electroweak group results in an explicit breaking of $SO(5)$, and the Higgs potential is generated through loop corrections. This leads to the spontaneous breaking of the EW group, and gives rise to the mass of SM gauge fields. In addition to the Higgs and EW bosons, the theory also describes the resonance σ with mass

$$m_* = g_* f. \tag{2.63}$$

From Eq. (2.14) we read the part involving the Higgs doublet H

$$\frac{f^2}{2|H|^2}\sin^2\frac{\sqrt{2}|H|}{f}D_\mu H^\dagger D^\mu H + \frac{f^2}{8|H|^4}\left(2\frac{|H|^2}{f^2} - \sin^2\frac{\sqrt{2}|H|}{f}\right)\left(\partial_\mu|H|^2\right)^2 , \tag{2.64}$$

where in this expression we used the standard form of the Higgs covariant derivative

$$D_\mu H = \left(\partial_\mu - ig_0 W_\mu^\alpha\frac{\sigma_\alpha}{2} - ig_0' B_\mu\frac{I}{2}\right)H . \tag{2.65}$$

We can now explore the implications of Eq. (2.64). One way to tackle this is to compute this expression in the unitary gauge defined in Eq. (2.49). The Higgs part of the Lagrangian now becomes

$$\frac{1}{2}\left(\partial_\mu\rho\right)^2 + \frac{g^2}{4}f^2\sin^2\frac{\langle h\rangle+\rho}{f}\left(|W|^2 + \frac{1}{2c_w^2}Z^2\right) , \tag{2.66}$$

where W and Z denote the SM mass and charge eigenstate fields and c_w denotes the cosine of the weak mixing angle defined by $\tan\theta_w = \frac{g_0'}{g_0}$. Now in the expression of this Lagrangian, the mass of the SM W bosons are given by

$$m_W = c_w m_Z = \frac{gf}{2}\sin\frac{\langle h\rangle}{f} = \frac{gv}{2} . \tag{2.67}$$

From the expression above, we obtain the relation between $\langle h\rangle$ and the EWSB scale $v = 246$ GeV:

$$\xi = \frac{v^2}{f^2} = \sin^2\epsilon , \tag{2.68}$$

where $\epsilon = \langle h\rangle / f$. This equation is in analogy to the Abelian Higgs model [4]. We note again in this case that v is not defined as the composie Higgs VEV, but rather it is related to it and the parameter f. Apart from the vector boson masses, we can also extract an infinite set of interactions involving two gauge bosons and an arbitrary number of Higgs field by Taylor-expanding the Lagrangian around $\rho = 0$. The first few terms of this expression are

$$\frac{g^2v^2}{4}\left(|W|^2 + \frac{1}{2c_w^2}Z^2\right)\left[2\sqrt{1-\xi}\frac{\rho}{f} + (1-2\xi)\frac{\rho^2}{v^2} - \frac{4}{3}\xi\sqrt{1-\xi}\frac{\rho^3}{v^3} + \ldots\right] \tag{2.69}$$

where $\langle h\rangle$ and f were traded for the EWSB scale v and ξ. From this expression, we see that the single Higgs and double Higgs vertices are modified with respect to the SM and higher dimensional vertices with more Higgs fields emerge. In the limit $\xi \to 0$ which occurs where $f \to \infty$, for a fixed value of v, the couplings reach their SM forms and the higher dimensional interactions are suppressed. The disappearance of the new

effects means that the composite Higgs then becomes the elementary SM Higgs. We could also inspect the implication of Eq. (2.64) by expanding it for large f. From the full expression, terms up to dimension 6 are found to be [26]

$$D_\mu H^\dagger D^\mu H - \frac{2}{3f^2}|H|^2 D_\mu H^\dagger D^\mu H + \frac{1}{6f^2}\partial_\mu (H^\dagger H)\partial^\mu (H^\dagger H) + \dots . \tag{2.70}$$

One could notice that the first term is just the kinetic term of the SM Higgs, and in the limit $f \to \infty$ this will be the only relevant term. This result also illustrates that the composite Higgs reduces to the elementary SM for small ξ. If we consider a model with a generic $\mathcal{G} \to \mathcal{H}$ symmetry breaking, what we find out might be different since in this situation there will be more Goldstone bosons than just one Higgs doublet. The model might not approach the SM model when f is sent to infinity, but rather a theory with an extended Higgs sector.

Chapter 3

Top-partners in explicit composite-Higgs models

The models we studied in our work correspond to the case where the Higgs iss the pNGB of a strong sector with a global symmmetry $SO(5) \times U(1)_X$, which is spontaneously broken to $SO(4) \times U(1)_X$ at the scale f. In the model construction, there is also an explicit breaking of this $SO(5) \times U(1)_X$ group as described below. The models structure were previously studied in ref. [24]. In our work, we also extend their analysis by including an additional top partner multiplet in each of the models in section 3.2, and show how the mass and Yukawa coupling of each of the top partners, in this scenario, vary as functions of the fundamental parameters of the models in section 3.5. Furthermore, in both one and two top partner cases, we also study the CP-odd couplings which arise in the fourplet models. In one top partner case, we derive the analytical form of these CP-odd couplings, whereas in the two top partner case, we again discuss how these couplings vary as functions of the fundamental parameters of the models. All the SM fields are considered to be elementary, except for the right-handed top quark t_R. In these models, t_R is a totally composite bound state of the stong sector, and is also considered to be a singlet of the multiplet of the unbroken $SO(4)$ subgroup. Assumptions about the SM gauge fields, W_μ and B_μ, and the elementary left-handed doublet $q_L = (t_L, b_L)$ are also made. SM electroweak boson couplings arise from gauging the SM subgroup of the global symmetry of the strong sector as described above. From the partial compositeness, it is also assumed that the elementary left-handed doublet q_L couples linearly to the strong sector, as follows

$$\mathcal{L} = y \left(\overline{Q}\right)_i O^i + \text{h.c.}\,, \tag{3.1}$$

where Q_i is used to denote the embeddings of q_L in $SO(5) \times U(1)_X$ multiplets, and O^i represents an operator of the strong sector. The operator O^i consists of combinations of top partners in representations of $SO(4)$, whose explicit form will be given in Eq. (3.5), and the σ-Goldstone boson matrix U [24, 34]. Hence, O^i can be decomposed into various representation of $SO(4)$. As O^i contains the top partner fields, the coupling in the form given in Eq. (3.1) gives rise to the couplings between the SM fields and the top partner. The SM fermions can also obtain their masses as a result of including this type of mixing in the theory.Considering the definition of U in Eq. (2.11), it can be seen that the form of U in a given model depends on the representation of $\vec{h}$. In the $SO(5) \times U(1)_X$ spontaneously broken to $SO(4) \times U(1)_X$ at hand, the representation of $\vec{h}$ is given in Eq. (2.47), which is related to H in Eq. (2.48). If we consider the component of the doublet H in unitary gauge, given in Eq. (2.49), it can be seen that this leads to the form of U described in Eq. (2.50). Since, O^i is consisted of U, this means that O^i is also dependent on the representation of H. If no additional external states are introduced, the elementary quark doublet q_L cannot completely fill a $SO(5)$ multiplet, and the coupling is not invariant under $SO(5)$. The mixing in the form given in Eq. (3.1) then gives rise to the explicit breaking of $SO(5)$. In our work, we considered only the third generation quark of the SM and the relevant field when we consider the elementary-composite mixing terms. The operators O^i were considered to be in either the $\mathbf{5_{2/3}}$ or $\mathbf{14_{2/3}}$ representations of $SO(5) \times U(1)_X$. In order to generate the mass of the top after EWSB, the $U(1)_X$ charge of the operators O^i must be the same as that of the right-handed top quark t_R. In the low energy theory, the terms in Eq. (3.1) must be equivalent to $q_L H t_R$, and hence can give rise to the mass of the top.

The structure of the top-partner effective field theory (EFT) used in our work is based on the standard CCWZ model [31, 32]. In particular, we use the matrix U in unitary gauge, as written in Eq. (2.50), and the d_μ symbol constructed out of U and its derivative. In the model we study, the top-partner multiplet Ψ transforms in the $\mathbf{1_{2/3}}$ and $\mathbf{4_{2/3}}$ representations of $SO(4)$, and we constructed operators O^i in $SO(5)$ representations consisting of Ψ and the matrix U, as outlined above. The embedding

Q_i of the SM doublet will be in $\mathbf{5_{2/3}}$ and $\mathbf{14_{2/3}}$ of $SO(5) \times U(1)_X$. These are given by

$$Q_L^5 = \frac{1}{\sqrt{2}} \begin{pmatrix} ib_L \\ b_L \\ it_L \\ -t_L \\ 0 \end{pmatrix} \quad , Q_L^{14} = \begin{pmatrix} 0 & 0 & 0 & 0 & ib_L \\ 0 & 0 & 0 & 0 & b_L \\ 0 & 0 & 0 & 0 & it_L \\ 0 & 0 & 0 & 0 & -t_L \\ ib_L & b_L & it_L & -t_L & 0 \end{pmatrix} , \tag{3.2}$$

where Q_L^5 and Q_L^{14} denote the embedding in $\mathbf{5}$ and $\mathbf{14}$ respectively. The right-handed top quark can be written in the $\mathbf{5}$ representation of $SO(5)$ as

$$t_R^1 = \begin{pmatrix} 0 & 0 & 0 & 0 & t_R \end{pmatrix}^T . \tag{3.3}$$

The top-partner multiplet can also be written in the $\mathbf{5}$ of $SO(5)$ as

$$\Psi^4 = \frac{1}{\sqrt{2}} \begin{pmatrix} iB - iX_{5/3} \\ B + X_{5/3} \\ iT + iX_{2/3} \\ -T + X_{2/3} \\ 0 \end{pmatrix} \quad , \Psi^1 = \begin{pmatrix} 0 \\ 0 \\ 0 \\ 0 \\ T \end{pmatrix} . \tag{3.4}$$

With these forms of the top partner multiplets, the operator O^i can be written as

$$O^5 = U\Psi \quad , O^{14} = U\Psi U^T , \tag{3.5}$$

where O^5 and O^{14} denote the operators in the $\mathbf{5}$ and $\mathbf{14}$ representations of $SO(5)$ respectively. In these expressions, Ψ denoted the top partner multiplets in the $\mathbf{1}$ and $\mathbf{4}$, as written in Eq. (3.4). When the SM quarks are embedded as shown in Eq. (3.2) and Eq. (3.3), the hypercharge of the q_L doublet is fixed to $Y = 1/6$, and that of the right-handed top quark is fixed to $Y = X = 2/3$. It is worth mentioning that the $U(1)_X$ charges of all the fermion fields described above are fixed by the hypercharge of the right-handed top. The top partners in the $\mathbf{4}$ decompose into two $SU(2)_L$ doublets: (T, B) which have the same quantum numbers as the SM doublet, and an exotic doublet $(X_{5/3}, X_{2/3})$ where $X_{2/3}$ has the same charge as the top quark and $X_{5/3}$ is a state of exotic charge 5/3.

After decomposing O^i, in both $\mathbf{5}$ and $\mathbf{14}$ representations, under the unbroken $SO(4)$, we obtain $\mathbf{5_{2/3}} = \mathbf{4_{2/3}} + \mathbf{1_{2/3}}$ and $\mathbf{14_{2/3}} = \mathbf{4_{2/3}} + \mathbf{1_{2/3}} + \mathbf{9_{2/3}}$ respectively. The embedding of the SM doublet in Eq. (3.2), the right-handed top quark in Eq. (3.3), the top partner

multiplets in Eq. (3.4) and the operators constructed from the top partner multiplets in Eq. (3.5) are all written in representations of $SO(5)$. Moreover, the mixing in the form shown in Eq. (3.1) constructed out of these objects will be invariant under $SO(5)$. This means that without including the **9** in the theory, it is still possible to construct a $SO(5)$ invariant Lagrangians. Studying of the $\mathbf{9_{2/3}}$ is beyond the scope of our project, and hence, will not be considered anywhere in this thesis.

It is important to emphasise that the model employed in our work is a simplified one which only catches the important features of top-partner states relevant for phenomenological purposes as outlined in [24]. These are not complete concrete realisations and the structure of these models is not sufficient to allow one to make a calculable Higgs potential or to determine the fine-tuning for the model. This is because the models do not possess states and couplings necessary for the calculation of the Higgs potential. Because of these reasons we will assume that the mass of the Higgs in our models is the same as its observed value and lower levels of fine-tuning is implied by a lower mass for top-partners. However, it is still possible to calculate the top quark mass from the mixing between the SM top quark and top partners. This mass value will be a constraint on the parameters in our models. The structure of the models can, in fact, be improved [24]. More details about how to improve the structure of the models can be found in ref. [24], but in our work we deal with the minimal models only.

New composite resonances of different spin are expected to appear in composite Higgs models with masses near the compositeness scale which is defined in our work as m_* [24,35]. It is possible to integrate out from the effective field theory the states above this mass scale m_* if its value is sufficiently large. Nevertheless, we still need to include top-partners in our theory in order to achieve a natural EWSB. So, it is assumed that the lightest top-partners masses are below m_*, and cannot be integrated out. It our works, more than one top partner is allowed in contrast to the general approach where only one top partner lies below the scale m_*. Having more than one top partner in the theory would allow additional cascade of decays and changes in the relationship between the top-partner masses, couplings and the compositeness scale f.

The effective field theory in this work is constructed in the same way as in [24]. Depending on the SM doublet embeddings Q_i and whether the top-partners transform in the **1** or **4** of $SO(4)$, we considered four cases in this work: $\mathbf{M4_5}$, $\mathbf{M4_{14}}$, $\mathbf{M1_5}$ and $\mathbf{M1_{14}}$.

3.1 One top-partner multiplet

In this section, we consider the situation where we have one set of top-partner multiplets for each of the models described before.

The M4$_5$ model. For the case where the embedding of SM left-hand doublet is in the **5** of $SO(5)$ and a top-partner multiplet transforms in the **4** of $SO(4)$, after integrating out the states heavier than m_*, the relevant effective Lagrangian for the SM particles and the top-partner is given by

$$\begin{aligned}\mathcal{L}_{\mathbf{M4_5}} = i\bar{q}_L \not{D} q_L + i\bar{t}_R \not{D} t_R + i\bar{\Psi}^{\mathbf{4}} \not{D} \Psi^{\mathbf{4}} - M_\Psi \bar{\Psi}^{\mathbf{4}} \Psi^{\mathbf{4}} + ic_1 \bar{\Psi}^{\mathbf{4}}_R d_\mu \gamma^\mu t_R \\ + yf \bar{Q}^{\mathbf{5}}_L U \Psi^{\mathbf{4}}_R + yf c_2 \bar{Q}^{\mathbf{5}}_L U t^{\mathbf{1}}_R \ + \ \text{h.c.}\end{aligned} \tag{3.6}$$

In the expression above, we used the standard notation $\not{D} = \gamma_\mu D^\mu$, where the Dirac gamma matrices obey the Clifford algebra

$$\{\gamma^\mu, \gamma^\nu\} \equiv \gamma^\mu \gamma^\nu + \gamma^\nu \gamma^\mu = 2g^{\mu\nu} \tag{3.7}$$

and the covariant derivatives associated with the SM gauge group are given by

$$\begin{aligned} D_\mu q_L &= \left(\partial_\mu - ig_0 W^{aL}_\mu T^{aL} - ig'_0 B_\mu T^{3R} - ig_S G_\mu\right) q_L \\ D_\mu t_R &= \left(\partial_\mu - i\frac{2}{3} g'_0 B_\mu T^{3R} - ig_S G_\mu\right) t_R \\ D_\mu \Psi &= \left(\partial_\mu - i\frac{2}{3} g'_0 B_\mu T^{3R} - ig_S G_\mu\right) \Psi \end{aligned} \tag{3.8}$$

where g_S is the $SU(3)_c$ gauge coupling. The top-partners form a colour triplet under $SU(3)_c$, so we included the gluon field G_μ in its associated covariant derivative. We note that in the Eq. (3.6), the $c_{1,2}$ are expected to be the order 1 coefficients, and y is the coupling mixing the elementary states with those from the strong sectors. The coupling proportional to c_1, mixing the totally composite t_R and the top-partner, is entirely generated by the strong sector and not mediated by the y coupling. Because of its nature, this term would have been suppressed if we consider the case of partial t_R compositeness, where in this situation t_R is not entirely generated from the strong sector. This term contains couplings involving the top quark, SM gauge fields and the top-partners [24].

The independent parameters in this model are f, c_1, y and the top-partner mass scale M_Ψ. The parameter c_2 is used to fix the mass of the top quark to ~ 173 GeV. As mentioned earlier in this section, a calculable Higgs potential cannot be constructed

for the models considered in this work and, as a result, it is not possible to investigate the relation between the Higgs mass and any of the parameters listed above. Hence, the mass of the Higgs does not eliminate any of the independent parameters.

We can write the mass matrix for the top and top-partners in the unitary gauge as

$$\begin{pmatrix} \bar{t}_L \\ \bar{T}_L \\ \bar{X}_{2/3,L} \end{pmatrix}^T \begin{pmatrix} -\frac{yfc_2}{\sqrt{2}} \sin\frac{h}{f} & \frac{y}{2}f(1+\cos\frac{h}{f}) & \frac{y}{2}f(1-\cos\frac{h}{f}) \\ 0 & -M_\Psi & 0 \\ 0 & 0 & -M_\Psi \end{pmatrix} \begin{pmatrix} t_R \\ T_R \\ X_{2/3,R} \end{pmatrix} . \tag{3.9}$$

Expanding the Higgs field h around its expectation value in the same way as in Eq. (2.49), we can write the mass matrix for the top and top-partners and its interaction with the Higgs field as

$$\begin{aligned} &\begin{pmatrix} \bar{t}_L \\ \bar{T}_L \\ \bar{X}_{2/3,L} \end{pmatrix}^T \begin{pmatrix} -\frac{yfc_2}{\sqrt{2}} s_\epsilon & \frac{y}{2}f(1+c_\epsilon) & \frac{y}{2}f(1-c_\epsilon) \\ 0 & -M_\Psi & 0 \\ 0 & 0 & -M_\Psi \end{pmatrix} \begin{pmatrix} t_R \\ T_R \\ X_{2/3,R} \end{pmatrix} \\ &+ \begin{pmatrix} \bar{t}_L \\ \bar{T}_L \\ \bar{X}_{2/3L} \end{pmatrix}^T \rho \begin{pmatrix} -\frac{yc_2}{\sqrt{2}} c_\epsilon & -\frac{y}{2}s_\epsilon & \frac{y}{2}s_\epsilon \\ 0 & 0 & 0 \\ 0 & 0 & 0 \end{pmatrix} \begin{pmatrix} t_R \\ T_R \\ X_{2/3,R} \end{pmatrix} , \end{aligned} \tag{3.10}$$

where ρ denotes the canonical Higgs field, $s_\epsilon = \sin\frac{\langle h\rangle}{f}$ and $c_\epsilon = \cos\frac{\langle h\rangle}{f}$. In Eq. (3.10), the first part is the matrix that will give rise to the masses of the top and the top partner, so we will refer to it as the mass matrix. The second part containing ρ will give rise to the interaction between the top, the top partner and the Higgs, so we will refer to this part as the interaction part.

Ignoring the interaction part for now, the mass matrix can be reduced by an orthogonal rotation of the form

$$\begin{pmatrix} t \\ T \\ X_{2/3} \end{pmatrix} \to \frac{1}{N} \begin{pmatrix} N & 0 & 0 \\ 0 & 1+c_\epsilon & 1-c_\epsilon \\ 0 & -1+c_\epsilon & 1+c_\epsilon \end{pmatrix} \begin{pmatrix} t \\ T \\ X_{2/3} \end{pmatrix} , \tag{3.11}$$

where $N = \sqrt{2+2\cos^2\epsilon} = \sqrt{2+2c_\epsilon^2}$ and we are left with a matrix containing a mixing between just one linear combination of the top-partner states and the q_L, while the orthogonal combination is then decoupled from the q_L and any other state. These combining states are given in terms of the original states as

$$\begin{aligned} T' &= \frac{1}{N}\left[(1+c_\epsilon)T + (1-c_\epsilon)X_{2/3}\right] , \\ X'_{2/3} &= \frac{1}{N}\left[(1+c_\epsilon)X_{2/3} - (1-c_\epsilon)T\right] . \end{aligned} \tag{3.12}$$

With the new states defined by Eq. (3.12), the resulting mass matrix reads

$$\begin{pmatrix} \bar{t}_L \\ \bar{T}'_L \\ \bar{X}'_{2/3,L} \end{pmatrix}^T \begin{pmatrix} -\frac{yfc_2}{\sqrt{2}} s_\epsilon & \frac{y}{2} f\sqrt{3+c_{2\epsilon}} & 0 \\ 0 & -M_\Psi & 0 \\ 0 & 0 & -M_\Psi \end{pmatrix} \begin{pmatrix} t_R \\ T'_R \\ X'_{2/3,R} \end{pmatrix} , \tag{3.13}$$

where $X'_{2/3}$ is not mixing with the top-quark and any other states in the mass matrix. From the block-diagonal form of this matrix, it is straightforward to diagonalise the matrix using the method known as bi-unitary transformation, as done for instance in [23]. This can be done by rotating this matrix on the right in a similar way that we performed in Eq. (3.11) but with a mixing angle θ_R, i.e. with a matrix of the form

$$U_R = \begin{pmatrix} \cos\theta_R & \sin\theta_R & 0 \\ -\sin\theta_R & \cos\theta_R & 0 \\ 0 & 0 & 1 \end{pmatrix} , \tag{3.14}$$

and rotating on the left with a rotation matrix U_L, characterised by a mixing angle θ_L, defined by

$$U_L = \begin{pmatrix} \cos\theta_L & \sin\theta_L & 0 \\ -\sin\theta_L & \cos\theta_L & 0 \\ 0 & 0 & 1 \end{pmatrix} . \tag{3.15}$$

Note that these two rotating matrices have the same form. After performing these rotations, the diagonal elements of the mass matrix will be identified as the physical top quark mass m_t and the physical mass of the remaining top partner M_T. The off-diagonal elements of the mass matrix will be set to zero, so that, given the masses m_t and M_T, they will yield constraints on the parameters of the theory y, c_2, f, M_Ψ. Since this bi-unitary transformation will be applicable to the other models studied in our work, it is important to emphasise how to define the rotation angles $\theta_{L,R}$. Starting, for example, from the matrix in Eq. (3.13), it is possible to write this matrix in the form

$$-\begin{pmatrix} \bar{t}_L \\ \bar{T}'_L \end{pmatrix}^T \begin{pmatrix} m & \Delta \\ 0 & M_\Psi \end{pmatrix} \begin{pmatrix} t_R \\ T'_R \end{pmatrix} , \tag{3.16}$$

where we ignore the contribution from fields that do not mix with any other states, e.g. $X'_{2/3}$ in this case. Then, we can define a parameter η as the ratio of the off-diagonal mixing term in the mass matrix before its diagonalisation, denoted in our work as Δ, and the top-partner mass parameter M_Ψ, i.e. $\eta = \frac{\Delta}{M_\Psi}$. As an example, in this model the η is defined as

$$\eta = -\frac{y}{2}\frac{f}{M_\Psi}\sqrt{3+c_{2\epsilon}} , \tag{3.17}$$

since

$$\Delta = -\frac{y}{2} f \sqrt{3 + c_{2\epsilon}} \tag{3.18}$$

in this case. The rotating angle θ_R is then given in general by

$$\theta_R = \frac{1}{2} \arcsin\left(\frac{2 M_T m_t \eta}{M_T^2 - m_t^2}\right) . \tag{3.19}$$

The relationship between the angle θ_R and the left-handed angle θ_L is given by

$$\tan\theta_L = \frac{M_T}{m_t} \tan\theta_R \, . \tag{3.20}$$

Note that the method of diagonalising the mass matrix from the form in Eq. (3.10) described above leaves the kinetic term invariant. After diagonalisation of the mass matrix described above, the state $X'_{2/3}$ has mass M_Ψ, while the mass of the top-partner T' is shifted from this value. Not only $X'_{2/3}$, but also $X_{5/3}$ maintains its original mass $m_{5/3} = M_\Psi$. This $X_{5/3}$ state cannot mix with the other state due to its exotic charge and, therefore, its mass value has to stay the same. So, the $X_{2/3}$ and the exotic state $X_{5/3}$ are degenerate states. This property arises as a result of the pNGB nature of the Higgs, and the composite nature of t_R. If the t_R were treated as a partially composite state, the mass matrix would contain additional entries that could possibly result in mixing between $X_{2/3}$ and other states [24, 33].

The interaction matrix of the Eq. (3.10) must then be rewritten in terms of the mass eigentstates. The diagonal elements of this matrix give the Yukawa couplings of the top and top partner. The off-diagonal terms give the couplings between the Higgs and different top partner states. However, they are not relevant in our study, since they will not be involved in the Higgs plus jet production process.

The $\mathbf{M4_{14}}$ model. For the case where the embedding of SM left-hand doublet is in the **14** of $SO(5)$ and the top-partner multiplet transforms in the **4** of $SO(4)$, the relevant terms in the effective Lagrangian are

$$\begin{aligned} \mathcal{L}_{\mathbf{M4_{14}}} = \; & i\bar{q}_L \not{D} q_L + i\bar{t}_R \not{D} t_r + i\bar{\Psi}^{\mathbf{4}} \not{D} \Psi^{\mathbf{4}} - M_\Psi \bar{\Psi}^{\mathbf{4}} \Psi^{\mathbf{4}} + i c_1 \bar{\Psi}^{\mathbf{4}}_R d_\mu \gamma^\mu t_R \\ & + y f \mathrm{Tr}\left(\bar{Q}_L^{\mathbf{14}} U \Psi^{\mathbf{4}}_R U^T\right) + y f \mathrm{Tr}\left(\bar{Q}_L^{\mathbf{14}} U t_R^{\mathbf{1}} U^T\right) . \end{aligned} \tag{3.21}$$

In Eq. (3.21), the composite states, the top-partners and t_R, are embedded in an operator in the **14** of $SO(5)$ when they are coupling with the SM doublet, and they are in the **5** elsewhere. With the same particle content as in the $\mathbf{M4_5}$ case, the mass matrix

is similar to the one in Eq. (3.10) [24]

$$\begin{pmatrix} \bar{t}_L \\ \bar{T}_L \\ \bar{X}_{2/3,L} \end{pmatrix}^T \begin{pmatrix} -\frac{c_2 yf}{2\sqrt{2}} \sin\frac{2h}{f} & \frac{yf}{2}(\cos\frac{h}{f} + \cos\frac{2h}{f}) & \frac{yf}{2}(\cos\frac{h}{f} - \cos\frac{2h}{f}) \\ 0 & -M_\Psi & 0 \\ 0 & 0 & -M_\Psi \end{pmatrix} \begin{pmatrix} t_R \\ T_R \\ X_{2/3,R} \end{pmatrix} . \tag{3.22}$$

We can then expand the Higgs field around its VEV, and obtain

$$\begin{aligned} &\begin{pmatrix} \bar{t}_L \\ \bar{T}_L \\ \bar{X}_{2/3,L} \end{pmatrix}^T \begin{pmatrix} -\frac{c_2 yf}{2\sqrt{2}} s_{2\epsilon} & \frac{yf}{2}(c_\epsilon + c_{2\epsilon}) & \frac{yf}{2}(c_\epsilon - c_{2\epsilon}) \\ 0 & -M_\Psi & 0 \\ 0 & 0 & -M_\Psi \end{pmatrix} \begin{pmatrix} t_R \\ T_R \\ X_{2/3,R} \end{pmatrix} \\ &+ \begin{pmatrix} \bar{t}_L \\ \bar{T}_L \\ \bar{X}_{2/3,L} \end{pmatrix}^T \rho \begin{pmatrix} -\frac{c_2 y}{\sqrt{2}} c_{2\epsilon} & -\frac{y}{2}(s_\epsilon + 2s_{2\epsilon}) & -\frac{y}{2}(s_\epsilon - 2s_{2\epsilon}) \\ 0 & 0 & 0 \\ 0 & 0 & 0 \end{pmatrix} \begin{pmatrix} t_R \\ T_R \\ X_{2/3,R} \end{pmatrix} , \end{aligned} \tag{3.23}$$

where, in analogy to the $\mathbf{M4_5}$ model, $s_{2\epsilon} = \sin\frac{2\langle h\rangle}{f}$, and $c_{2\epsilon} = \cos\frac{2\langle h\rangle}{f}$. Similar to the $\mathbf{M4_5}$ case, it is possible to rotate this matrix with the rotation of the form

$$\begin{pmatrix} t \\ T \\ X_{2/3} \end{pmatrix} \to \frac{1}{N} \begin{pmatrix} N & 0 & 0 \\ 0 & c_\epsilon + c_{2\epsilon} & c_\epsilon - c_{2\epsilon} \\ 0 & -c_\epsilon + c_{2\epsilon} & c_\epsilon + c_{2\epsilon} \end{pmatrix} \begin{pmatrix} t \\ T \\ X_{2/3} \end{pmatrix} , \tag{3.24}$$

where $N = \sqrt{2 + c_{2\epsilon} + c_{4\epsilon}}$, and $c_{4\epsilon} = \cos\frac{4\langle h\rangle}{f}$, so that in the part of the matrix contributing to the mass only one combination of the top partners couples to the SM field and the Higgs. We are left with the resulting mass matrix

$$\begin{pmatrix} \bar{t}_L \\ \bar{T}'_L \\ \bar{X}'_{2/3,L} \end{pmatrix}^T \begin{pmatrix} -\frac{yfc_2}{2\sqrt{2}} s_{2\epsilon} & \frac{yf}{2}\sqrt{2 + c_{2\epsilon} + c_{4\epsilon}} & 0 \\ 0 & -M_\Psi & 0 \\ 0 & 0 & -M_\Psi \end{pmatrix} \begin{pmatrix} t_R \\ T'_R \\ X'_{2/3,R} \end{pmatrix} . \tag{3.25}$$

In the same way as in $\mathbf{M4_5}$, the $X'_{2/3R}$ has decoupled. This state and $X_{5/3}$ have the same mass M_Ψ. The mass matrix in Eq. (3.25) can be diagonalised by the method of bi-unitary transformation described previously and setting the off-diagonal elements to zero. The interaction part of the matrix in Eq. (3.23) must then be rewritten in terms of the mass eigenstates in order obtain the expressions for the Yukawa couplings.

The $\mathbf{M1_5}$ model. In the case where the embedding of the SM left-handed doublet is in the **5** of $SO(5)$, and the top-partner is in the **1** of $SO(4)$, the relevant parts of the

effective Lagrangian are given by

$$\begin{aligned}\mathcal{L}_{\mathbf{M1_5}} = \; & i\bar{q}_L \not{D} q_L + i\bar{t}_R \not{D} t_R + i\bar{\Psi}^{\mathbf{1}} \not{D} \Psi^{\mathbf{1}} - M_\Psi \bar{\Psi}^{\mathbf{1}} \Psi^{\mathbf{1}} \\ & + yf \bar{Q}_L^{\mathbf{5}} U \Psi_R^{\mathbf{1}} + yf c_2 \bar{Q}_L^{\mathbf{5}} U t_R^{\mathbf{1}} \; + \; \text{h.c.} \end{aligned} \tag{3.26}$$

With a top-partner in the **1**, we can have only one top-partner state T with identical quantum numbers as t_R. The term with c_1 coefficient is now absent from this model. It is possible to add this mixing term to Eq. (3.26), but this term could be removed from the theory by a field redefinition. The mass matrix in this model takes a simpler form than in the case where we have top-partners in the **4**, and it reads [24]

$$\begin{pmatrix} \bar{t}_L \\ \bar{T}_L \end{pmatrix}^T \begin{pmatrix} -\frac{yfc_2}{\sqrt{2}} \sin\frac{h}{f} & \frac{yf}{\sqrt{2}} \sin\frac{h}{f} \\ 0 & -M_\Psi \end{pmatrix} \begin{pmatrix} t_R \\ T_R \end{pmatrix} . \tag{3.27}$$

After expanding the Higgs field, this mass matrix becomes

$$\begin{pmatrix} \bar{t}_L \\ \bar{T}_L \end{pmatrix}^T \begin{pmatrix} -\frac{yfc_2}{\sqrt{2}} s_\epsilon & \frac{yf}{\sqrt{2}} s_\epsilon \\ 0 & -M_\Psi \end{pmatrix} \begin{pmatrix} t_R \\ T_R \end{pmatrix} + \begin{pmatrix} \bar{t}_L \\ \bar{T}_L \end{pmatrix}^T \rho \begin{pmatrix} -\frac{yc_2}{\sqrt{2}} c_\epsilon & \frac{y}{\sqrt{2}} c_\epsilon \\ 0 & 0 \end{pmatrix} \begin{pmatrix} t_R \\ T_R \end{pmatrix} . \tag{3.28}$$

We can obtain the masses and Yukawa couplings of the top quark and the top partner from this matrix by simply rotating it with the bi-unitary transformation, but now in the 2×2 form

$$U_R = \begin{pmatrix} \cos\theta_R & \sin\theta_R \\ -\sin\theta_R & \cos\theta_R \end{pmatrix} , \tag{3.29}$$

and

$$U_L = \begin{pmatrix} \cos\theta_L & \sin\theta_L \\ -\sin\theta_L & \cos\theta_L \end{pmatrix} , \tag{3.30}$$

and sending the off-diagonal elements of the mass part to zero. Again, writing the interaction matrix in terms of the mass eigenstates gives the Yukawa couplings.

The $\mathbf{M1_{14}}$ model. In the case where the SM left-handed doublet is embedded in the **14** of $SO(5)$, and the top-partner transforms in the **1** of $SO(4)$, the relevant effective Lagrangian is

$$\begin{aligned}\mathcal{L}_{\mathbf{M1_{14}}} = \; & i\bar{q}_L \not{D} q_L + i\bar{t}_R \not{D} t_R + i\bar{\Psi}^{\mathbf{1}} \not{D} \Psi^{\mathbf{1}} - M_\Psi \bar{\Psi}^{\mathbf{1}} \Psi^{\mathbf{1}} \\ & + yf \,\text{Tr}\left(\bar{Q}_L^{\mathbf{14}} U \Psi_R^{\mathbf{1}} U^T\right) + yf c_2 \,\text{Tr}\left(\bar{Q}_L^{\mathbf{14}} U t_R^{\mathbf{1}} U^T\right) \; + \; \text{h.c.} \end{aligned} \tag{3.31}$$

Analogously to the $\mathbf{M4_{14}}$ model, we have embedded the composite states in a **14** of $SO(5)$ when they couple to the SM doublet in the expression above. The mass matrix takes a similar form to the one in Eq. (3.27) and is given by

$$\begin{pmatrix} \bar{t}_L \\ \bar{T}_L \end{pmatrix}^T \begin{pmatrix} -\frac{yfc_2}{2\sqrt{2}} \sin 2\frac{h}{f} & \frac{yf}{2\sqrt{2}} \sin 2\frac{h}{f} \\ 0 & -M_\Psi \end{pmatrix} \begin{pmatrix} t_R \\ T_R \end{pmatrix} , \tag{3.32}$$

which becomes

$$\begin{pmatrix} \bar{t}_L \\ \bar{T}_L \end{pmatrix}^T \begin{pmatrix} -\frac{yfc_2}{2\sqrt{2}} s_{2\epsilon} & \frac{yf}{2\sqrt{2}} s_{2\epsilon} \\ 0 & -M_\Psi \end{pmatrix} \begin{pmatrix} t_R \\ T_R \end{pmatrix} + \begin{pmatrix} \bar{t}_L \\ \bar{T}_L \end{pmatrix}^T \rho \begin{pmatrix} -\frac{yc_2}{\sqrt{2}} c_{2\epsilon} & \frac{y}{\sqrt{2}} c_{2\epsilon} \\ 0 & -M_\Psi \end{pmatrix} \begin{pmatrix} t_R \\ T_R \end{pmatrix} , \tag{3.33}$$

after we expand the Higgs field around its VEV.

From the mass matrix of each of the models, one would expect that after expanding $h \to \langle h \rangle + \rho$ and diagonalising them, the Higgs will have non-zero Yukawa couplings to the top partners. It was found that this is the case, and we will show the result later on in this thesis. Hence, top-partner loops will contribute to the gluon initiated Higgs production, as well as that of the Higgs production in association with jets. We also found that the $X_{2/3}$ top partner decouples from the Higgs and the Yukawa coupling of this state is zero. This follows from the form of the mass matrices in Eqs. (3.13) and (3.25). This knowledge will be useful when we will repeat the analysis for the situation where we have two top partner multiplets, since we will be able to decouple the $X_{2/3}$ states from the Higgs.

In this thesis, we want to investigate the impact of the existence of top-partner multiplets on Higgs production, in particular we want to use the process $pp \to h + \text{jet}$ as a probe of the mass and coupling of top partners in specific composite Higgs models. Similar analyses have been presented in Refs. [23, 36, 37]. In Ref. [23] studied the sensitivity of $pp \to h + \text{jet}$ to the mass and coupling of a single top partner in a generic composite Higgs model with $f \gg v$. Many of the techniques used in our work were first exploited there. In Ref. [36], an analysis on $pp \to h + \text{jet}$ production with very boosted Higgs and a jet with High p_T was presented. In particular, the effect of CP-odd couplings to the amplitudes for $pp \to h + \text{jet}$ were presented in that work as well. In our work, we find that, in the models with top-partner multiplet transforming in the **4** representation of $SO(4)$, described in this Chapter, there exist CP-odd couplings which would result in similar effect on the amplitude of the production process. The detailed procedure for deriving these couplings will be presented in Section 3.3. In Ref. [37], for $h + \text{jet}$ production, the boosted Higgs transverse momentum shape was studied as a

mean to analyse the modification of the top Yukawa coupling which arises from mixing with the top partner in both composite Higgs model and minimal supersymmetric SM (MSSM). In these studies, the analyses were carried out using an EFT that encompassed the common features of various models. In our study, however, we consider concrete realisations of perturbative composite Higgs models. Furthermore, in section 3.2, we extend previous studies by including an additional top partner multiplet in the model.

3.2 Two top partner multiplets

Adding one top-partner multiplet to the models can be done straightforwardly. In order to keep the models simple, we assume that all the top partner multiplets couple to the SM with the same strength and each of them would only have different influence on the SM model due to its mass parameters. The top-partner multiplets are denoted by Ψ_i^4 and Ψ_i^1 with their masses denoted by M_{Ψ_i}. The components of the multiplets are labelled as T^i, B^i, $X^i_{2/3}$, $X^i_{5/3}$, and T^i.

For the $\mathbf{M1_5}$ and $\mathbf{M1_{14}}$ models, additional top-partner multiplets can be included in the models in a simple way since we are dealing with top partners in the singlet representaion. As an example to illustrate how to deal with this situation, the mass matrices for these models when we have two top partner multiples are given by

$$\begin{pmatrix} \bar{t}_L \\ \bar{T}^1_L \\ \bar{T}^2_L \end{pmatrix}^T \begin{pmatrix} -\frac{yfc_2}{\sqrt{2}} s_\epsilon & \frac{yf}{\sqrt{2}} s_\epsilon & \frac{yf}{\sqrt{2}} s_\epsilon \\ 0 & -M_{\Psi 1} & 0 \\ 0 & 0 & -M_{\Psi 2} \end{pmatrix} \begin{pmatrix} t_R \\ T^1_R \\ T^2_R \end{pmatrix} \tag{3.34}$$

for $\mathbf{M1_5}$ and

$$\begin{pmatrix} \bar{t}_L \\ \bar{T}^1_L \\ \bar{T}^2_L \end{pmatrix}^T \begin{pmatrix} -\frac{yfc_2}{2\sqrt{2}} s_{2\epsilon} & \frac{yf}{2\sqrt{2}} s_{2\epsilon} & \frac{yf}{2\sqrt{2}} s_{2\epsilon} \\ 0 & -M_{\Psi 1} & 0 \\ 0 & 0 & -M_{\Psi 2} \end{pmatrix} \begin{pmatrix} t_R \\ T^1_R \\ T^2_R \end{pmatrix} \tag{3.35}$$

for $\mathbf{M1_{14}}$.

For the $\mathbf{M4_5}$ and $\mathbf{M4_{14}}$ models, the situation is very similar. The mass matrix for

$\mathbf{M4_5}$ with two top partner multiplets is

$$\begin{pmatrix} \bar{t}_L \\ \bar{T}'^1_L \\ \bar{X}'^1_{2/3,L} \\ \bar{T}'^2_L \\ \bar{X}'^2_{2/3,L} \end{pmatrix}^T \begin{pmatrix} -\frac{yfc_2}{\sqrt{2}}s_\epsilon & \frac{y}{2}f(1+c_\epsilon) & \frac{y}{2}f(1-c_\epsilon) & \frac{y}{2}f(1+c_\epsilon) & \frac{y}{2}f(1-c_\epsilon) \\ 0 & -M_{\Psi 1} & 0 & 0 & 0 \\ 0 & 0 & -M_{\Psi 1} & 0 & 0 \\ 0 & 0 & 0 & -M_{\Psi 2} & 0 \\ 0 & 0 & 0 & 0 & -M_{\Psi 2} \end{pmatrix} \begin{pmatrix} t_R \\ T'^1_R \\ X'^1_{2/3,R} \\ T'^2_R \\ X'^2_{2/3,R} \end{pmatrix} . \tag{3.36}$$

Similarly, the mass matrix for $\mathbf{M4_{14}}$ reads

$$\begin{pmatrix} \bar{t}_L \\ \bar{T}'^1_L \\ \bar{X}'^1_{2/3,L} \\ \bar{T}'^2_L \\ \bar{X}'^2_{2/3,L} \end{pmatrix}^T \begin{pmatrix} -\frac{yfc_2}{\sqrt{2}}s_\epsilon & \frac{yf}{2}(c_\epsilon + c_{2\epsilon}) & \frac{yf}{2}(c_\epsilon - c_{2\epsilon}) & \frac{yf}{2}(c_\epsilon + c_{2\epsilon}) & \frac{yf}{2}(c_\epsilon - c_{2\epsilon}) \\ 0 & -M_{\Psi 1} & 0 & 0 & 0 \\ 0 & 0 & -M_{\Psi 1} & 0 & 0 \\ 0 & 0 & 0 & -M_{\Psi 2} & 0 \\ 0 & 0 & 0 & 0 & -M_{\Psi 2} \end{pmatrix} \begin{pmatrix} t_R \\ T'^1_R \\ X'^1_{2/3,R} \\ T'^2_R \\ X'^2_{2/3,R} \end{pmatrix} . \tag{3.37}$$

When additional top partner multiplets are included in the models where the top partners are in the **4**, one needs to rotate each $(T^i, X^i_{2/3})$ pair separately, so that from each multiplet only one linear combination of top partner states couples to the top quark and the Higgs. With two top-partner multiplets in each of the fourplet models, such rotation can be done by the tranformations

$$\begin{pmatrix} t \\ T^1 \\ X^1_{2/3} \\ T^2 \\ X^2_{2/3} \end{pmatrix} \to \frac{1}{N} \begin{pmatrix} N & 0 & 0 & 0 & 0 \\ 0 & 1+c_\epsilon & 1-c_\epsilon & 0 & 0 \\ 0 & -1+c_\epsilon & 1+c_\epsilon & 0 & 0 \\ 0 & 0 & 0 & 1+c_\epsilon & 1-c_\epsilon \\ 0 & 0 & 0 & -1+c_\epsilon & 1+c_\epsilon \end{pmatrix} \begin{pmatrix} t \\ T^1 \\ X^1_{2/3} \\ T^2 \\ X^2_{2/3} \end{pmatrix} \tag{3.38}$$

for $\mathbf{M4_5}$ with $N = \sqrt{2 + 2\cos^2\epsilon}$, and

$$\begin{pmatrix} t \\ T^1 \\ X^1_{2/3} \\ T^2 \\ X^2_{2/3} \end{pmatrix} \to \frac{1}{N} \begin{pmatrix} N & 0 & 0 & 0 & 0 \\ 0 & c_\epsilon + c_{2\epsilon} & c_\epsilon - c_{2\epsilon} & 0 & 0 \\ 0 & -c_\epsilon + c_{2\epsilon} & c_\epsilon + c_{2\epsilon} & 0 & 0 \\ 0 & 0 & 0 & c_\epsilon + c_{2\epsilon} & c_\epsilon - c_{2\epsilon} \\ 0 & 0 & 0 & -c_\epsilon + c_{2\epsilon} & c_\epsilon + c_{2\epsilon} \end{pmatrix} \begin{pmatrix} t \\ T^1 \\ X^1_{2/3} \\ T^2 \\ X^2_{2/3} \end{pmatrix} \tag{3.39}$$

for $\mathbf{M4_{14}}$ with $N = \sqrt{2 + c_{2\epsilon} + c_{4\epsilon}}$. It is important to note that one can decouple the $X_{2/3}$ states form the top quark and the Higgs irrespective of how many top partners

there are in the models. Similar to the case where we have only one top partner multiplet in the model, the mass matrices for the cases where there are two top partner multiplets in the models can be written as

$$\begin{pmatrix} \bar{t}_L \\ \bar{T}'^1_L \\ \bar{X}'^1_{2/3,L} \\ \bar{T}'^2_L \\ \bar{X}'^2_{2/3,L} \end{pmatrix}^T \begin{pmatrix} -\frac{yfc_2}{\sqrt{2}}s_\epsilon & \frac{yf}{2}\sqrt{3+c_{2\epsilon}} & 0 & \frac{yf}{2}\sqrt{3+c_{2\epsilon}} & 0 \\ 0 & -M_{\Psi 1} & 0 & 0 & 0 \\ 0 & 0 & -M_{\Psi 1} & 0 & 0 \\ 0 & 0 & 0 & -M_{\Psi 2} & 0 \\ 0 & 0 & 0 & 0 & -M_{\Psi 2} \end{pmatrix} \begin{pmatrix} t_R \\ T'^1_R \\ X'^1_{2/3,R} \\ T'^2_R \\ X'^2_{2/3,R} \end{pmatrix} \tag{3.40}$$

for $\mathbf{M4_5}$ and

$$\begin{pmatrix} \bar{t}_L \\ \bar{T}'^1_L \\ \bar{X}'^1_{2/3,L} \\ \bar{T}'^2_L \\ \bar{X}'^2_{2/3,L} \end{pmatrix}^T \begin{pmatrix} -\frac{yfc_2}{2\sqrt{2}}s_{2\epsilon} & \frac{yf}{2}\sqrt{2+c_{2\epsilon}+c_{4\epsilon}} & 0 & \frac{yf}{2}\sqrt{2+c_{2\epsilon}+c_{4\epsilon}} & 0 \\ 0 & -M_{\Psi 1} & 0 & 0 & 0 \\ 0 & 0 & -M_{\Psi 1} & 0 & 0 \\ 0 & 0 & 0 & -M_{\Psi 2} & 0 \\ 0 & 0 & 0 & 0 & -M_{\Psi 2} \end{pmatrix} \begin{pmatrix} t_R \\ T'^1_R \\ X'^1_{2/3,R} \\ T'^2_R \\ X'^2_{2/3,R} \end{pmatrix} \tag{3.41}$$

for $\mathbf{M4_{14}}$. We did not show the full form of the interaction parts of the mass matrices in this discussion, but they can be worked out in the same way as we described in the cases where we have only one top partner multiplet in the models. Even though, it is not shown in this thesis, the top partners do not need to be in the same $SO(4)$ representation as each other, i.e. there can be one or more top partners in the singlet and the fourplet representation in the same model.

3.3 The CP-odd Yukawa Coupling

We now discuss the effect of the terms with coefficient c_1 in Eqs. (3.6) and (3.21). Writing the d_μ symbol in the unitary gauge, we find that the term $ic_1\bar{\Psi}^{\mathbf{4}}_R d_\mu \gamma^\mu t_R$ contains the term [24]

$$ic_1\left[\bar{X}_{2/3,R} - \bar{T}_R\right]\frac{\not{\partial}\rho}{f}t_R\,, \tag{3.42}$$

which is a derivative coupling between the top partners and the Higgs boson. This derivative coupling would result in a CP-odd Yukawa coupling, i.e. in the form of the coupling between the Higgs and $i\bar{\psi}\gamma_5\psi$, where ψ represents either the top or top partners, plus couplings with higher order in the Higgs boson, and i ensures hermiticity.

This term is P-odd and C-even, so CP-odd, as can be checked from any QFT textbook [38]. This coupling scales as $\mathrm{Im}(c_1)$. In the SM, the term $ic_1\bar{\Psi}^{\mathbf{4}}_R d_\mu \gamma^\mu t_R$ doesn't exist, and there exists only the coupling between the Higgs and $\bar{\psi}\psi$, which is a CP-even contribution.

The detail of this procedure will be explained in this thesis for the $\mathbf{M4_5}$ model with one top partner case only since it can be analogously applied to the $\mathbf{M4_{14}}$ model, and the case where we have more than one top partner multiplets in the theory. Starting with the coupling in Eq. (3.42), we can perform an integration by parts on this term, which results in

$$ic_1 \left[(\bar{X}_{2/3})_R - \bar{T}_R\right] \frac{\not{\partial}\rho}{f} t_R = -ic_1 \partial_\mu \left(\left[(\bar{X}_{2/3})_R - \bar{T}_R\right] \gamma^\mu t_R\right) \frac{\rho}{f} \,. \tag{3.43}$$

Then, the states must be rotated to the mass eigenstates. This amounts to performing the following substitution in Eq. (3.42):

$$\begin{aligned} X_{2/3} &= \frac{1}{N}\left[T'\,(1-c_\epsilon) + X'_{2/3}\,(1+c_\epsilon)\right], \\ T &= \frac{1}{N}\left[T'\,(1+c_\epsilon) - X'_{2/3}\,(1-c_\epsilon)\right] \end{aligned} \tag{3.44}$$

where $N = \sqrt{2+2\cos^2\epsilon}$ for $\mathbf{M4_5}$. This is simply the reverse of Eq. (3.12), which leaves us with

$$ic_1[(\bar{X}_{2/3})_R - \bar{T}_R]\frac{\not{\partial}\rho}{f} t_R = -ic_1\partial_\mu \left([(\bar{X}'_{2/3})_R - \bar{T}'_R \frac{2c_\epsilon}{N}]\gamma^\mu t_R\right) \frac{\rho}{f} \,, . \tag{3.45}$$

We then rotate the states t_R and T'_R with the angle θ_R used in bi-unitary transformation which corresponds to performing the substitution

$$\begin{aligned} T'_R &= \cos\theta_R T''_R + \sin\theta_R t''_R \,, \\ t_R &= \cos\theta_R t''_R - \sin\theta_R T''_T \,, \\ X'_{2/3R} &= X''_{2/3R} \,, \end{aligned} \tag{3.46}$$

where t''_R and T''_R are the mass eigenstates of the right-handed top quark and top partner respectively. We then arrive at

$$ic_1[(\bar{X}_{2/3})_R - \bar{T}_R]\frac{\not{\partial}\rho}{f} t_R = -ic_1 \cos\theta_R \sin\theta_R \frac{2c_\epsilon}{N}\partial_\mu \left(\bar{T''_R}\gamma^\mu T''_R - \bar{t''_R}\gamma^\mu t''_R\right)\frac{\rho}{f} + \ldots \,. \tag{3.47}$$

The terms presented in this expression are the only terms relevant to the Higgs plus jet production process studied in our work. In fact, the omitted terms involve mixing between different mass eigenstates, hence they do not contribute to the amplitude for

Higgs plus jet production. Note that the kinetic term is left invariant by this rotation. Applying the product rule on the expression above, we obtain

$$\begin{aligned} ic_1[(\bar{X}_{2/3})_R - \bar{T}_R]\frac{\not{\partial}\rho}{f}t_R = -ic_1\cos\theta_R\sin\theta_R\frac{2c_\epsilon}{N}\left(\left(\partial_\mu\bar{T}''_R\right)\gamma^\mu T''_R + \bar{T}''_R\gamma^\mu\left(\partial_\mu T''_R\right)\right)\frac{\rho}{f} \\ ic_1\cos\theta_R\sin\theta_R\frac{2c_\epsilon}{N}\left(\left(\partial_\mu\bar{t}''_R\right)\gamma^\mu t''_R + \bar{t}''_R\gamma^\mu\left(\partial_\mu t''_R\right)\right)\frac{\rho}{f} + \dots . \end{aligned} \tag{3.48}$$

Now, consider Dirac equation of motion

$$\left(i\gamma^\mu\partial_\mu - m\right)\psi\left(x\right) = 0\,. \tag{3.49}$$

Multiplying $\frac{1-\gamma^5}{2}$ on both sides of Eq. (3.49), we obtain

$$\begin{aligned} \frac{1-\gamma^5}{2}\left(i\gamma^\mu\partial_\mu - m\right)\psi\left(x\right) &= \left(i\gamma^\mu\left(\frac{1+\gamma^5}{2}\right)\partial_\mu - m\left(\frac{1-\gamma^5}{2}\right)\right)\psi\left(x\right) \\ &= i\gamma^\mu\partial_\mu\psi_R\left(x\right) - m\psi_L\left(x\right) \\ &= 0 \end{aligned} \tag{3.50}$$

where above we used the expressions of the left and right handed fields

$$\psi_L = \frac{1-\gamma^5}{2}\psi\,, \qquad \psi_R = \frac{1+\gamma^5}{2}\psi\,, \tag{3.51}$$

and the relations among gamma matrices

$$\begin{aligned} \left(\gamma^5\right)^\dagger &= \gamma^5 \\ \left\{\gamma^5,\gamma^\mu\right\} &= \gamma^5\gamma^\mu + \gamma^\mu\gamma^5 = 0 \\ \left(\gamma^5\right)^2 &= I_4\,. \end{aligned} \tag{3.52}$$

From this, we obtain

$$i\gamma^\mu\partial_\mu\psi_R = m\psi_L\,. \tag{3.53}$$

For the conjugate transpose of Eq. (3.49)

$$-i\left(\partial_\mu\psi^\dagger\right)\gamma^0\gamma^\mu - m\psi^\dagger\gamma^0 = 0 \tag{3.54}$$

multiplying this expression on $\frac{1+\gamma^5}{2}$, we obtain

$$\left[-i\left(\partial_\mu\psi^\dagger\right)\gamma^0\gamma^\mu - m\psi^\dagger\gamma^0\right]\frac{1+\gamma^5}{2} = 0\,. \tag{3.55}$$

Then, using

$$\psi_L^\dagger = \psi^\dagger\left(\frac{1-\gamma^5}{2}\right), \quad \psi_R^\dagger = \psi^\dagger\left(\frac{1+\gamma^5}{2}\right), \tag{3.56}$$

we obtain

$$-i\left(\partial_\mu\psi^\dagger\right)\left(\frac{1+\gamma^5}{2}\right)\gamma^0\gamma^\mu - m\psi^\dagger\left(\frac{1-\gamma^5}{2}\right)\gamma^0 = -i\left(\partial_\mu\psi_R^\dagger\right)\gamma^0\gamma^\mu - m\psi_L^\dagger\gamma^0\,. \quad (3.57)$$

So, we obtain

$$-i\partial_\mu\bar{\psi}_R\gamma^\mu = m\bar{\psi}_L\,. \quad (3.58)$$

Using Eqs. (3.53) and (3.58) on Eq. (3.48) results in

$$\begin{aligned} ic_1[(\bar{X}_{2/3})_R - \bar{T}_R]\frac{\not{\partial}\rho}{f}t_R = &-ic_1\cos\theta_R\sin\theta_R\frac{2c_\epsilon}{N}\left(iM_T\bar{T}''_LT''_R - iM_TT''_R\bar{T}''_L\right)\frac{\rho}{f} \\ &+ic_1\cos\theta_R\sin\theta_R\frac{2c_\epsilon}{N}\left(im_t\bar{t}''_Lt''_R - im_tt''_R\bar{t}''_L\right)\frac{\rho}{f}. \end{aligned} \quad (3.59)$$

Now, taking into account the hermitian conjugate term of this expression, we obtain

$$\begin{aligned} &ic_1[(\bar{X}_{2/3})_R - \bar{T}_R]\frac{\not{\partial}\rho}{f}t_R + \text{ h.c.} = \\ &-\left(ic_1 - ic_1^*\right)\cos\theta_R\sin\theta_R\frac{2c_\epsilon}{N}\left(iM_T\bar{T}''_LT''_R - iM_TT''_R\bar{T}''_L\right)\frac{\rho}{f} \\ &+\left(ic_1 - ic_1^*\right)\cos\theta_R\sin\theta_R\frac{2c_\epsilon}{N}\left(im_t\bar{t}''_Lt''_R - im_tt''_R\bar{t}''_L\right)\frac{\rho}{f}\,. \end{aligned} \quad (3.60)$$

Now, noting that

$$i(c_1 - c_1^*) = 2\text{Im}\,(c_1)\,, \quad (3.61)$$

we then obtain

$$\begin{aligned} ic_1[(\bar{X}_{2/3})_R - \bar{T}_R]\frac{\not{\partial}\rho}{f}t_R + \text{ h.c.} = &\,2\text{Im}\,(c_1)\cos\theta_R\sin\theta_R\frac{2c_\epsilon}{N}\left(im_t\bar{t}''_Lt''_R - im_tt''_R\bar{t}''_L\right)\frac{\rho}{f} \\ &-2\text{Im}\,(c_1)\cos\theta_R\sin\theta_R\frac{2c_\epsilon}{N}\left(iM_T\bar{T}''_LT''_R - iM_TT''_R\bar{T}''_L\right)\frac{\rho}{f}\,. \end{aligned} \quad (3.62)$$

Consider now the gamma matrices structure in this expression,

$$\bar{t}''_Lt''_R = t''^\dagger\frac{1-\gamma^5}{2}\gamma^0\frac{1+\gamma^5}{2}t'' = t''^\dagger\gamma^0\frac{1+\gamma^5}{2}t''\,, \quad (3.63)$$

and

$$\bar{t}''_Rt''_L = t''^\dagger\frac{1+\gamma^5}{2}\gamma^0\frac{1-\gamma^5}{2}t'' = t''^\dagger\gamma^0\frac{1-\gamma^5}{2}t''\,, \quad (3.64)$$

we arrive at

$$\bar{t}''_Lt''_R - \bar{t}''_Rt''_L = \bar{t}''\gamma^5t''\,. \quad (3.65)$$

The same consideration can be applied to the top partner mass eigenstate. Eq. (3.62), then gives

$$\begin{aligned} ic_1[(\bar{X}_{2/3})_R - \bar{T}_R]\frac{\not{\partial}\rho}{f}t_R + \text{ h.c.} = &\,2\text{Im}\,(c_1)\cos\theta_R\sin\theta_R\frac{2c_\epsilon}{N}\left(im_t\bar{t}''\gamma^5t''\frac{\rho}{f}\right) \\ &-2\text{Im}\,(c_1)\cos\theta_R\sin\theta_R\left(iM_T\bar{T}''\gamma^5T''\right)\,. \end{aligned} \quad (3.66)$$

This is the CP-odd coupling that arrive as a result of the mixing between the right handed top partner states and the right hand top in the fourplet models in our study. We would like to denote here that there is an alternative method to derive this coupling, that we present in appendix A. In that calculation, we make use of field redefinitions and we obtain the same result as the one presented here.

Including the CP-odd couplings, the general effective Lagrangian for the top quark $t_{L,R}$ and the top partner states with charge 2/3, which does not decouple from the top quark, $T_{L,R}$, can be written as

$$\begin{aligned}\mathcal{L}_{\text{EFT}} = \mathcal{L}_{\text{kinetic}} - m_t\bar{t}t - m_b\bar{b}b - M_T^j\bar{T}_jT_j - \kappa_t\frac{m_t}{v}\bar{t}t\rho - \kappa_b\frac{m_b}{v}\bar{b}b\rho \\ +\kappa_T^j\frac{M_T^j}{v}\bar{T}_jT_j\rho + i\tilde{\kappa}_t\frac{m_t}{v}\bar{t}\gamma_5 t\rho + i\tilde{\kappa}_T^j\frac{M_T^j}{v}\bar{T}_j\gamma_5T_j\rho\,,\end{aligned} \tag{3.67}$$

where j indicates the sum over the number of the top partner multiplets. Note that in the equation above, t and T denote the mass eigenstates of the top quark and top partner respectively. In the SM, the anomalous couplings κ_i will have the values $\kappa_t = 1$, and $\kappa_T = \tilde{\kappa}_{t,T} = 0$. The CP-odd couplings in the second line of the equation above will be present only in the models with the top partner multiplets in the **4** representation, i.e. $\mathbf{M4_5}$ and $\mathbf{M4_{14}}$, and they will be functions of $\text{Im}(c_1)$ and the mixing angles.

Electron and neutron Electric Dipole Moment experiments have put constraints on the c_1 parameter [25]. For the case where we include up to two top partner multiplets in the models with the c_1 parameter of these multiplet written as $c_{1,1}$ and $c_{1,2}$, the EDM results in ref. [25] indicate that the imaginary part of the parameter must have the value $\lesssim 0.2$. Since the CP-odd Higgs couplings are derived from these parameters, this must also affect the possible value that we could impose on $c_{1,1}$ and $c_{1,2}$. Since the purpose of our study does not involve with the effects of these parameters on the EDMs, we took value of $\text{Re}\,(c_{1,1})$, $\text{Re}\,(c_{1,2})$, $\text{Im}\,(c_{1,1})$ and $\text{Im}\,(c_{1,2})$ to be less than 0.2 in our study.

In section 3.4, we will discuss how the masses and Yukawa couplings respond to the change of the input parameters in the cases where we have either one or two top partner multiplets in all the four models.

3.4 Couplings for one top partner multiplet

In the case where there is only one top partner multiplet in the models, after expanding the Higgs fields to its VEV and its physical field ρ, and diagonalising the mass matrix,

we found the Yukawa couplings of the top and the top partner to have the analytical forms

$$
\begin{aligned}
\mathbf{M1_5}: \quad & \kappa_t = c_\epsilon \cos^2\theta_L\,, \\
& \kappa_T = c_\epsilon \sin^2\theta_L\,, \\
\mathbf{M1_{14}}: \quad & \kappa_t = \frac{c_{2\epsilon}}{c_\epsilon}\cos^2\theta_L\,, \\
& \kappa_T = \frac{c_{2\epsilon}}{c_\epsilon}\sin^2\theta_L\,, \\
\mathbf{M4_5}: \quad & \kappa_t = c_\epsilon\left(\cos^2\theta_R - \frac{s_\epsilon^2}{1+c_\epsilon^2}\left(\cos^2\theta_L - \cos^2\theta_R\right)\right)\,, \\
& \kappa_T = c_\epsilon\left(\sin^2\theta_R - \frac{s_\epsilon^2}{1+c_\epsilon^2}\left(\sin^2\theta_L - \sin^2\theta_R\right)\right)\,, \\
\mathbf{M4_{14}}: \quad & \kappa_t = \left(\frac{c_{2\epsilon}}{c_\epsilon}\cos^2\theta_R - \frac{s_\epsilon\left(s_{2\epsilon}+2s_{4\epsilon}\right)}{2\left(c_\epsilon^2+c_{2\epsilon}^2\right)}\left(\cos^2\theta_L - \cos^2\theta_R\right)\right)\,, \\
& \kappa_T = \left(\frac{c_{2\epsilon}}{c_\epsilon}\sin^2\theta_R - \frac{s_\epsilon\left(s_{2\epsilon}+2s_{4\epsilon}\right)}{2\left(c_\epsilon^2+c_{2\epsilon}^2\right)}\left(\sin^2\theta_L - \sin^2\theta_R\right)\right)\,,
\end{aligned}
\tag{3.68}
$$

where in the $\mathbf{M4_5}$ and $\mathbf{M4_{14}}$ models the κ_T values are those for the T field, since the combination $X_{2/3}$ interacts with the Higgs field only with T, and hence this interaction is not a Yukawa coupling contributing to Higgs plus jet production. As mentioned above, the CP-odd $\tilde{\kappa}$ coefficients can be calculated from Eq. (3.43). Following the procedure outline above, the couplings with Higgs derivative in Eq. (3.43) are thus re-cast into CP-odd Yukawa couplings

$$
\begin{aligned}
\mathbf{M4_5}: \quad & \tilde{\kappa_t} = -\tilde{\kappa}_T = \frac{4c_\epsilon s_\epsilon}{\sqrt{2+2c_\epsilon^2}}\mathrm{Im}(c_1)\sin\theta_R\cos\theta_R\,, \\
\mathbf{M4_{14}}: \quad & \tilde{\kappa_t} = -\tilde{\kappa}_T = \frac{4s_\epsilon(1-2s_\epsilon^2)}{\sqrt{2+c_{2\epsilon}+c_{4\epsilon}}}\mathrm{Im}(c_1)\sin\theta_R\cos\theta_R\,,
\end{aligned}
\tag{3.69}
$$

and couplings to higher powers of the Higgs field. Note that the mass of the bottom quark is also generated via partial compositeness. However, the right-handed bottom is not a totally composite state, unlike the right-handed top, and the mixing of the bottom quark with the composite sector is much smaller. In each of the models, the Yukawa coupling of the bottom quark is shifted by the same factors of c_ϵ or $c_{2\epsilon}/c_\epsilon$ as the top quark, and we can make the assumption that the mixing angles with the composite sector are negligible. So, the anomalous couplings of the bottom quark are $\kappa_b^{\mathbf{5}} = c_\epsilon$ and $\kappa_b^{\mathbf{14}} = \frac{c_{2\epsilon}}{c_\epsilon}$ for models with the top pratner in $\mathbf{5}$ and $\mathbf{14}$ representations respectively. Since the CP-odd couplings are also proportional to the mixing with the composite sector, we can assume that they are absent for the bottom quark.

An important remark is now in order concerning which parameters one can fix in each composite Higgs model. Inspecting on eq. (3.19), one could realises there are restrictions on the values of the parameters in models that we can consider. In all of the models considered in our work, for a fixed value of θ_R, if f is sent to ∞ while the top partner mass M_T is kept at a constant value, then it is implied that the value of y must be sent to infinity in order to keep value of the top mass at the observed value. A similar issue occurs when the value of M_T is sent to infinity while the scale f and the angle θ_R are kept at constant values. In this case, y must again be sent to infinity. Moreover, it seems to be inevitable to sent y to infinity in the situation where f and M_T are both sent to infinity, while the ratio of f/M_T is constant, so that the mass of the top is kept at the correct value. From this argument, it seemed that y must be sent to infinity in the case where one of the parameters in the model is sent to infinity. In fact, y cannot simply be sent to infinity, because this would correspond to a non-perturbative regime. Therefore, in this work, the perturbative range of y is taken to be $y < 3$ [24]. From this constraint on y, the top-partner mass and the mixing angles have to be constrained to have only certain values. In order to investigate these constraints, it is useful to express the off-diagonal term Δ in terms of a mixing angle. Starting from the expression of one mixing angle, i.e. $\theta_{L,R}$ in terms of the other

$$\cos^2\theta_R = \frac{M_T^2\cos^2\theta_L}{M_T^2\cos^2\theta_L + m_t^2\sin^2\theta_L}, \quad \cos^2\theta_L = \frac{m_t^2\cos^2\theta_R}{m_t^2\cos^2\theta_R + M_T^2\sin^2\theta_R}, \tag{3.70}$$

we could derive the expression for Δ

$$\Delta = \frac{M_T^2 - m_t^2}{\sqrt{m_t^2\cos^2\theta_R + M_T^2\sin^2\theta_R}}\frac{\sin(2\theta_R)}{2} = \frac{M_T^2 - m_t^2}{\sqrt{M_T^2\cos^2\theta_L + m_t^2\sin^2\theta_L}}\frac{\sin(2\theta_L)}{2}. \tag{3.71}$$

Due to the different scaling of Δ in terms of v and f, the model parameters will be restricted differently in the singlet and fourplet models. In the singlet model, Δ scales as yv. From this scaling and eq. (3.71), for the singlet models, $y \sim M_T/v\tan\theta_L$ for moderate mixing angle $\theta_L \lesssim \pi/4$ and $M_T \gg m_t$. This means that θ_L, and hence θ_R must have a very small value if M_T is going to have a very large value. This is equivalent to stating that a very heavy top partner will be decoupled from the theory, and this feature occurs for all value of f. For fourplet models, the scaling of Δ is given by $\Delta \sim yf$. From this scaling, for moderate value of the mixing angle, if f is sufficiently large, we could send the M_T to a large value in the fourplet model without violating the perturbativity bound. This discussion shows that it might not be possible to have

a perturbative composite Higgs model from a simplified model by simply determining the mixing angle and the mass of the top partner in the model.

From this discussion, we see that the top partner mass M_T cannot be sent to infinity by fixing all other parameter because the perturbativity bound forbids this to happen. Within the perturbativity bounds, it is however possible to take the limit $f \to \infty$. In such limit, the Yukawa coupling derived in eq. (3.68) takes the form

$$\begin{aligned} \mathbf{M1_5}, \mathbf{M1_{14}}: &\quad \kappa_t = \cos^2\theta_L, \quad \kappa_T = \sin^2\theta_L \\ \mathbf{M4_5}, \mathbf{M4_{14}}: &\quad \kappa_t = \cos^2\theta_R \quad \kappa_T = \sin^2\theta_R \end{aligned} \tag{3.72}$$

while all CP-odd Yukawa couplings derived in eq. (3.69) vanish.

3.5 Mass Spectrum for two top partner multiplets

In the case where there are two light top partner multiplets in each of the models, we will only study the relationship among the fundamental parameters of the models, i.e. mass parameters of the top partner multiplets, the decay constant f, and the couplings in each of the models, to the physical top-partner masses and the Yukawa couplings instead of trying to obtain analytical results in the same way we did for the one top partner multiplet case. The parameters $y, f, M_{\Psi 1}, M_{\Psi 2}$ and c_1 are taken as free parameters in our analysis, while c_2 is used to fix the mass of the top quark to 173 GeV.

The plot for the Yukawa couplings and masses of T^1 or T^2 as a function of the heavier vector-like mass for $M_{\Psi 1} = 1200$ GeV, $y = 1$, and $f = 600/1000$ GeV are shown in Figures 3.1 and 3.2. In each of the plots, the masses and couplings of a single top partner are labelled T^1 only. They are plotted with the same values of y and f, and $M_\Psi = M_{\Psi_1}$. We note here that, for the plots in this section, the cases labelled T^1 only indicates the situation where there is only one top partner left in the theory, i.e. the limit where any other top-partner is decoupled. Also, the label T^1 is used to indicate the lighter top partner. From Figure 3.1, we can see that, in all the models except for $\mathbf{M4_{14}}$, when M_{Ψ_1} is similar to M_{Ψ_2}, the Yukawa coupling of the heavier top partner can becomes larger than that of the lighter top partner. As the gap between the mass parameters of the multiplets increases, the coupling to the Higgs of the heavier top partner decreases and the Yukawa coupling of the lighter top partner is approaching the value we expect to see when there is only one top partner present in the model. For the models with fourplet top partner multiplets, in particular $\mathbf{M4_5}$ model, there is a large region in which the coupling of the heavier top partner dominates that of

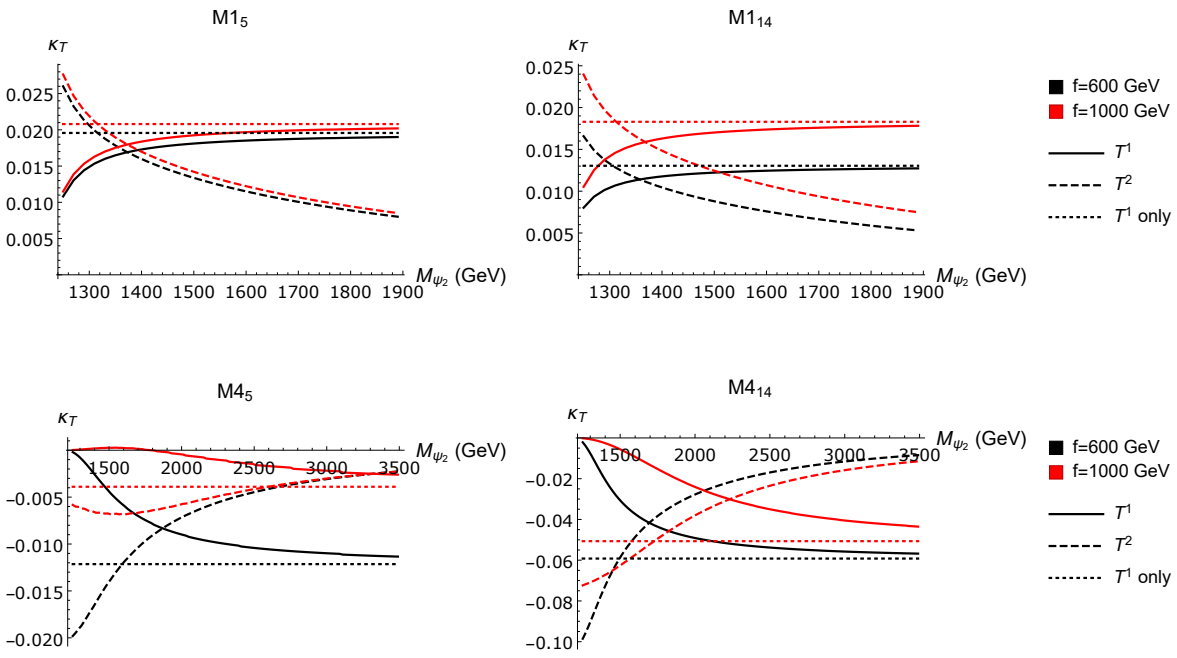

Figure 3.1: The Yukawa couplings for the two T^1 or T^2 top-partners as functions of M_{Ψ_2}, for $M_{\Psi 1} = 1200$ GeV, $y = 1$, and $f = 600/1000$ GeV. The results presented in 'T^1 only' case can be verified from Eqs. (3.68).

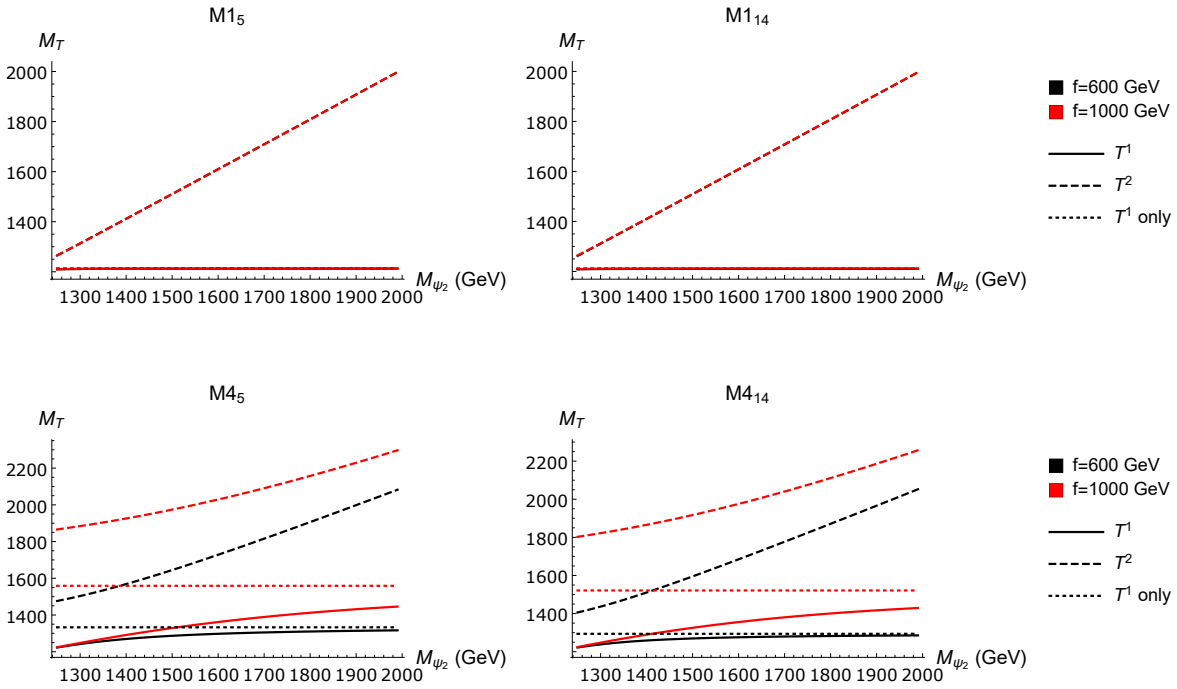

Figure 3.2: The masses of the top-partners T^1 or T^2 as functions of M_{Ψ_2}, for $M_{\Psi 1} = 1200\,\mathrm{GeV}$, $y = 1$, and $f = 600/1000\,\mathrm{GeV}$.

the lighter top partner. Notably, the Yukawa coupling of the lighter top partner can be suppressed when there is a heavier top partner having the same charge but slightly heavier mass.

From Fig. 3.2, we can see that, in the models $\mathbf{M1_5}$ and $\mathbf{M1_{14}}$, the vector-like mass and the mass of the T^2 almost form mass degenerate states. Also, the behaviour of M_T is the same for $f = 600$ GeV and $f = 1000$ GeV scenarios for the singlet models, since in these models the mass matrix is largely insensitive to f. In the models with fourplet top partner multiplets, however, this behaviour could only be appreciated if the mass of one of the top partners is much larger than the other. This is because the mass matrix in these models is no longer insensitive to the scale f. Note that $M_{\Psi_{1,2}}$ are the masses of the $X^{1,2}_{2/3}$ and $X^{1,2}_{5/3}$ states, in the fourplet models, hence such states have the same mass as T^2 for $M_{\Psi_2} \gg M_{\Psi_1}$.

In figure 3.3 aims at displaying the effect of the elementary-composite mixing parameter y on the physical masses and Yukawa couplings in the model $\mathbf{M4_5}$ and $\mathbf{M4_{14}}$ with $M_{\Psi 1} = 1200$ GeV and $M_{\Psi 2} = 1300$ GeV.

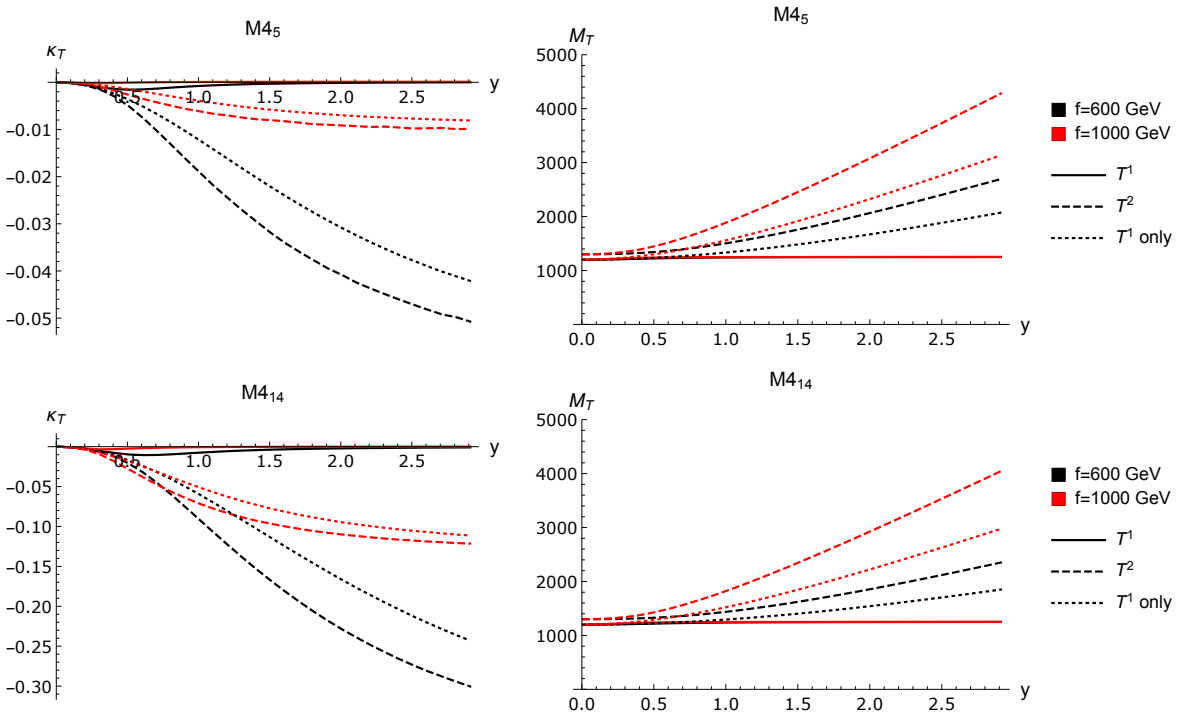

Figure 3.3: The masses and Yukawa couplings of the two T top-partners from the $\mathbf{M4_5}$ and $\mathbf{M4_{14}}$ model as functions of the elementary-composite coupling y, for $M_{\Psi_1} = 1200$ GeV, $M_{\Psi_2} = 1300$ GeV, and $f = 600/1000$ GeV.

From this figure, one first notices that, at small values of y, the top-partner Yukawa couplings approach zero, and their masses approach the multiplet mass parameters $M_{\Psi_{1,2}}$. This behaviour arises because, in this limit, the top partners are gradually decoupled from the top quark and the Higgs, while the mass of the top quark is kept at the observed value by a large c_2 coupling. When we increase the value of y, the difference between T^1 and T^2 becomes more significant, the masses of the lighter top partner is still close to M_{Ψ_1} while the mass of the heavier state is increased. As can be seen from the left panel of this figure, the behaviour of the Yukawa couplings as y varies is less trivial and shows strong dependence on the value of f.

In figure 3.4, we show the behaviour of the masses and Yukawa couplings as we vary the value of the parameter f in the models $\mathbf{M4_5}$ and $\mathbf{M4_{14}}$ with $M_{\Psi_1} = 1200$ GeV and $M_{\Psi 2} = 1300$ GeV. In this plot, we fixed the value of y to 1 and 3.

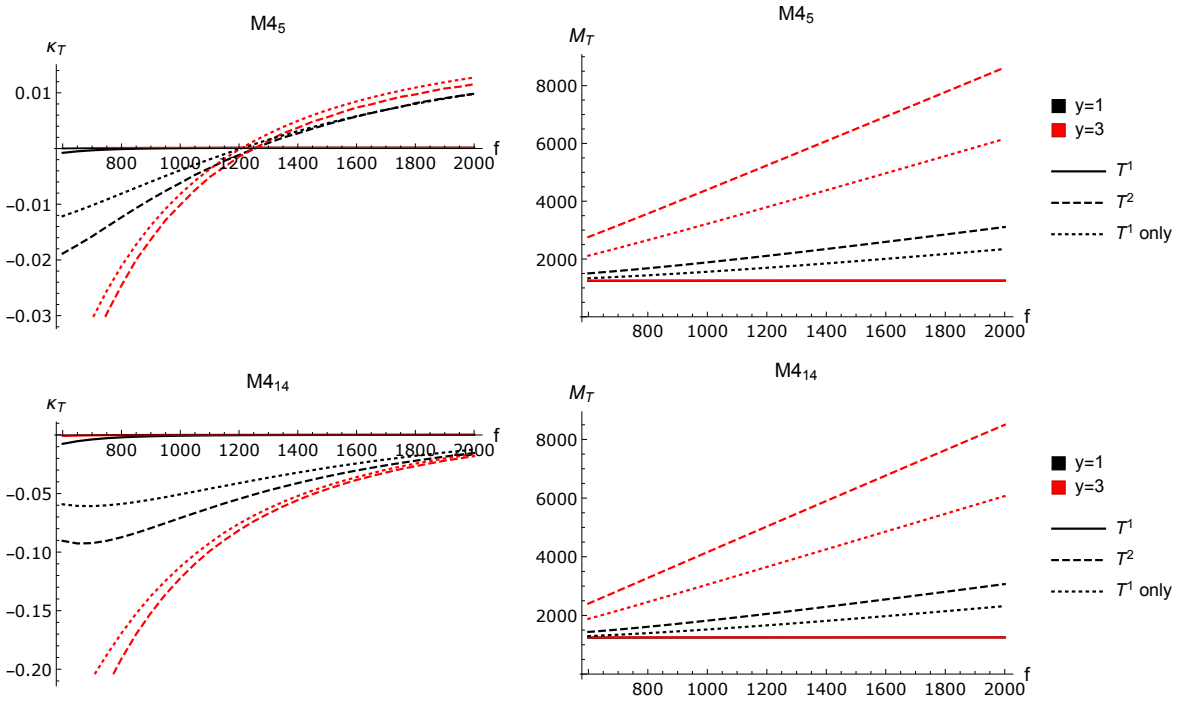

Figure 3.4: The masses and Yukawa couplings of the two T top-partners from the $\mathbf{M4_5}$ and $\mathbf{M4_{14}}$ model as functions of the scale f, for $M_{\Psi_1} = 1200$ GeV, $M_{\Psi_2} = 1300$ GeV, and $y = 1, 3$.

In this figure, we can see that as the value of f is increased one top partner effectively remains light and decouples from the Higgs, while for the other its mass keep increasing and its Yukawa coupling approaches those of a single top-partner. Note here that as we increase the value of f, the ratio v/f becomes small. This indicates that more fine-tuning will be required for the Higgs potential to reproduce the observed Higgs mass and vacuum expectation value.

So far we have not discussed the top quark Yukawa coupling, which is expected to deviate from what is expected in the SM. The top Yukawa coupling as a function of the compositeness scale f for the four models is plotted in Figure 3.5. In this Figure, we set $M_\Psi = M_{\Psi_1}$ in the case where there is only one top-partner multiplet in the considered model. Comparing to Figure 3.1, this plot gives a good representation of the case where $M_{\Psi_1} \ll M_{\Psi_2}$. As can be observed from the figure, apart from small values of f, the top quark anomalous Yukawa coupling do not depend largely on f because at large f this anomalous coupling is dominated by the mixing angles between the top and the

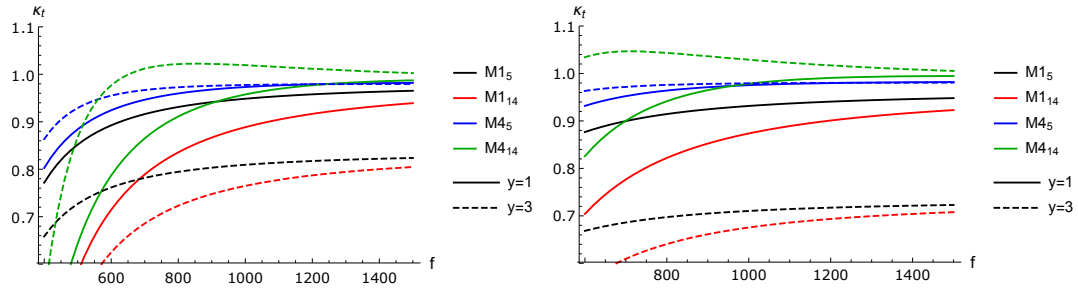

Figure 3.5: The Yukawa coupling of the top quark in each of the models as a function of the scale f, for $M_{\Psi_1} = 1200$ GeV, $M_{\Psi_2} = 1300$ GeV, and $y = 1, 3$, for one top partner (left) and two top partners (right).

top partners. The one top partner (the left panel of Fig. 3.5) and two top partner (the right panel of Fig. 3.5) cases show similar dependence on y. For the singlet models the y-dependence is much stronger than that of the fourplet models, with roughly 30% suppression with respect to the SM for larger value of y. There are large deviations from the standard model for low values of f, particularly in the singlet models. In fact, the recent observation of associated Higgs production with a top quark pair by ATLAS experiment [39] set the 2σ lower bound $\kappa_t \gtrsim 0.8$, which puts the values with $y = 3$ for the singlet models in both one and two top partner cases for the all value of f shown in tension with data. Therefore, in the other plots in this section the value of y is restricted to $y = 1$ when there is a comparison between the singlet and fourplet models.

Last, we discuss the couplings of the top partners to the Higgs derivatives in $\mathbf{M4_5}$ and $\mathbf{M4_{14}}$ models, in the case where we have two top partners. These couplings come from the following contribution to the effective Lagrangian

$$\begin{aligned}\mathcal{L} \supset & - ic_{1,1}\bar{T}_1 d_\mu \gamma^\mu t_R - ic_{1,2}\bar{T}_2 d_\mu \gamma^\mu t_R + \text{ h.c.} \\ = & - i\frac{\partial_\mu \rho}{f}\bar{\psi} C \psi + \text{ h.c.}\end{aligned} \tag{3.73}$$

with

$$\psi = \begin{pmatrix} t_R \\ T_R^1 \\ T_R^2 \end{pmatrix} \quad \text{and} \quad C = \begin{pmatrix} 0 & 0 & 0 \\ c_{1,1} & 0 & 0 \\ c_{1,2} & 0 & 0 \end{pmatrix}. \tag{3.74}$$

In order to calculate the couplings between the quark and the Higgs derivatives in the mass eigenbasis, the matrix C must be rotated by the rotations used to diagonalise

the mass matrix. Hence in the mass eigenbasis, we write $\tilde{C} = O_R(C - C^\dagger)O_R^T$, where O_R is the matrix used to diagonalise the right-handed fields of the mass matrix. We can then use the equations of motion, or perform the field redefinition, in a similar way to the case with one top partner multiplet to change the coupling between quark and derivative of the Higgs Eq. (3.73) into CP-odd Yukawa couplings and couplings to higher powers of the Higgs boson. For the CP-odd Yukawa couplings, we get:

$$\begin{aligned}
\mathbf{M4_5}: \quad & \tilde{\kappa}_t = \frac{2c_\epsilon s_\epsilon}{\sqrt{2+2c_\epsilon^2}}\tilde{C}_{11}, \quad \tilde{\kappa}_{T,1} = \frac{2c_\epsilon s_\epsilon}{\sqrt{2+2c_\epsilon^2}}\tilde{C}_{22}, \quad \tilde{\kappa}_{T,2} = \frac{2c_\epsilon s_\epsilon}{\sqrt{2+2c_\epsilon^2}}\tilde{C}_{33} \\
\mathbf{M4_{14}}: \quad & \tilde{\kappa}_t = \frac{2s_\epsilon(1-2s_\epsilon^2)}{\sqrt{2+c_{2\epsilon}+c_{4\epsilon}}}\tilde{C}_{11}, \quad \tilde{\kappa}_{T,1} = \frac{2s_\epsilon(1-2s_\epsilon^2)}{\sqrt{2+c_{2\epsilon}+c_{4\epsilon}}}\tilde{C}_{22}, \quad \tilde{\kappa}_{T,2} = \frac{2s_\epsilon(1-2s_\epsilon^2)}{\sqrt{2+c_{2\epsilon}+c_{4\epsilon}}}\tilde{C}_{33}.
\end{aligned} \tag{3.75}$$

Then, in Figures. 3.6 and 3.7, we show how the CP-odd couplings of the top and the top partner, respectively, scale as a function of the input parameters. In these figures, we are considering the scenario in which the determining parameters of the CP-odd couplings are universal, i.e. $\mathrm{Re}\,(c_{1,1}) = \mathrm{Im}\,(c_{1,1}) = \mathrm{Re}\,(c_{1,2}) = \mathrm{Im}\,(c_{1,2}) = c$. Also, we study the variation with the scale f for different values of y and c for the CP-odd top Yukawa couplings and the variation with the multiplet mass parameters $M_{\Psi_{1,2}}$ for $y = 1$ and two different values of f for the CP-odd top partner Yukawa couplings. We note here that when one top partner mass is taken to be very heavy, the CP-odd coupling of that top partner diminishes, and in this limit, the CP-odd couplings of the top and the lighter top partner are equal and opposite, as in the case with one top partner. In

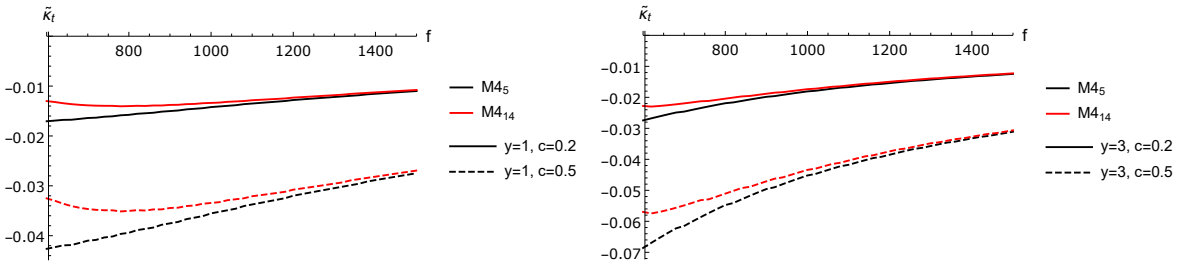

Figure 3.6: The CP-odd Yukawa coupling of the top quark in the fourplet models as a function of the scale f, for $M_{\Psi_1} = 1200$ GeV, $M_{\Psi 2} = 1300$ GeV, and for different values of the parameters y and c.

order to compare with Figures 3.6, for one top partner case, we plotted Figures 3.8 to

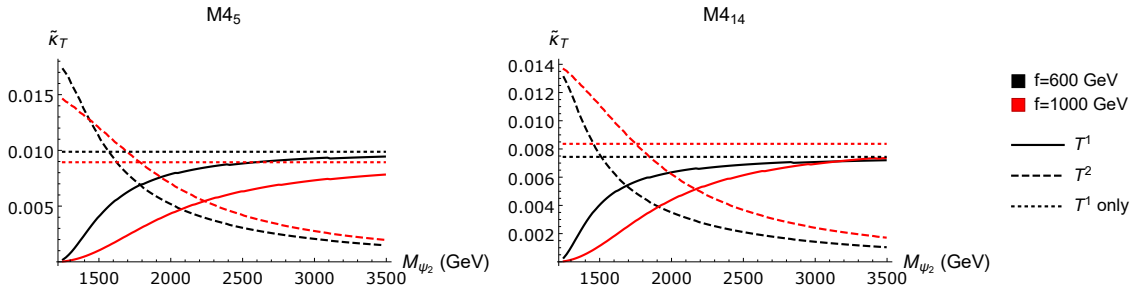

Figure 3.7: The CP-odd Yukawa couplings of the two T top-partners as functions of the heavier vector-like mass, for $M_{\Psi_1} = 1200$ GeV, $y = 1$, $c = 0.2$ and $f = 600/1000$ GeV.

show how the CP-odd top-quark Yukawa coupling varies as a function of f for different values of the parameters y and c.

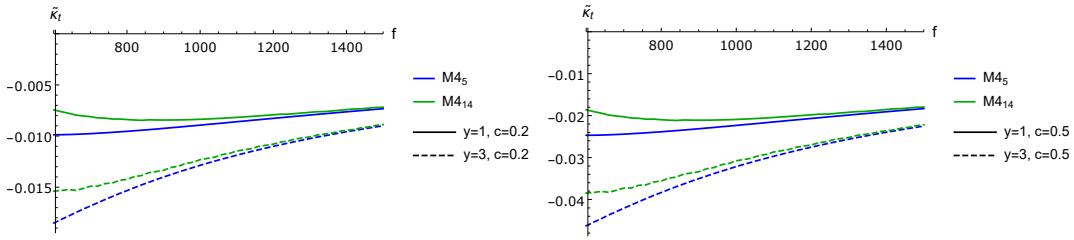

Figure 3.8: The CP-odd top-quark Yukawa coupling varies in the fourplet models in the case where there is only one top-partner multiplet as a function of f, for $M_{\Psi 1} = 1200$ GeV, and for different values of the parameters y and c.

Chapter 4

Top-partners in Higgs production

4.1 Higgs plus jet production process

In this section we compare the discovery potential of the total Higgs cross section, and Higgs production plus one jet. In particular, we investigate the sensitivity of the transverse momentum disgtribution of the Higgs to the masses of the top partners in the composite-Higgs models considered so far.

4.1.1 Higgs production through gluon fusion

Gluon fusion is the main Higgs production mechanism at hadron colliders. This process appears at one loop level in the minimally coupled theories. Since the $SU(3)_C$ QCD symmetry is not broken, the gluon sits in a different gauge group than that of the Higgs field and this process cannot appear at tree level. The Higgs is not charged under $SU(3)_c$ and so does not couple to gluons. The main contributions to this mechanism come from loops of the particles that couple strongly to the Higgs. The Higgs boson couplings to the SM particles will be proportional to their masses. In the SM, the top quark is the only particle to have significant effect in this process. In BSM theories, however, additional coloured particles can also give significant contribution on this Higgs production process. In composite-Higgs models, despite the presence of one or more top partners, the total Higgs production cross-section has been shown to be essentially independent of the masses of the top partners in the model.[1] This low-energy effect rendering the cross section insensitive to the mass spectrum of the top partners occurs

[1] An actual Born-level calculation shows in fact a small percent-level difference between the contribution of top and top partners to the Higgs cross-section.

because, in composite Higgs models, the Higgs is a pseudo Nambu-Goldstone boson.

The authors of ref. [40] studied the effect from the new coloured fermions, along with other less significant effects, to gluon fusion Higgs production in composite Higgs models by using the method of effective Lagrangians. In their study, they investigated new physics effects to Higgs coupling from the higher dimensional operators made out of the SM fields. These operators are

$$\mathcal{O}_H = \partial^\mu (H^\dagger H)\partial_\mu (H^\dagger H), \quad \mathcal{O}_y = H^\dagger H \bar{f}_L H f_R, \quad \mathcal{O}_g = H^\dagger H G_{\mu\nu} G^{\mu\nu}. \tag{4.1}$$

In particular, they showed that, in composite Higgs models, the gluon fusion production rate of the composite Higgs depends on the decay constant f only, and is insensitive to masses of new particles.

The same fact was illustrated in [22]. There it was shown with a different approach that the contribution to gluon fusion Higgs production from the top partners is hard, if not impossible to appreciated. For $pp \to h$, even though top-partners do contribute to Higgs production through loops, it was shown that there is a low energy cancellation that renders this process basically insensitive to the mass of the top-partners. Even though the work in [22] was performed for a model with top partners in the **5**, their argument holds for all composite-Higgs models discussed in chapter 3. The low-energy cancellation can be understood as follows. A generic contribution to the Lagrangian from a model with heavy fermions is given in the physical mass basis by [22]

$$\Delta\mathcal{L} = \sum M_j(v)\bar{\psi}_j\psi_j + \sum Y_{ij}\bar{\psi}_i\psi_j H(x). \tag{4.2}$$

At Born level, a fermion will give a contribution to the ggh production cross-section given by [22]

$$\hat{\sigma}_{gg\to H} = \frac{\alpha_s^2 m_H^2}{576\pi}\left|\sum_j \frac{Y_{jj}}{M_j} A_{1/2}(\tau_j)\right|^2 \delta(\hat{s} - m_H^2), \tag{4.3}$$

where Y_{jj} is the Yukawa coupling of fermion j of mass M_j to the Higgs boson, $\hat{s}$ is the partonic centre-of-mass energy squared, and $A_{1/2}(\tau_j)$ is the following function of $\tau_j = m_H^2/(4M_j^2)$:

$$A_{1/2}(\tau) = -2\left[\tau + (\tau-1)f(\tau)\right]/\tau^2, \qquad f(\tau) = \begin{cases} \arcsin^2\sqrt{\tau} & \tau \le 1 \\ -\frac{1}{4}\left[\ln\frac{1+\sqrt{1-\tau^{-1}}}{1-\sqrt{1-\tau^{-1}}}\right]^2 & \tau > 1 \end{cases}. \tag{4.4}$$

In the limit where the fermions participating in the loop are massive, we have $A_{1/2}(\tau \to 0) \to 1$. The contribution to ggh of fermions with a mass larger than the mass of the Higgs is given by

$$\delta g_{Hgg} \propto \sum_{M_j > m_H} \frac{Y_{jj}}{M_j} \tag{4.5}$$

where the sum is performed over states that are heavier than the Higgs. This contribution can be rewritten as

$$\sum_j \frac{Y_{jj}}{M_j} - \sum_{M_j < m_H} \frac{Y_{jj}}{M_j} = \mathrm{Tr}(Y M^{-1}) - \sum_{M_j < m_H} \frac{Y_{jj}}{M_j} \tag{4.6}$$

where M is a matrix whose eigenvalues are the masses of the fermions and Y incorporates the corresponding Yukawa couplings. Moreover, it can be shown [22] that

$$\mathrm{Tr}(Y M^{-1}) = \frac{\partial \log(\det M)}{\partial \langle h \rangle} \,. \tag{4.7}$$

The above representation of the sum in eq. (4.6) makes the calculation of the ggh coupling more efficient, since there is no need to perform the calculation in the mass eigenstates explicitly.

If we repeat the analysis of ref. [22] for our composite Higgs models we find that, for the models $\mathbf{M1_5}$ and $\mathbf{M4_5}$, we have

$$\frac{\partial \log(\det M)}{\partial \langle h \rangle} = \frac{1}{f} \cot\left(\frac{\langle h \rangle}{f}\right) = \frac{c_\epsilon}{v} \,, \tag{4.8}$$

whereas for the models $\mathbf{M1_{14}}$ and $\mathbf{M4_{14}}$ we obtain

$$\frac{\partial \log(\det M)}{\partial \langle h \rangle} = \frac{2}{f} \cot\left(\frac{2\langle h \rangle}{f}\right) = \frac{c_{2\epsilon}}{v\, c_\epsilon} \,, \tag{4.9}$$

which are independent of the masses and couplings of the top partners. For a single top partner, the above results can be checked explictly by computing the Higgs partonic cross section as in eq. (4.3) using the Yukawa couplings obtained from eq. (3.68).

Note that in ref. [22], the same analysis was performed on a composite Higgs model where a top-partner multiplet is in the $\mathbf{5}$ of $SO(5) \times U(1)_X$. The form of the top partner in this representation can be written in the same way as in Eq. (3.4). A field redefinition of the composite quark

$$\Psi^5 \to U^\dagger \Psi^5 \,, \tag{4.10}$$

where U is defined in Eq. (2.50), was also performed to simplify the analysis. This redefined field mixes with the elementary top quark, and the relevant terms in the action are given by [22]

$$\mathcal{L} = M_5 \overline{\Psi}^5_R \Psi^5_L + \lambda_q \bar{q}_L P_q U^\dagger \Psi^5_R + \lambda_t \bar{t}_R P_t U^\dagger \Psi^5_L + Y f (\overline{\Psi}^5_R \sigma_0)(\sigma_0^\dagger \Psi^5_L) + \mathrm{h.c.} \tag{4.11}$$

where P_q and P_t are used to project out the components of the composite multiplet with the quantum numbers of the left- and right-handed top quark respectively and the standard vacuum configuration σ_0 is defined as

$$\sigma_0 = \begin{pmatrix} 0 & 0 & 0 & 0 & 1 \end{pmatrix}^T . \tag{4.12}$$

From this equation, it is possible to derive the mass matrix for the top quark and the top partners [22]

$$M = \begin{pmatrix} 0 & \frac{\lambda_q(\cos(\langle h\rangle/f)+1)}{2} & \frac{\lambda_q(\cos(\langle h\rangle/f)+1)}{2} & \frac{i\lambda_q \sin(\langle h\rangle/f)}{\sqrt{2}} \\ \frac{-i\lambda_t^* \sin(\langle h\rangle/f)}{\sqrt{2}} & M_5 & 0 & 0 \\ \frac{-i\lambda_t^* \sin(\langle h\rangle/f)}{\sqrt{2}} & 0 & M_5 & 0 \\ \lambda_t^* \cos(\langle h\rangle/f) & 0 & 0 & M_5 + Yf \end{pmatrix} . \tag{4.13}$$

In Eq. (4.13), we can see that there is no Higgs dependence in the composite sub-block of the matrix which benefits from using the field redefinition in Eq. (4.10). This property will be true in any basis because the determinant of a matrix will stay the same under unitary transformations. Moreover, the composite part of the mass matrices will be independent of the Higgs for each different charge species individually since the generator of electric charge commutes with the matrix U. Using Eq. (4.6), the contribution to Higgs coupling to gluons from the top quark and the top partners in this model is found to be

$$\frac{\partial \log(\det M)}{\partial v} = \frac{2}{f}\cot(\frac{2\langle h\rangle}{f}) \tag{4.14}$$

for a light Higgs with $m_H \ll m_t$. In this model, the only fermion in loops with a mass smaller that m_H is the bottom quark, whose Yukawa coupling is not dependent on the top-partner masses and couplings, since it does not couple to the top partners. Hence, $\sum_{M_j<m_H} \frac{Y_{jj}}{M_j}$ is not dependent on the masses and couplings of the top partners. From the result calculated in Eq. (4.14), δg_{Hgg} from Eq. (4.5) will show no dependency on the the top partner masses and couplings. So, the modification to the ggh effective coupling in Eq. (4.3), calculated from this sample model shows no dependence on the masses and coupling strength of the top partners. The same argument applies to the results of the composite Higgs models studied in this thesis in Eqs. (4.8) and (4.9) as well.

4.1.2 Higgs plus jet production

In contrast to single Higgs production, in the Higgs plus jet production process $pp \to h + j$, the cross section of this process will be dependent on the top partners' masses.

In fact, as shown in ref. [23], the low-energy theorem that renders the cross section insensitive to the masses of the loop fermions does not hold any longer in $pp \to h + j$. At the lowest order, in this production process $p_{T,h} = p_{T,j}$. When the transverse momentum p_T of either the Higgs or the jet in the final states is large, it is not possible to use the low-energy theorem assumption. In order to get a better idea of how this comes about, we consider what happens when this p_T takes high or low values. At parton level, there are four processes contributing to $pp \to h + j$:

$$gg \to h + g, gq \to h + q, \hat{q}g \to h + \hat{q}, q\hat{q} \to h + g\,. \tag{4.15}$$

We now consider for instance $gg \to h + g$, but similar considerations hold for the other subprocesses as well. The partonic cross section of $gg \to h + g$ can be written in terms of a sum over different gluon helicity configurations and fermions running in the loop as [23]

$$\hat{\sigma}_{gg\to hg} = \frac{3}{2}\frac{\beta_H}{16\pi\hat{s}}\frac{\alpha_s^3}{4\pi v^2}\left(\sum_{\lambda_j=\pm}\left|\sum_{f_j}\mathcal{M}^j_{\lambda_1\lambda_2\lambda_3}\left(\hat{s},\hat{t},\hat{u},m_j,y_j\right)\right|^2\right), \tag{4.16}$$

where β_H is the final state velocity, λ_j are the helicities of the three gluons, and f_j is the indication of the different fermion species in the loop. The matrix element $\mathcal{M}^j_{\lambda_1\lambda_2\lambda_3}$ for one fermion species with mass m_f and Yukawa coupling $y = \frac{m_f}{v}\kappa_f$ running in the loop will behave differently for different p_T magnitude. Consider for instance, the amplitude $\mathcal{M}_{+++}$ in the limit where $p_T \gg m_f, m_H$. In this limit, the amplitude will take the form [23]

$$\mathcal{M}_{+++} \propto \frac{m_f^2\kappa_f}{p_T}\left(A_0 + A_1\ln\left(\frac{p_T^2}{m_f^2}\right) + A_2\ln^2\left(\frac{p_T^2}{m_f^2}\right)\right), \tag{4.17}$$

where A_0, A_1, A_2 are combination of constants and m_f-independent logarithms. It can be seen from this expression that the matrix element shows dependencies on both the mass and the coupling to the Higgs of the fermion running in the loop. For low p_T limit, the amplitude becomes

$$\mathcal{M}_{+++} \propto \kappa_f p_T\,, \tag{4.18}$$

where the dependence on fermion mass is absent. The expression in Eq. (4.18) is proportional to what one would obtain for $gg \to h$. If we consider the contributions from a top quark with mass m_t and Yukawa coupling $\frac{m_t}{v}\kappa_t$, and a top partner with mass M_T and Yukawa coupling $\frac{M_T}{v}\kappa_T$ to the matrix element $\mathcal{M}_{+++}$, the low energy theorm applies when the final states have low p_T. If the transverse momentum of the final state is increased to the range $m_t \ll p_T \ll M_T$, however, the contributions from the top can

be approximated to be in the high p_T limit, i.e., the one shown in Eq. (4.17), while the contribution from the top partner can be approximated to be in the low p_T limit shown in Eq. (4.18). In this kinemetic region, we then obtain

$$\mathcal{M}_{+++} \propto \frac{m_t^2 \kappa_t}{p_T} \left(A_0 + A_1 \ln\left(\frac{p_T^2}{m_t^2}\right) + A_2 \ln^2\left(\frac{p_T^2}{m_t^2}\right)\right) + \kappa_T p_T \,, \tag{4.19}$$

where the amplitude is only dependent on the top mass and the Yukawa couplings of the top and the top partner. The amplitude will show dependence on the top partner mass when the p_T is increased further to the region $p_T \gg m_t, m_H, m_T$. In this range of the final state transverse momentum, the contributions from both the top and the top partner will approximately be in the high-p_T limit, and we obtain [23]

$$\begin{aligned} \mathcal{M}_{+++} \propto & \frac{m_t^2 \kappa_t}{p_T} \left(A_{0,t} + A_{1,t} \ln\left(\frac{p_T^2}{m_t^2}\right) + A_{2,t} \ln^2\left(\frac{p_T^2}{m_t^2}\right)\right) \\ & + \frac{M_T^2 \kappa_T}{p_T} \left(A_{0,T} + A_{1,T} \ln\left(\frac{p_T^2}{M_T^2}\right) + A_{2,T} \ln^2\left(\frac{p_T^2}{M_T^2}\right)\right) . \end{aligned} \tag{4.20}$$

Even though, we show here only the approximated forms of $\mathcal{M}_{+++}$ when p_T is increased, the other matrix elements $\mathcal{M}^j_{\lambda_1\lambda_2\lambda_3}$ show a similar behaviour for different values of p_T. Numerical analyses were carried out in ref [23] to confirm the behaviour of the matrix elements, both at the parton level, and after including the effect of the parton distribution function (PDF).

4.2 One top partner multiplet

Having discussed the four models in our work, and derived the Yukawa couplings of the top quark and the top partners in each of the models in Eq. (3.68), we compute the p_T distributions for these models at the LHC with a centre-of-mass energy $\sqrt{s} = 14$ TeV. In this computation, we set the top quark mass $m_t = 173.5$ GeV, the bottom quark mass $m_b = 4.65$ GeV, and use MSTW2008NLO parton distribution function [41], corresponding to $\alpha_s(M_Z) = 0.12$. The data used to produce the plots in this section was obtained by interfacing the matrix elements of [42] contained in the program HERWIG 6.5 [43] with LHAPDF [41, 44, 45], using the PDF evolution toolkit HOPPET [46], to obtain the transverse momentum distribution $\frac{d\sigma}{dp_T}$ of a Higgs or a recoiling jet. The code was originally developed by my supervisor and used for the first time in [23]. In this thesis, the core of the code, which contains the details of the numerical integrations needed to obtain $d\sigma/dp_T$, was left untouched, and we have only modified the couplings

to the fermions in the loops contributing to Higgs plus jet (see appendix B.1 for details). Note that this is not the only way to integrate the matrix elements of [42]. For an example of an alternative implementation of the same calculation one could look at the SusHi program [47]. In particular, for this thesis, only the couplings of the particles involved in the process were modified and no edits to the main structure of the code have been performed. For the case with one top parter, the couplings of the particles are modified according to the relation

$$-\kappa_t \frac{m_t}{v} \bar{t}th - \kappa_T \frac{M_T}{v} \bar{T}Th - \kappa_b \frac{m_b}{v} \bar{b}bh \,. \tag{4.21}$$

The lowest-order amplitude for Higgs plus jet is then computed using these couplings, and convoluted with parton distribution functions to obtain $\frac{d\sigma}{dp_T}$. In particular, for the case with one top partner, the couplings $\kappa_t, \kappa_T, \kappa_b$ are automatically computed by the program simply from the input values of the scale f, the mixing angle $\sin^2\theta_{L,R}$, and an integer indicating one of the models. For the scenario with multiple top partners, the number of quark participating in the computation, the masses and couplings of each of the parton (bottom, top and top partners) are input from a file. More details on the modification made to the code, and basic instructions to run it, can be found in Appendix. B.1.

From the differential p_T spectrum, we construct the integrated transverse momentum distribution $\sigma\left(p_T > p_T^{\text{cut}}\right)$ defined as

$$\sigma\left(p_T > p_T^{\text{cut}}\right) = \int_{p_T^{\text{cut}}} dp_T \frac{d\sigma}{dp_T} \,. \tag{4.22}$$

The reason behind considering $\sigma\left(p_T > p_T^{\text{cut}}\right)$ is that, for large values of p_T, we do not have many events, so this observables aims at collecting as many events as possible.

With the above program, it would already be useful to analyse the difference between the observable $\sigma\left(p_T > p_T^{\text{cut}}\right)$ in each of the models considered in chapter 3 and in the SM as a mean to probe the compositeness of the Higgs. In our work, we studied instead the efficiency $\epsilon(p_T > p_T^{\text{cut}})$ defined as the fraction of events for which the Higgs (or at least one jet) has a transverse momentum larger than a given p_T cut

$$\epsilon(p_T > p_T^{\text{cut}}) = \frac{1}{\sigma} \int_{p_T^{\text{cut}}} dp_T \frac{d\sigma}{dp_T} \,. \tag{4.23}$$

The advantage of computing this quantity can be appreciated when two spectra are different just by an overall factor due to different total cross section. Since no information about the presence of top partners can be assessed when this difference occurs,

it will be better to avoid this discrepancy by studying dicrepancy from the SM of the efficiency rather than of the cross section in Eq. (4.22). More precisely, from the p_T distribution of the Higgs produced in each of the models, we studied $\epsilon_{\rm BSM}(p_T > p_T^{\rm cut})$, defined as the fraction of the events for which the Higgs, generated in one of the models studied in this work, has a transverse momentum larger than a given $p_T^{\rm cut}$. For the SM, we similarly studied $\epsilon_{\rm SM}(p_T > p_T^{\rm cut})$, which is defined as the fraction of the events for which the SM Higgs has a transverse momentum larger than a given $p_T^{\rm cut}$. We then produce contour plots for $\delta(p_T^{\rm cut})$ defined as the deviation of the efficiency of the BSM from that of the SM

$$\delta(p_T^{\rm cut}) \equiv \frac{\epsilon_{\rm BSM}(p_T > p_T^{\rm cut})}{\epsilon_{\rm SM}(p_T > p_T^{\rm cut})} - 1\,. \tag{4.24}$$

These contour plos are computed in percentage, as a function of the top partner mass M_T and the compositeness scale f using Mathematica. We note here that in the SM case, the value $\delta(p_T^{\rm cut})$ will be zero. Since in ref. [23], the case $f \gg M_T$ has already been considered, in these contour plots, M_T and f values are in the range that are not excluded by current measurements, and there is no specific hierarchy between these two parameters. In line with ref. [23], in the single top-partner case, we also fix the value of the mixing angle between the top and the top partner. In particular, for the contour plots of the singlet models, we fix the value of $\sin^2\theta_L$, whereas for those of the fourplet models, we fix the value of $\sin^2\theta_R$. Different mixing angles are fixed in the singlet and fourplet models because in the singlet model the Yukawa coupling modification depends only on $\sin^2\theta_L$ which becomes increasingly large with the top partner mass according to Eq. (3.20). The contribution of the top gets smaller as the value of f get larger, and the spectrum is dominated by the top-partner contribution. For the fourplet models, on the other hand, the Yukawa coupling is largely dependent on $\sin^2\theta_R$ for large values of f. However, when the top-partner masses are increasing, for a finite f, the Yukawa couplings contains a negative contribution proportional to $\sin^2\theta_L$ for the top partner and $\cos^2\theta_L$ for the top quark. We would like to stress here that the predictions presented in our work correspond to those presented in ref. [23] in the limit $f \gg v$. We then decided to fix the same parameters in order to assess the impact of choosing a finite value of f. This choice exposes us to problems with perturbativity of the models. In fact, as discussed in section 3.4, fixing $\sin^2\theta_{L,R}$ might not correspond to any perturbative composite-Higgs model. In all the contour plots of $\delta(p_T^{\rm cut})$ for models with a single top partner, we include lines corresponding to fixed values of y, so that the region where y is in the perturbative regime can be clearly distinguished. Furthermore,

the lower bound on κ_t mentioned in chapter 3 further constrains the value of mixing angles in both singlets and fourplet models. This results in the fact that singlet models with $\sin^2\theta_L > 0.2$ are in strong tension with data, so we have deviced not to show any contour plots for those.

In Fig. 4.1, contour plots of $\delta(p_T^{\text{cut}})$ for $p_T^{\text{cut}} = 200$ GeV and $\sin^2\theta_L = 0.1$ are shown for singlet models. Similarly, with $\sin^2\theta_R = 0.1$, the contour plots of $\delta(p_T^{\text{cut}})$ are presented in Fig. 4.3 for fourplet models and for the same value of p_T^{cut}. The first thing

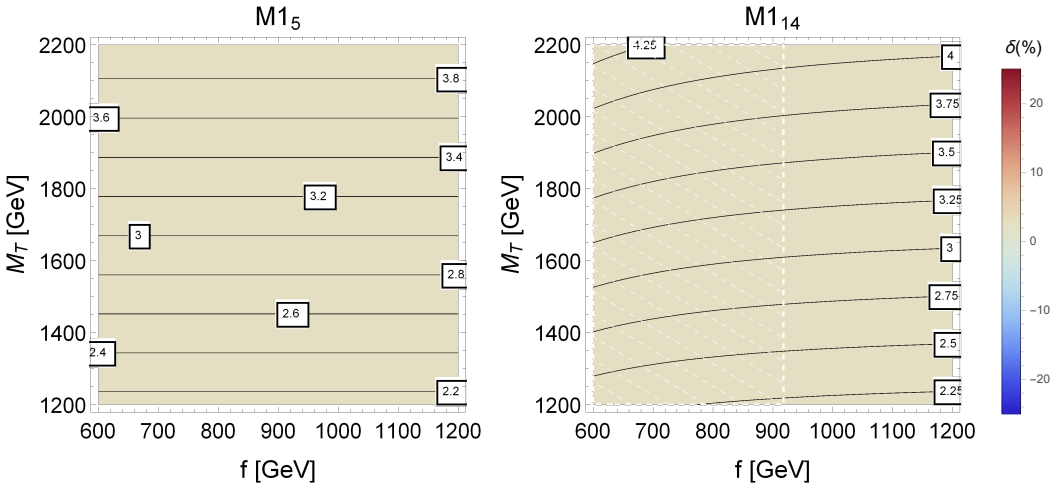

Figure 4.1: The contour plots of $\delta(p_T^{\text{cut}})$ with $\sin^2\theta_L = 0.1$ and $p_T^{\text{cut}} = 200$ GeV for each of the singlet models with only one top partner multiplet included in each of the models. The solid lines indicates constant values of the coupling y. The region marked by dashed white lines corresponds to the case where $\kappa_t \leq 0.8$.

that can be observed from these figures is that the deviation from the SM is not large. This arises from the fact that the spectrum of the integrated transverse momentum is dominated by the lowest p_T values, where the top still behaves as a heavy particle in loops. The cancellation between top and top partner contribution still has an effect in this range of p_T, and results in this small deviation. Nevertheless, the difference in the behaviour of the singlet (Fig. 4.1) and fourplet (Fig. 4.3) models can still be noticed. For singlet models, when the values of M_T is increased, the deviation from the SM slightly increases. For fourplet models, as the value of f is increased, the SM deviation increases. This behaviour appears because when the value of f is increased, the negative contributions from the Yukawa coupling depending on $\sin^2\theta_L$ and $\cos^2\theta_L$ are getting smaller. We denote here that, for $\mathbf{M4_{14}}$, when the value of f is small, these

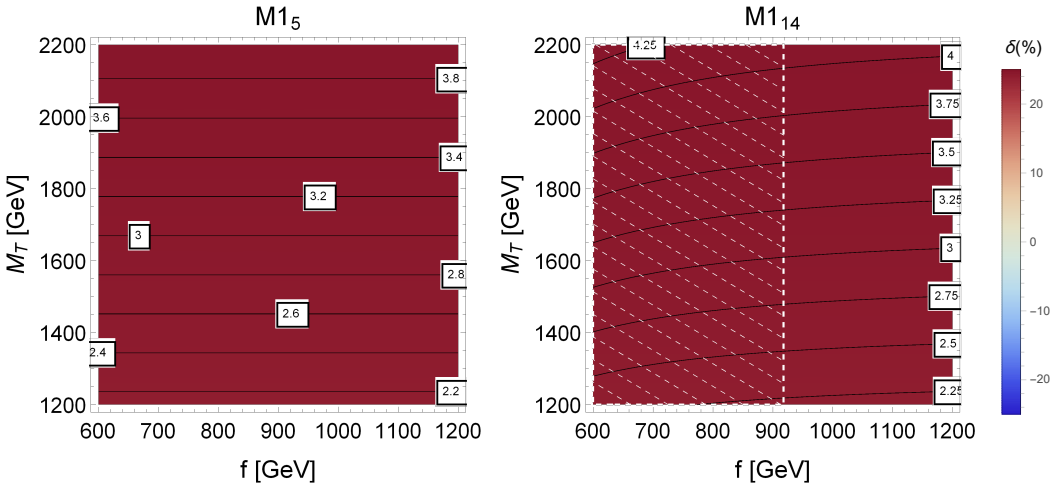

Figure 4.2: The contour plots of $\delta(p_T^{\rm cut})$ with $\sin^2\theta_L = 0.1$ and $p_T^{\rm cut} = 600$ GeV for each of the singlet models with only one top partner multiplet included in each of the models. The corresponding values of y are shown by the solid lines. The region marked by dashed white lines corresponds to the case where $\kappa_t \leq 0.8$.

negative contributions dominate, which in turn results in negative interference between the contribution of the top and the top partner. In both Figs. 4.1 and 4.3, and all remaining contour plots in this section, we include the solid lines indicating the fixed values of the parameter y, so that one can then determine if the corresponding choice of parameters correspond to a perturbative composite Higgs model. Recall that the value of y must fall in the range $y < 3$ due to the perturbativity requirement, it is possible to observe that one cannot legitimately probe M_T above 1600 GeV for singlet models. In the fouplet models, however, the range of parameters chosen here results in predictions that are almost always allowed by the perturbativity requirement.

Keeping the values of $\sin^2\theta_{L,R} = 0.1$ and increasing the value of $p_T^{\rm cut}$ to 600 GeV, we show the corresponding contour plots of $\delta(p_T^{\rm cut})$ as a function of M_T and f in Figs. 4.2 and 4.4. In this case, The values of p_T are high enough so that the cancellation between the contribution of a top and a top-partner in loops are broken. This results in large deviations from the SM for singlet models. For the fourplet models, we observe again that the deviation decreases when the value of f is decreased. This is again because of the fact that the negative contribution to the Yukawa couplings proportional to $\sin^2\theta_L$ and $\cos^2\theta_L$ becomes more relevant for small values of f, and eventually vanishes when $f \to \infty$. For $\mathbf{M4_{14}}$ model, the most significant features can be noticed when one look

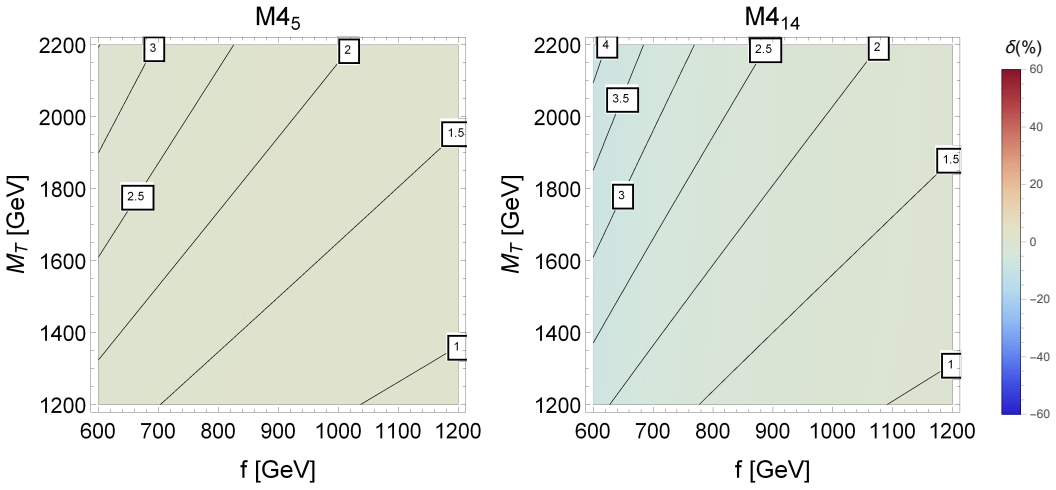

Figure 4.3: The contour plots of $\delta(p_T^{\rm cut})$ with $\sin^2\theta_R = 0.1$ and $p_T^{\rm cut} = 200$ GeV for each of the fourplet models with only one top partner multiplet included in each of the models. The solid lines indicates constant values of the coupling y. No parameter space on these plots corresponds to $\kappa_t \leq 0.8$.

small value of f. In this range of f, a large negative interference between top and top-partner contributions can be seen. Note that the contour plots show also a shaded region that corresponds to $\kappa_t < 0.8$, to highlight a region in parameter space that is in tension with current data for Higgs production in association with a top-antitop pair.

In order to have a full comparison with the results presented in [23], we should then repeat the same analysis for $\sin^2\theta_{L,R} = 0.4$. Unfortunately, in the singlet models, if $\sin^2\theta_L = 0.4$, it would result in the case that are not allowed by perturbative regime. We are then left with the choice to consider only fourplet models with $\sin^2\theta_R = 0.4$. With this value of $\sin^2\theta_R$, we show the contour plots with $p_T^{\rm cut} = 200\,\text{GeV}$ in Fig. 4.5. In this case, we again observe a moderate deviation form the SM, which occurs from the same reasons as the corresponding case where we set $\sin^2\theta_R = 0.1$. In addition, since $\sin^2\theta_R$ is set at a larger value, the negative contributions to the Yukawa couplings due to $\cos^2\theta_L$ and $\sin^2\theta_L$ become less important. Then, for fourplet model, we increase the value of $p_T^{\rm cut}$ to $600\,\text{GeV}$ while keeping the value of $\sin^2\theta_R = 0.4$, and show the corresponding contour plots in Fig. 4.6. The larger value of the mixing angle, $\sin^2 = 0.4$ prevents the negative contributions to take over. So, the top quark in the loops gives the contribution which is smaller than compared to the contribution from the top partner, giving a sizeable deviation from the SM.

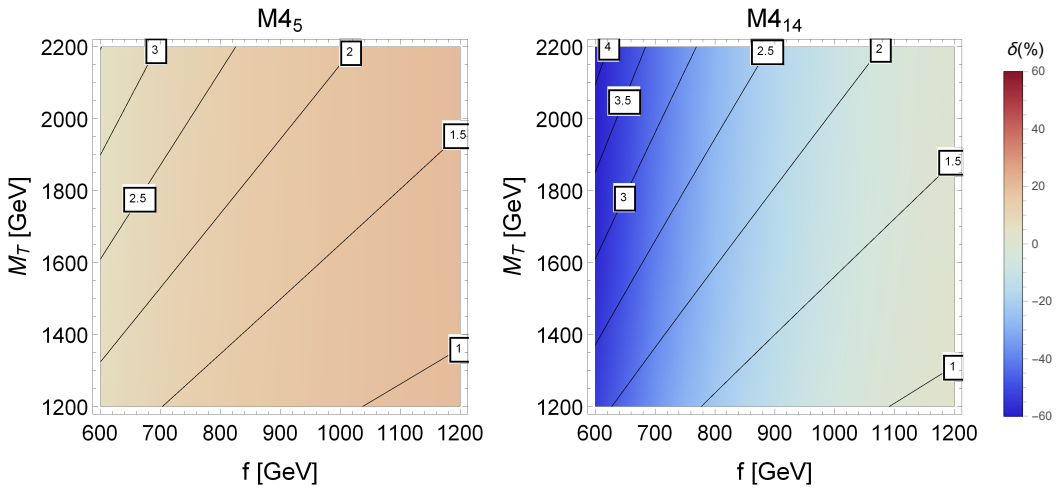

Figure 4.4: The contour plots of $\delta(p_T^{\rm cut})$ with $\sin^2\theta_R = 0.1$ and $p_T^{\rm cut} = 600$ GeV for each of the fourlet models with only one top partner multiplet included in each of the models. The corresponding values of y are shown by the solid lines. No parameter space on these plots corresponds to $\kappa_t \leq 0.8$.

The next thing to consider is the CP-odd contributions induced by the couplings $\tilde{\kappa_t}$ and $\tilde{\kappa_T}$ in Eq. (3.69), which exist only in the fourplet models. Since these contributions cannot interfere with the SM, their contribution to $\delta(p_T^{\rm cut})$ is very small, at sub-percent level for most of the choices of $\sin^2\theta_R$ considered in our work. There is an exception for $\sin^2 = 0.4$ with $p_T^{\rm cut} = 600$ GeV, for which the deviation from the SM is of a few percent. We show the corresponding contour plots in Fig. 4.7.

We also consider an extra example in the singlet models, with $\sin^2\theta_L = 0.025$, in order to have a better idea of the deviation one would expect from this type of models for acceptable values of the parameters. With this value of $\sin^2\theta_L$, we show the contour plots with $p_T^{\rm cut} = 200$ GeV in Fig. 4.8, and those with $p_T^{\rm cut} = 600$ GeV in Fig. 4.9. From comparison between these figures, it can be observed again that by increasing the value of $p_T^{\rm cut}$, the cancellation between the contribution from the top and top partner in the loop is overcome, and hence in Fig. 4.9 the deviation from the SM is more significant. In addition, we observe in both figures that the behaviour approaches that of the SM when the value of the compositeness scale f is increased.

To summarise this section, with one top partner there exist a variety of deviations from the SM, reflecting the different ways Yukawa couplings are modified according to the fundamental parameter of each model. In particular, in the singlet models, the

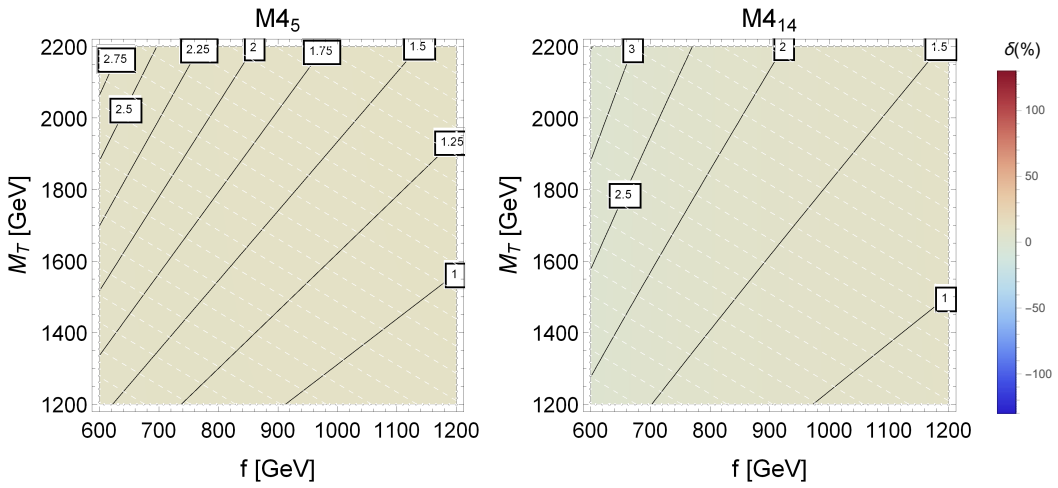

Figure 4.5: The contour plots of δ with $\sin^2\theta_R = 0.4$ and $p_T^{\text{cut}} = 200$ GeV for each of the fourplet models with only one top partner multiplet included in each of the models. The corresponding values of y are shown by the solid lines. As shown by the dashed white lines, all the points on these plots corresponds to $\kappa_t \leq 0.8$.

deviations from the SM can be huge even from a mild mixing of right-handed fermions. So, the parameters considered in these models will be the easiest to access through Higgs production in association with a jet. For fourplet models, the analysis must be carried on a case-by-case basis for each choice of the parameters because of non-trivial cancellations between different contributions to the Yukawa couplings. From the analysis presented in this section, it is promising though that one can expect to see sizeable deviations from the SM for large mixings angle with high values of p_T^{cut}.

4.3 Two top-partner multiplets

For the two top-partner case, we extend the analysis used in the case of one top partner by considering a number of benchmark scenarios, obtained by fixing some of the fundamental parameters of the theory as described in section 3.5, instead of varying the physical top partner mass M_T and the scale f. In the first three scenarios, we considered the cases where the CP-odd couplings $c_{1,1}$ and $c_{1,2}$ are both set to zero. Then, in the fourth scenario, the CP-odd couplings have non-zero values:

1. $y = 1$, $M_{\Psi_1} = 1200\,\text{GeV}$, $1300\,\text{GeV} < M_{\Psi_2} < 3000\,\text{GeV}$, $f = 800\,\text{GeV}$ (see Figs. 3.2, 3.1).

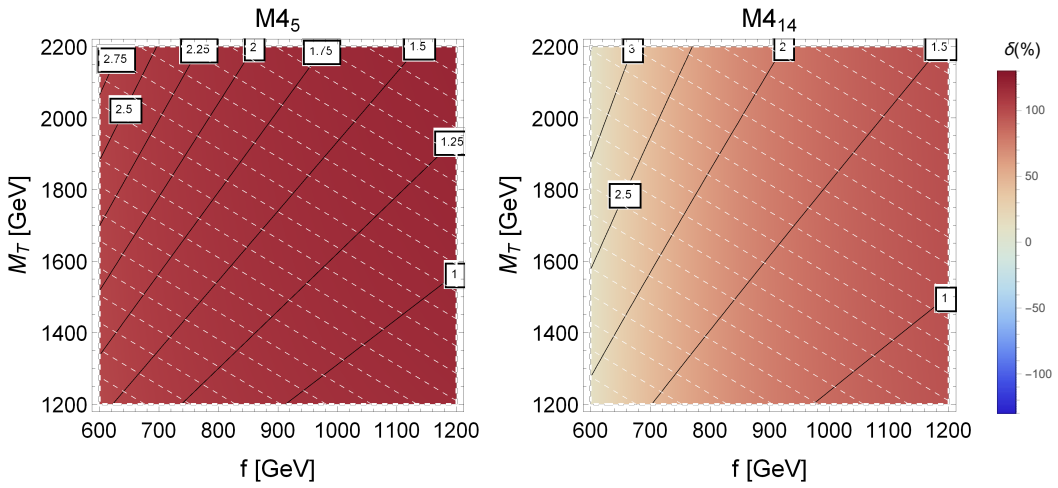

Figure 4.6: The contour plots for δ with $\sin^2\theta_R = 0.4$ and $p_T^{\rm cut} = 600$ GeV for each of the fourplet models with only one top partner multiplet included in each of the models. The corresponding values of y are shown by the solid lines. As shown by the dashed white lines, all points on these plots corresponds to $\kappa_t \leq 0.8$.

2. $0.5 < y < 3$, $M_{\Psi_1} = 1200\,\text{GeV}$, $M_{\Psi_2} = 1300\,\text{GeV}$, $f = 800\,\text{GeV}$ (see Fig. 3.3) (fourplet models only).

3. $y = 1$, $M_{\Psi_1} = 1200\,\text{GeV}$, $M_{\Psi_2} = 1300\,\text{GeV}$, $800\,\text{GeV} < f < 2000\,\text{GeV}$ (see Figs. 3.5, 3.4).

4. $y = 2$, $M_{\Psi_1} = 1200\,\text{GeV}$, $M_{\Psi_2} = 1300\,\text{GeV}$, $800\,\text{GeV} < f < 1400\,\text{GeV}$, $c_{1,1} = c_{1,2} = 0.2i$ (see Figs. 3.6 and 3.7).

From all these scenarios, the deviation from SM $\delta\,(p_T^{\rm cut})$ are plotted as a function of $p_T^{\rm cut}$, for the selected values of the parameters that are varied in these scenarios.

In benchmark 1, we investigate the impact of varying the mass parameter of the top partner multiplet M_{Ψ_2}, from the case in which this parameter is quasi-degenerate with the mass M_{Ψ_1} to the case which $M_{\Psi_2} \gg M_{\Psi_1}$, where the second top partner is decoupled from the theory. In this scenario, the compositeness scale is set to the value $f = 800$ GeV, which is an intermediate value between the two chosen in Figs. 3.1, 3.2. From the data files computed in this scenario, we plot the deviation from the SM $\delta\,(p_T^{\rm cut})$ as a function of $p_T^{\rm cut}$ in Figure 4.10, for selected values of M_{Ψ_2} (the solid curves). In the same figure, we also include the plots for the case where there is only one top partner in the model (the dashed curve), with the same value of y and $M_\Psi = M_{\Psi_1}$ and $f = 800$

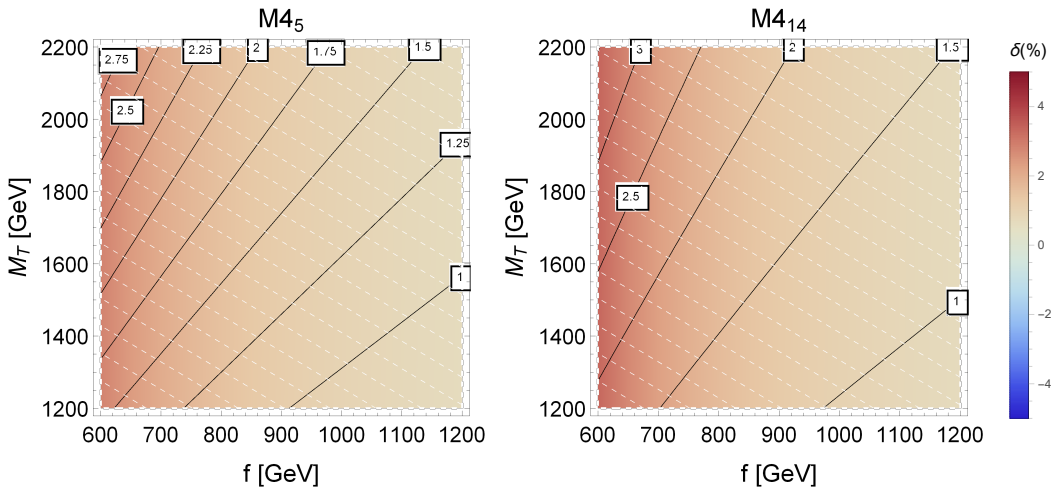

Figure 4.7: The contour plots of the contribution to δ with $\sin^2\theta_R = 0.4$ and $p_T^{\rm cut} = 600$ GeV for each of the fourplet models with only one top partner multiplet included in each of the models. In this figure, only the CP-odd Yukawa coupling is taken into account. The corresponding values of y are shown by the solid lines. As shown by the dashed white lines, all points on these plots corresponds to $\kappa_t \leq 0.8$.

GeV. In this figure, we can see that there is an enhancement in the with respect to the SM for singlet models, while there is a depletion, due to negative interference, for the fourplet models. The dependence on M_{Ψ_2} is appreciable in all of the models, which is in accordance with the behaviour of the Yukawa coupling shown in Fig. 3.1. As the value of M_{Ψ_2} gets bigger the deviation approaches that with the single top partner, since the heavier top-partner is decoupled from the models. This is also expected from Figs. 3.1 and 3.2, where we can see that as the value of M_{Ψ_2} is increased the masses and couplings of the lighter top partner tend to those of the models with only one top partner multiplet.

In benchmark 2, we investigate the effect of varying the parameter y in models with two top partner, occurring as a result of including two top partner multiplets with similar masses, which is plotted as the solid curves in Fig. 4.11. Again, in the same figure, we also include the corresponding curves for the same models with one top partner only (the dashed curves) with $M_\Psi = M_{\Psi_1}$. Since the experimental constraint $\kappa_t > 0.8$ forces the value of y to be less than one in singlet models, we presented in Fig. 4.11 the results for fourplet models only, where y is allowed to take a larger value. A variety of features are present in this case. For $\mathbf{M4_5}$, the transverse momentum

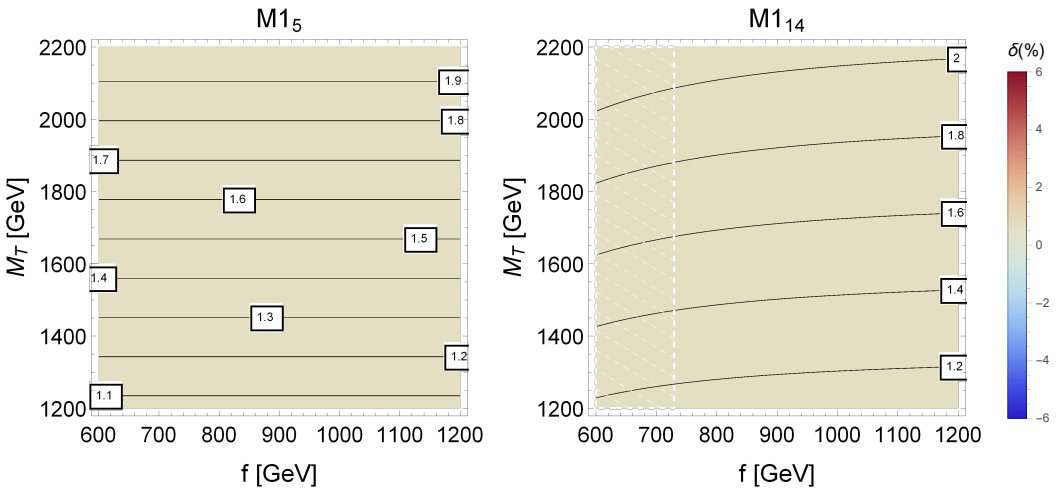

Figure 4.8: The contour plots of $\delta(p_T^{\rm cut})$ with $\sin^2\theta_L = 0.025$ and $p_T^{\rm cut} = 200$ GeV for the singlet models with only one top partner multiplet included in each of the models. The corresponding values of y are shown by the solid lines. The region marked by dashed white lines corresponds to the case where $\kappa_t \leq 0.8$.

distribution is suppressed in comparison to that of the SM because of a persistent negative interference between the top and top-partner contributions, as can be seen in Fig. 3.3. In $\mathbf{M4_{14}}$, negative interference is only dominant when the value y is not too large. When y and $p_T^{\rm cut}$ are increased, the interference can become as large as the contribution of the SM. So, in this range of parameters, the amplitude square of the heavier top partner dominates, as can be understood from considering Eq. (4.18). This results in the positive values of $\delta\left(p_T^{\rm cut}\right)$ at large $p_T^{\rm cut}$.

In benchmark 3, we investigate the impact of varying the compositeness scale f in the case where in the models there are two quasi-degenerate vector-like quarks (the solid lines in Fig. 4.12) and where there is only a top partner with $M_\Psi = M_{\Psi_1}$ in the model (the dashed lines in Fig. 4.12). As shown in section 3.5, in this situation the heavier top partner can have a larger anomalous Yukawa coupling than that of the lighter top partner. For each of the models considered in our study, $\delta\left(p_T^{\rm cut}\right)$ is plotted as a function of $p_T^{\rm cut}$ for some selected values of f. In the singlet models, the values of the parameters considered in this benchmark lead to the SM deviation that are not too big, and are largely independent of the f scale. This is what one would expect from looking at the upper panel of Figs. 3.1, where there is a small different in Yukawa coupling when varying the compositeness scale for singlet models. We would like to

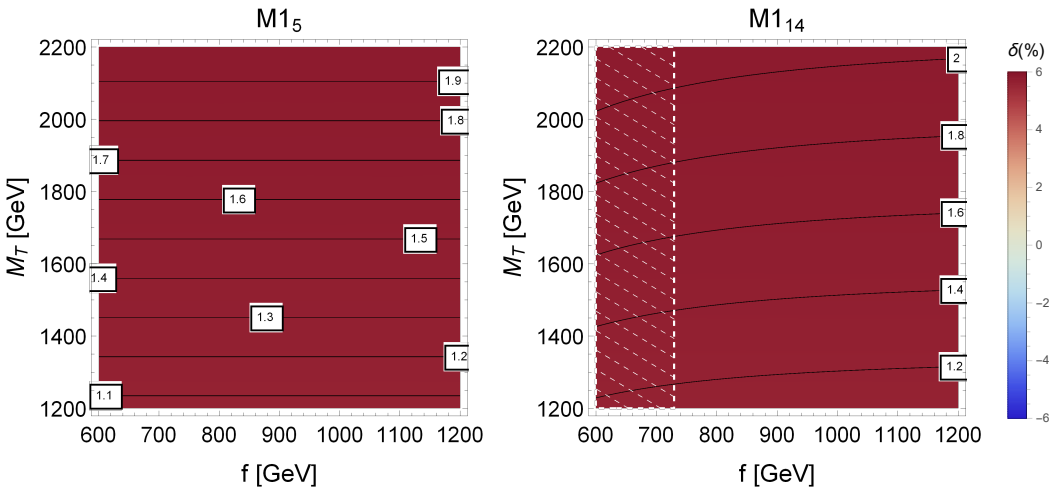

Figure 4.9: The contour plots of $\delta(p_T^{\rm cut})$ with $\sin^2\theta_L = 0.025$ and $p_T^{\rm cut} = 600$ GeV for the singlet models with only one top partner multiplet included in each of the models. The corresponding values of y are shown by the solid lines. The region marked by dashed white lines corresponds to the case where $\kappa_t \leq 0.8$.

denote that we also observe the same behaviour in the one top partner case as shown in Figs. 4.1 and 4.2 for the singlet models. For the two top-partner case, the deviations from the SM are approximately twice as large as that of the case where there is only a single top partner in the models because the Yukawa couplings of both top partners are close to the one top-partner case for the parameters selected here. For fourplets models, the situation is more interesting since we observe negative deviations from the SM results in both $\mathbf{M4_5}$ and $\mathbf{M4_{14}}$ models. This negative deviation can be understood when one considers the negative values of the Yukawa couplings in the fourplet models in Figs. 3.1. For $\mathbf{M4_5}$ model, the deviation from the SM result is not large, but it is strongly dependent on the compositeness scale, which can be inferred from considering the left panel of Fig. 3.4. In this case, it can be seen that the deviation from the SM reaches zero when the scale f is equal to the value of the mass parameter M_{Ψ_1}, before becoming positive for larger f scale. A strong dependence on f can also be appreciated in $\mathbf{M4_{14}}$ because of the fact that for smaller value of the compositeness scale f the negative anomalous Yukawa couplings are larger.

Lastly, benchmark 4 investigates the impact of the CP-odd contributions in the models $\mathbf{M4_5}$ and $\mathbf{M4_{14}}$. As the case where we have one top partner in the models, only the ratio between the CP-odd contribution and the SM result is plotted (the solid

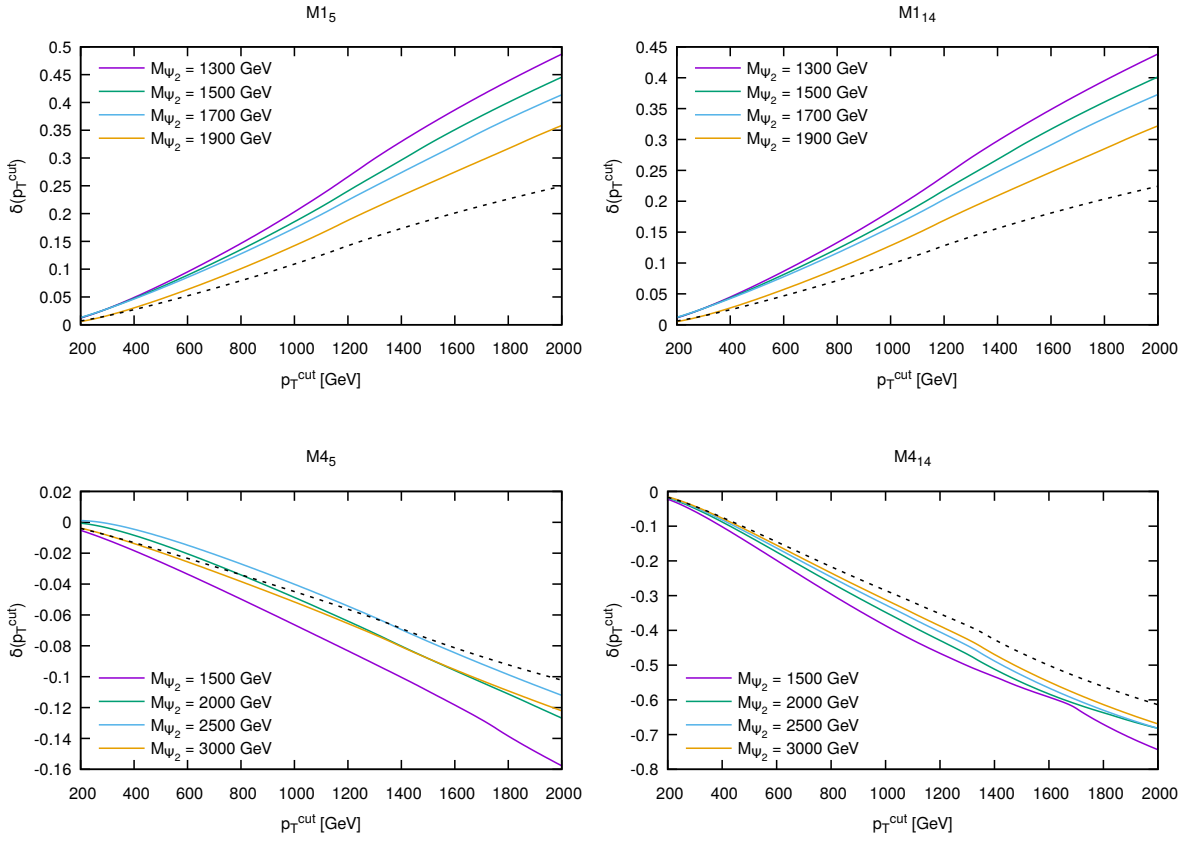

Figure 4.10: The distribution of $\delta(p_T^{\text{cut}})$ computed from the data files generated with the parameters in benchmark scenario 1 and the four models considered in section 3.5.

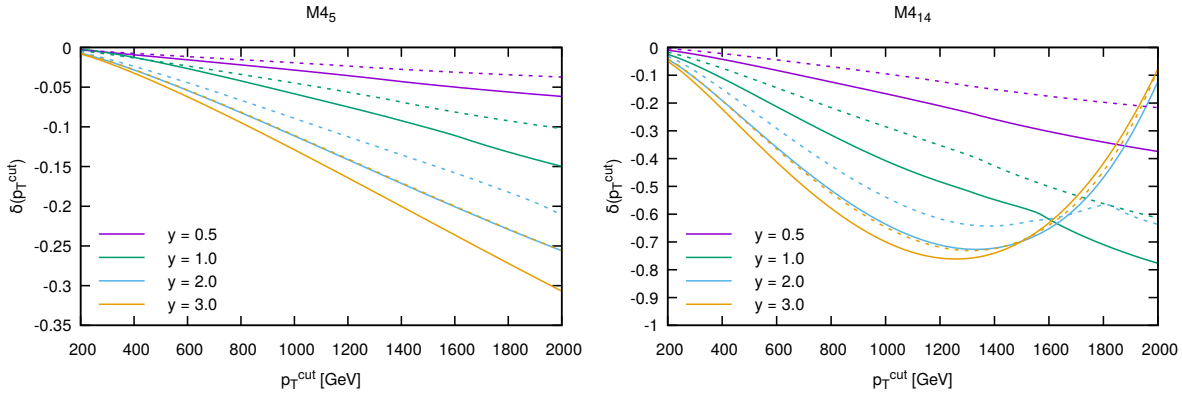

Figure 4.11: The distribution of $\delta(p_T^{\text{cut}})$ computed from the data files generated with the parameters in benchmark scenario 2 and the fourplet models considered in section 3.5.

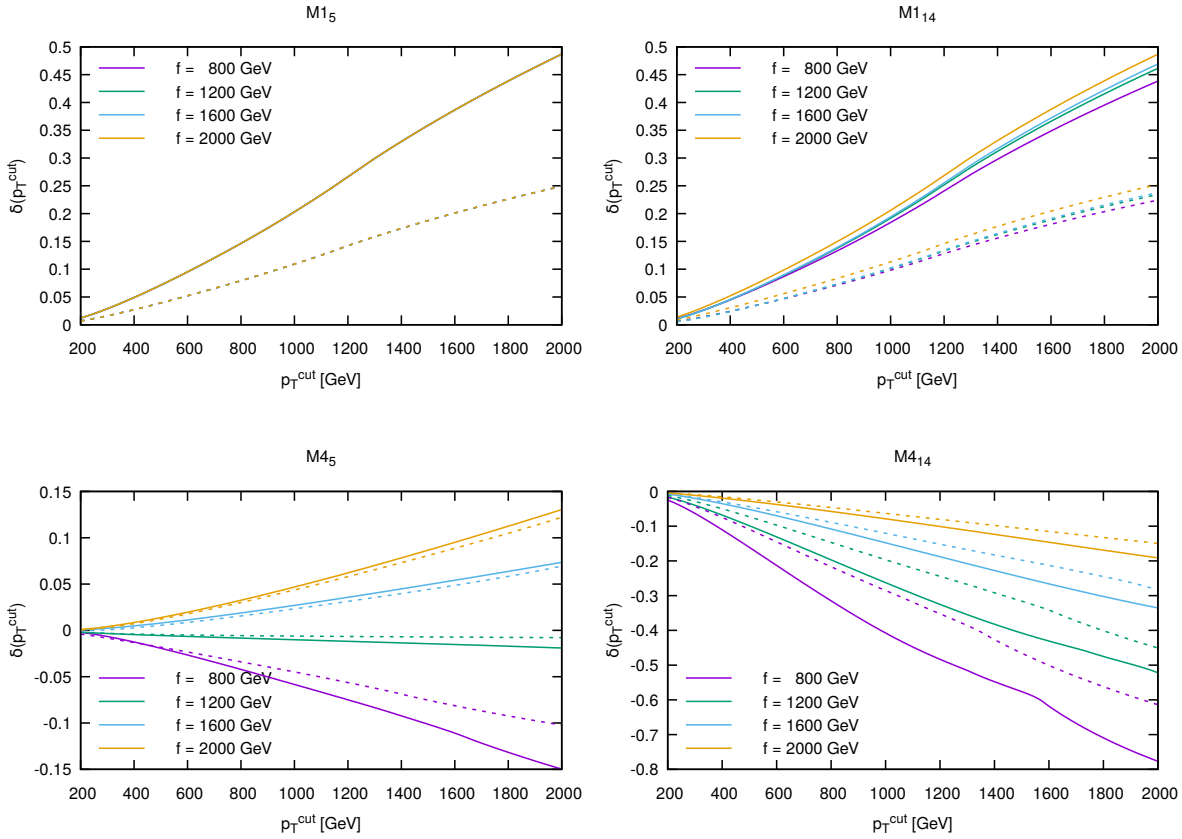

Figure 4.12: The distribution of $\delta(p_T^{\text{cut}})$ computed from the data files in benchmark scenario 3 and the four models considered in section 3.5.

curves in Fig. 4.13), since there is no interference between the CP-odd terms and the SM amplitude. In Fig. 4.13, we also include the plot for one top partner case for the same value of y and $M_\Psi = M_{\Psi_1}$ (the dashed curves in Fig. 4.13). For both of these models,

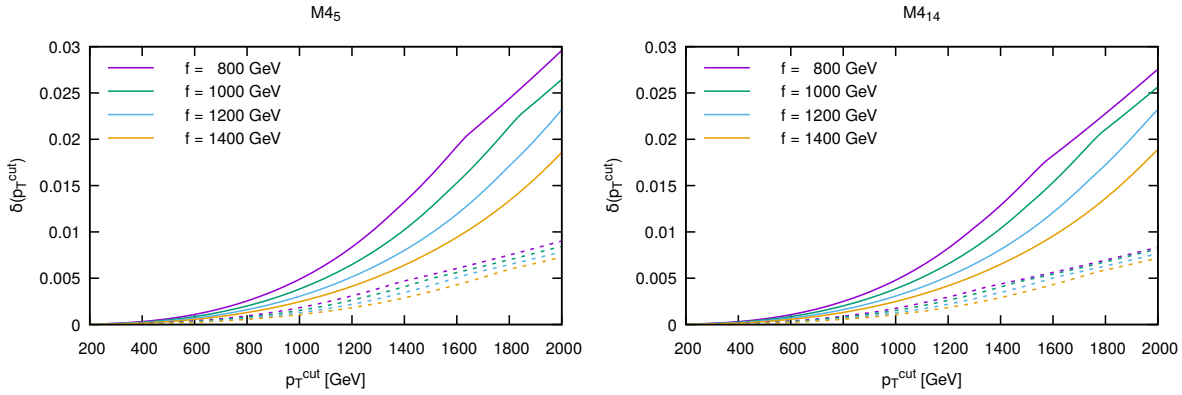

Figure 4.13: The distribution of $\delta(p_T^{\text{cut}})$ computed from the data files generated with the parameters in benchmark scenario 4 and the fourplet models considered in section 3.5.

the expected deviation from the SM are less than 10%, which is rather small, for the whole range of the considered values of p_T^{cut}, with the deviations in $\mathbf{M4_{14}}$ are slightly larger than those of the $\mathbf{M4_5}$. One remarkable feature one can see in Fig. 4.13 is that, the deviations are roughly two times as big in the two top partner case compared to the one top-partner case, which can also be appreciated from inspection on Fig. 3.7. This is a peculiar feature that arises from the fact that the values of the masses parameters M_{Ψ_1} and M_{Ψ_2} are very close in this benchmark scenario. If the value of the larger mass (M_{Ψ_2} in this case) increases, the CP-odd Yukawa coupling of the lighter mass (M_{Ψ_2} in this case) approaches that of the case with a single top partner. To better understand this effect, one would need to observe how the CP-odd coupling vary with the underlying parameters in the models as shown in Figs. 3.6 and 3.7, where the CP-odd couplings in the case with two top-partner are significantly larger than in the one top-partner case for the selected values of the parameters in Fig. 4.13.

To summarise, there is a variety of deviations from the SM in the p_T spectrum of the Higgs boson or a jet exhibited by models with two top partners. From the fact that the deviation shows strong dependency on p_T^{cut}, it is implied that a shape analysis of the p_T distribution is the best way to exclude large fractions of parameter space for composite Higgs models. In order to make the most use of such analysis, it is required to develop an appropriate model of the irreducible SM background to Higgs production, including

detailed acceptance cuts and experimental systematic uncertainties for the Higgs decay products. Though this is very interesting topic, it is beyond the scope of the work carried out in this thesis.

We would like to mention here that there is yet any measurement on the $\delta\left(p_T^{\rm cut}\right)$. Instead, the information that one could gain from the current experimental data is that of the $\frac{d\sigma}{dp_T}$ distribution. The measurement cross section with $P_T > 200$ GeV with an integrated luminosity around 80 fb^{-1} at $\sqrt{s}$ =13 TeV [48, 49] seems to suggest at most a deviation of 20%. So, it would be safe to exclude the results present in this chapter where the percentage of $\delta\left(p_T^{\rm cut}\right)$ was greater than 20%. However, we need to keep in mind that the data of refs. [48, 49] correspond to Higgs decaying in two photons and a pair of Z bosons. Our analysis only consider modifications to the production cross section, and not to the Higgs decays. Therefore, any constraints from those data has to be taken with a grain of salt.

The results presented in this chapter has been involved only with indirect searches on top partner, as a complement to most of the results presented in literatures that focus on the direct search for top partner (see for instance ref. [50] and some of the references therein). As mentioned in Chapter 1, the direct searches for top partner depends on the model used to determine the decay channels the search will be focussed on, and knowledge on the background processes involved. On the other hand, in our study, even though the investigation has been concentrated on specific models, the methods discussed in this thesis should be applicable on a model independent basis. In addition, the result presented here are carried out on a more concrete perturbative composite-Higgs models than those studied in the literature, e.g. in Ref [23]. Including a second top partner in each of the models also lead to a variety of deviations from the SM, especially in the case of two quasi-degenerate top-partner masses.

We conclude with some very simplified arguments on the potential of increasing luminosity in LHC experiments to exclude the models considered in this thesis. First, in order to make use of our results, we need that at least one event could be detected. For a physical process, the expected number of events can be calculated from the relation

$$\sigma\mathcal{L} = N\,, \tag{4.25}$$

where σ is used to denote the total cross-section of the physical process, $\mathcal{L}$ denotes the integrated luminosity and N denote the number of expected events. From this relation,

we construct the significance parameter [51]

$$\text{Significance} = \frac{S}{\sqrt{B}}\,. \tag{4.26}$$

where S is used to denote the expected number of signal events, which in our case, it is the $h+\text{jet}$ in the composite-Higgs scenario, and B is used to denote the expected number of background, i.e. SM Higgs plus one jet and the corresponding irreducible background. In Eq. (4.26), S is defined as

$$S = \left(\sigma_{\rm BSM}(p_T^{\rm cut}) - \sigma_{\rm SM}(p_T^{\rm cut})\right)\mathcal{L} \tag{4.27}$$

where $\sigma_{\rm BSM}(p_T^{\rm cut})$ is the $h+\text{jet}$ total cross section computed in our composite Higgs scenario and $\sigma_{\rm SM}(p_T^{\rm cut})$ is the cross section of the Higgs plus jet production computed in the SM. B is defined as

$$B = (\sigma_{\rm SM}(p_T^{\rm cut}) + \sigma_{\rm B}(p_T^{\rm cut})\mathcal{L} \simeq \sigma_{\rm B}(p_T^{\rm cut})\mathcal{L}\,. \tag{4.28}$$

where $\sigma_{\rm B}(p_T^{\rm cut})$ denotes the cross section for all the processes that give an irreducible background to Higgs production. Eq. (4.26) can used to determine the probability to find the signal event of $h+\text{jet}$ process from the populated background events in the LHC. Focusing on the decay $h \to \gamma\gamma$, with an integrated luminosity of 3000 ab^{-1}, we obtain at most one event for $p_T^{\rm cut}$ around 1 TeV. At the moment, the efficiency in eq. (4.23) is not measured. Nevertheless, we can still ask what relative deviations from the SM could be appreciated, using the integrated p_T distribution. In particular, we can consider the relative deviation with respect to the SM, as follows

$$\delta_{\rm BSM}(p_T^{\rm cut}) \equiv \frac{\sigma_{\rm BSM}(p_T^{\rm cut}) - \sigma_{\rm SM}(p_T^{\rm cut})}{\sqrt{\sigma_{\rm SM}(p_T^{\rm cut})}}\,. \tag{4.29}$$

In term of this quantity, the significance in Eq. (4.26) can be rewritten in the form

$$\text{Significance} = \delta_{\rm BSM}(p_T^{\rm cut})\frac{\sigma_{\rm SM}(p_T^{\rm cut})}{\sqrt{\sigma_{\rm B}(p_T^{\rm cut})}}\sqrt{\mathcal{L}}\,. \tag{4.30}$$

By convention, a given BSM scenario is excluded if the significance is bigger than 2. This gives that, with an integrated luminosity $\mathcal{L}$, we can probe values of $\delta_{\rm BSM}(p_T^{\rm cut})$ as large as $2\sqrt{\sigma_{\rm B}/\mathcal{L}}/\sigma_{\rm SM}$. This depends crucially on the value of $\sigma_{\rm B}$, which has to be made as small as possible, but still much larger than $\sigma_{\rm SM}$. Such an analysis requires a detailed study of the backgrounds to Higgs production with appropriate acceptance cuts, and is beyond the scope of the present thesis.

Chapter 5

Conclusions

The purpose of this thesis is to investigate the effect of including one or two top-partner multiplets in composite-Higgs models, where the Higgs boson is a bound state of a strong sector rather than an elementary particle, to the distributions of transverse momentum of the jet radiated in Higgs production in association with a jet. This study can lead to an effective way to probing the compositness of the Higgs. If the p_T distribution of the jet (or Higgs) produced in the Higgs plus jet production shows sensitivity to the top-partner masses, this is expected to be a good indication that the Higgs is not an elementary particle, but instead a composite particle.

After the discussion on basic structure of a general composite Higgs model, including how this particle occur out of the symmetry breaking pattern of the model, in chapter 2, we then discuss, in chapter 3, the structure of the models studied in our work, and the procedure to diagonalise the matrices and obtain the Yukawa couplings, both in the generic case where there is only one top partner multiplet in the model and the case where we include two top partner multiplets in the models. These models are based on the work in ref. [24], where the top partner multiplets are categorised in either the singlet or fourplet representation of $SO(4)$ and the right-handed top quark is a totally composite particle arising from the strong sector. From these models, we derive the analytical formulae of the Yukawa couplings of the top and top partner in the situation where we have one top partner multiplet in each of the models. These formulae are expressed in terms of the mixing angles θ_L and θ_R used to diagonalise the mass matrices in the theory. In contrast to the similar analysis presented in Ref. [23], we find that in the singlet model the anomalous couplings of both the top and the top partner are dependent on θ_L instead of θ_R, and in the fourplet models the anomalous couplings of both types of the quarks are functions of both θ_L and θ_R. Also, as a result of assuming

that the top partner is a totally composite quark, we find, in the fourplet models, CP-odd Yukawa couplings for both top quark and top partner, and we compute their analytical forms in terms of the mixing angles. For the case where there are two top partner multiplets in the models, the fundamental parameters of the models are varied to see how the masses and couplings to the Higgs of the top and top partners respond to this change. Various features arise, the most intersting is the fact that, when the two top partners have similar masses, the heavier top-partner can have a larger coupling to the Higgs than the lighter top-partner. When the difference between the mass parameters of the two top partner multiplets gets larger, the heavier top partner begins to decouple from the Higgs.

After discussing the argument stated in ref. [23] that in the Higgs production in association with one jet, the presence of a top partner induces deviation from the SM in the transverse momentum distribution of either the Higgs or the jet, we then prove this point in the situation where a single top partner multiplet in both representations is included in the theory by presenting contours plots of the parameter $\delta(p_T^{\text{cut}})$, related to the integrated p_T distribution down to a lower bound p_T^{cut}, as a function of the physical top partner mass M_T and the compositeness scale f. The contours plots are presented for different values of $\sin^2\theta_R$ and p_T^{cut} for the singlet models discussed in chapter 3 and for different values of $\sin^2\theta_L$ for the fourplet models discussed in the same chapter. It is found that for the singlet models the deviation from the SM is huge, even for small values of $\sin^2\theta_R$. Increasing the value of the p_T^{cut} leads to a huge deviation from the SM in these models. For the model with the top-partners in the **4**, the difference from the SM p_T spectrum must be analysed on a case-to-case basis, with the highest values for both $\sin^2\theta_L$ and p_T^{cut} giving the most promising deviation from the SM.

For the situation where we have two top partner multiplets in the models, we studied the deviation from the SM as a function of p_T^{cut}. We find a variety of deviations from the SM, but the fact that all plots show strong dependence on p_T^{cut} suggests that an analysis on p_T distribution gives promise to exclude large fractions of parameter space for composite Higgs models.

We believe that a shape analysis of the Higgs transverse momentum spectrum is the best observable to probe masses and couplings of top partners. Moreover, if one normalises this quantity to the total cross section, it will be possible to disentangle also the effect of the compositeness scale resulting in a trivial change in normalisation of the spectrum. Assessing whether this is feasible or not with present or future

colliders requires a careful analysis of the ireducible background to Higgs production. This is beyond the scope of this thesis, but opens the way to many interesting further phenomenological studies.

Appendix A

An alternative method for deriving the CP-odd Higgs couplings

We would like to present an alternative method for deriving the CP-odd Higgs couplings from the mixing in Eq. (3.42). The starting point of this procedure is to rotate the $\bar{T}_R$ and $(\bar{X}_{2/3})_R$ states to the mass eigenstates with the rotations used to diagonalise the mass matrix in each of the models. Substituting Eq. (3.44) on Eq. (3.42), we first arrive at

$$ic_1[(\bar{X}_{2/3})_R - \bar{T}_R]\frac{\not{\partial}\rho}{f}t_R = ic_1[(\bar{X'}_{2/3})_R - \bar{T'}_R\frac{2c_\epsilon}{N}]\frac{\not{\partial}\rho}{f}t_R\,. \tag{A.1}$$

Using then Eq. (3.46), we are then left with

$$ic_1[(\bar{X}_{2/3})_R - \bar{T}_R]\frac{\not{\partial}\rho}{f}t_R = ic_1\cos\theta_R\sin\theta_R\frac{2c_\epsilon}{N}\bar{T}''_R\frac{\not{\partial}\rho}{f}T''_R - ic_1\cos\theta_R\sin\theta_R\frac{2c_\epsilon}{N}\bar{t}''_R\frac{\not{\partial}\rho}{f}t''_R + \dots\,. \tag{A.2}$$

We show here only the relevant terms for the Higgs plus jet production since the other terms will involve mixing between two different right-handed states and those cannot participate in fermion loops contributing to the process. From this expression, we could expect that these terms will interfere with all other terms in the theory that involve only the same species of the right-handed fields. Before rotating to the eigenstates, the terms in the original Lagrangian involving only the right-handed states are

$$ic_1\bar{\Psi}^{\mathbf{4}}_R d_\mu\gamma^\mu t_R + i\bar{t}_R\not{\partial}t_R + i\bar{T}_R\not{\partial}T_R + i\bar{X}_{2/3R}\not{\partial}X_{2/3R} + \text{ h.c.} \tag{A.3}$$

The kinetic terms of all the right handed fields are invariant under the rotation to the mass eigenstates, i.e.

$$i\bar{t}_R\not{\partial}t_R + i\bar{T}_R\not{\partial}T_R + i\bar{X}_{2/3R}\not{\partial}X_{2/3R} = i\bar{t}''_R\not{\partial}t''_R + i\bar{T}''_R\not{\partial}T''_R + i\bar{X}''_{2/3R}\not{\partial}X''_{2/3R}\,, \tag{A.4}$$

so their contributions can be handled straightforwardly. Let us consider $ic_1\bar{\Psi}^{\mathbf{4}}_R d_\mu \gamma^\mu t_R$ and its hermitian conjugate term. Their contributions read

$$\begin{aligned}&\left(ic_1 - ic_1^\dagger\right)\left(\cos\theta_R \sin\theta_R \frac{2c_\epsilon}{N}\left(\bar{T}''_R \frac{\not{\partial}\rho}{f} T''_R - \bar{t}''_R \frac{\not{\partial}\rho}{f} t''_R\right)\right)\\ &= 2\,\mathrm{Im}(c_1)\left(\cos\theta_R \sin\theta_R \frac{2c_\epsilon}{N}\left(\bar{t}''_R \frac{\not{\partial}\rho}{f} t''_R - \bar{T}''_R \frac{\not{\partial}\rho}{f} T''_R\right)\right).\end{aligned} \tag{A.5}$$

Then, in order to analyse how the terms in Eq. (A.3) combine with one another we act on the contribution in Eq. (A.5) with a field redefinition

$$t''_R \to (1 + \frac{\tilde{c}\rho}{f}) t''_R\,, \tag{A.6}$$

where $\tilde{c}$ is a complex constant to be defined. This leaves us with

$$\begin{aligned}&2\,\mathrm{Im}(c_1)\cos\theta_R \sin\theta_R \frac{2c_\epsilon}{N}\left(\left(1 + \tilde{c}^\dagger \frac{\rho}{f}\right)\bar{t}''_R \frac{\not{\partial}\rho}{f}\left(1 + \tilde{c}\frac{\rho}{f}\right) t''_R - \bar{T}''_R \frac{\not{\partial}\rho}{f} T''_R\right)\\ &= 2\,\mathrm{Im}(c_1)\cos\theta_R \sin\theta_R \frac{2c_\epsilon}{N}\left(\bar{t}''_R \frac{\not{\partial}\rho}{f} t''_R - \bar{T}''_R \frac{\not{\partial}\rho}{f} T''_R\right) + \dots\,,\end{aligned} \tag{A.7}$$

where we neglect higher order terms in ρ since only terms with single Higgs field contribute to the Higgs production process in association with a jet. At the lowest power in ρ, this field redefinition does not change any contributions from the terms in Eq. (A.5). However, once this redefinition is applied on $i\bar{t}''_R \not{\partial} t''_R$, we obtain

$$\begin{aligned}&i\bar{t}''_R \not{\partial} t''_R \to i\left(\bar{t}''_R + \frac{\tilde{c}^\dagger\rho}{f}\bar{t}''_R\right)\not{\partial}\left(t''_R + \tilde{c}\frac{\rho}{f} t''_R\right)\\ &= i\bar{t}''_R \not{\partial} t''_R + i\bar{t}''_R \not{\partial}\left(\tilde{c}\frac{\rho}{f} t''_R\right) + i\frac{\tilde{c}^\dagger\rho}{f}\bar{t}''_R \not{\partial} t''_R + \mathcal{O}\left(\rho^2\right).\end{aligned} \tag{A.8}$$

From this expression, only the second and third terms could contribute to the Higgs plus jet production process since they are the only terms containing a single Higgs field. They are the only terms that can participate in the fermion loop of the process. Unlike in Eq. (A.7), the terms with a single Higgs field contain either a factor of $\tilde{c}$ or $\tilde{c}^\dagger$. Carrying out integration by parts on the second and third terms of the last line in Eq. (A.8), we obtain

$$i\bar{t}''_R \not{\partial}\left(\tilde{c}\frac{\rho}{f} t''_R\right) + i\frac{\tilde{c}^\dagger\rho}{f}\bar{t}''_R \not{\partial} t''_R = -i\left(\partial_\mu \bar{t}''_R\right)\gamma^\mu \frac{\tilde{c}\rho}{f} t''_R - i\left(\partial_\mu\left(\frac{\tilde{c}^\dagger\rho}{f}\bar{t}''_R\right)\right)\gamma^\mu t''_R\,. \tag{A.9}$$

If we then use the product rule on the second term of this expression, we obtain

$$-i\left(\partial_\mu \bar{t}''_R\right)\gamma^\mu \frac{\tilde{c}\rho}{f} t''_R - i\left(\partial_\mu \bar{t}''_R\right)\frac{\tilde{c}^\dagger\rho}{f}\gamma^\mu t''_R - i\bar{t}''_R \frac{\tilde{c}^\dagger \not{\partial}\rho}{f} t''_R\,. \tag{A.10}$$

Then, if we set $\tilde{c} = -\tilde{c}^\dagger$, we are left with only the $-i\bar{t}''_R \frac{\tilde{c}^\dagger \not{\partial}\rho}{f} t''_R$ term. This term can cancel the first term in the last line of the Eq. (A.7) by setting

$$\tilde{c} = -\tilde{c}^\dagger = 4i \,\mathrm{Im}(c_1) \cos\theta_R \sin\theta_R \frac{c_\epsilon}{N}. \tag{A.11}$$

We use the same trick on the top partner field, i.e. with another field redefinition

$$T''_R \to (1 + \frac{\tilde{c}_2 \rho}{f}) T''_R \tag{A.12}$$

where $\tilde{c}_2$ is a complex constant. If we go back to the Eq. (A.7), the effect of this field redefinition on last expression in this equation is

$$\begin{aligned} &2\,\mathrm{Im}(c_1) \cos\theta_R \sin\theta_R \frac{2c_\epsilon}{N} \left(\bar{t}''_R \frac{\not{\partial}\rho}{f} t''_R - \left(\bar{T}''_R + \frac{\tilde{c}_2^\dagger \rho}{f} \bar{T}''_R \right) \frac{\not{\partial}\rho}{f} \left(T''_R + \frac{\tilde{c}_2 \rho}{f} T''_R \right) \right) + \dots \\ &\qquad = 2\,\mathrm{Im}(c_1) \cos\theta_R \sin\theta_R \frac{2c_\epsilon}{N} \left(\bar{t}''_R \frac{\not{\partial}\rho}{f} t''_R - \bar{T}''_R \frac{\not{\partial}\rho}{f} T''_R \right) + \dots \,, \end{aligned} \tag{A.13}$$

which, similarly to the field redefinition in Eq. (A.6), does not change the contribution from the terms with one Higgs derivative. We can then perform this field redefinition on $i\bar{T}''_R \not{\partial} T''_R$ in the same way we applied Eq. (A.6) to the $i\bar{t}''_R \not{\partial} t''_R$. In this case, however, the terms involving one Higgs field emerging from the top partner kinetic will be able to cancel out the second term in the last line of Eq. (A.13) only if we set

$$\tilde{c}_2 = -\tilde{c}_2^\dagger = -4i \,\mathrm{Im}(c_1) \cos\theta_R \sin\theta_R \frac{c_\epsilon}{N} \,. \tag{A.14}$$

At the level of one Higgs field, the contributions from every terms in Eq. (A.3) cancel each other out, and it might seem to be the case that the c_1 parameter does not have any effect on the Higgs plus jet production at hand. However, we must also perform the field redefinitons in Eqs. (A.6) and (A.12) on the mass terms of the mass eigenstates. For the top mass eigenstate, the effect of the field redefinition reads

$$\begin{aligned} m_t \bar{t}''_L t''_R + m_t \bar{t}''_R t''_L &\to m_t \bar{t}''_L (1 + \frac{\tilde{c}\rho}{f}) t''_R + m_t \bar{t}''_R (1 + \frac{\tilde{c}^\dagger \rho}{f}) t''_L \\ &= m_t \bar{t}''_L t''_R + m_t \bar{t}''_L \frac{\tilde{c}\rho}{f} t''_R + m_t \bar{t}''_R t''_L + m_t \bar{t}''_R \frac{\tilde{c}^\dagger \rho}{f} t''_L \,, \end{aligned} \tag{A.15}$$

where the second and fourth terms are the contribution to the Higgs plus jet process. If we again set $\tilde{c} = -\tilde{c}^\dagger$, these two terms give

$$m_t \bar{t}''_L \frac{\tilde{c}\rho}{f} t''_R - m_t \bar{t}''_R \frac{\tilde{c}\rho}{f} t''_L \,. \tag{A.16}$$

If we consider the Gamma matrices structure of these terms then from $m_t \bar{t}''_L \frac{\tilde{c}\rho}{f} t''_R$, we obtain

$$m_t \bar{t}''_L \frac{\tilde{c}\rho}{f} t''_R = m_t \frac{\tilde{c}\rho}{f} t''^{\dagger} \frac{1-\gamma^5}{2} \gamma^0 \frac{1+\gamma^5}{2} t'' = m_t \frac{\tilde{c}\rho}{f} t''^{\dagger} \gamma^0 \frac{1+\gamma^5}{2} t'' \,, \tag{A.17}$$

where above we used the definition of the left and right handed fields Eq. (3.51) and the relations for the gamma matrices in Eq. (3.52). For $m_t \bar{t}''_R \frac{\tilde{c}\rho}{f} t''_L$, we similarly obtain

$$m_t \bar{t}''_R \frac{\tilde{c}\rho}{f} t''_L = m_t \frac{\tilde{c}\rho}{f} t''^{\dagger} \frac{1+\gamma^5}{2} \gamma^0 \frac{1-\gamma^5}{2} t'' = m_t \frac{\tilde{c}\rho}{f} t''^{\dagger} \gamma^0 \frac{1-\gamma^5}{2} t'' \,. \tag{A.18}$$

The resulting contribution then becomes

$$m_t \bar{t}''_L \frac{\tilde{c}\rho}{f} t''_R - m_t \bar{t}''_R \frac{\tilde{c}\rho}{f} t''_L = m_t \frac{\tilde{c}\rho}{f} t''^{\dagger} \gamma^0 \gamma^5 t'' \tag{A.19}$$

and we arrive with the CP-odd coupling for the top quark that we want. We could apply Eq. (A.12) to the mass term of the top partner eigenstate, and carry on with the steps described above to extract the CP-odd couplings for the top partner. In the case of the top partner, the coupling should have the opposite sign to the CP-odd coupling derived from the top quark. This whole procedure works for the $\mathbf{M4_{14}}$ model and in the situation where we have an infinite number of top partner multiplets in the models.

Appendix B

Computational Tools

We now discuss about the computational tools we used in our work. One is the Herwigjet program that we used to calculate the transverse momentum distribution of the radiated jet and the integrated transverse momentum distribution $\sigma\left(p_T > p_T^{\text{cut}}\right)$ defined in Eq. (4.22) [23]. The other is the PERL script we used to compute the ratio of efficiencies of the models studied in our work and the SM, i.e. $\frac{\epsilon_{\text{BSM}}(p_T > p_T^{\text{cut}})}{\epsilon_{\text{SM}}(p_T > p_T^{\text{cut}})}$. This PERL script is used in our work in the case with one top partner only. The last one is Mathematica codes that we used to make plots for the diviation of this distributions.

B.1 Herwigjet

Herwig is a Monte Carlo event generator written in the Fortran77 computing language. It can be used to generate event samples of physics processes with their respective properties, such as distributions of physical observables. In ref. [23], Herwig was interfaced with a numerical integrator in order to produce the transverse momentum in Higgs plus one jet events. The interface involves the packages HOPPET [46] and LHAPDFF [41,44,45] that perform the convolution of tree-level matrix element squared provided by Herwig with parton distribution functions. The program is modular, so in our case we were able to include the effect of top partner multiplets without touching its core structure. In particular, our high-level interface is such that for the cases where we have one top partner multiplet in each of the models, the p_T distribution of the radiated jet and the integrated distribution defined in Eq. (4.22) are computed from the programme by simply inputting the values of the scale f, the physical masses of the top and of the top partner, the mixing angle of the right-handed fields $\sin^2\theta_R$ and

an integer corresponding to one of the models described in chapter 3.

We have seen that, in the case of multiple top partners, simple analytical expressions are not practical. Therefore, we also modified the code so that arbitrary numbers of top-partners masses and couplings can be read from a file, and directly taken into account by the program to compute transverse momentum distributions.

In Herwig, there are only two main files that allow users to implement the programme for their purposes: the main program `h1jet.f90`, and the helper FORTRAN modules `mass_parameters.f90`. The `mass_parameters.f90` file provide subroutines used for calculating masses and Yukawa couplings of the particles involving in physical processes. These subroutines are used by the file `mass_helper.f90` and `hwhig_helper.f` to compute the Higgs (or jet) transverse momentum distribution. The file `mass_helper.f90` contains the matrix element squared and subroutines for numerical integration. Some of these functions call subroutines from `mass_parameters.f90` to have access to the couplings and masses of the particles involved. The `hwhig_helper.f` file contains the amplitude for Higgs plus one jet with an arbitrary number of fermions running in loops. It also contains functions necessary for the subroutine constructed in this file, such as function to calculate one loop scalar integrals. Some of the subroutines from `hwhig_helper.f` are called by functions in `mass_helper.f90`. The `h1jet.f90` file is dedicated to computing the kinematics distributions, and input/output procedure. This file also allows user to input specific parameters for the computation such as setting renormalisation and factorisation scales, as well as parton distribution functions. Users will be able to execute the program herwig via the executable file `h1jet`.

We will now discuss the modification we made to the file `mass_parameters.f90`. For the case where there is one top partner in each of the models studied in our work, we set up the program, so that it implements analytical formulae for each model, as well as the limit where the model should correspond to the SM. In order to achieve this, we add the following statements

```
sthRsq = sthsq
cthRsq = one-sthRsq
tanthLsq = (mtp/mt)**2*sthRsq/cthRsq
cthLsq = one/(one+tanthLsq)
sthLsq = one-cthLsq
if (invfscale == zero) then
     select case(model)
```

```
      case(M1_5, M1_14)
         yt = yt*cthLsq
         ytp = ytp*sthLsq
      case(M4_5,M4_14)
         yt = yt*cthRsq
         ytp = ytp*sthRsq
      case default
         call wae_error('set_mass_parameters','unrecognised model: ',&
              &intval=model)
      end select
   else
      seps = vev*invfscale
      ceps = sqrt(one-seps**2)
      select case(model)
      case(M1_5)
         yt = yt*cthLsq*ceps
         ytp = ytp*sthLsq*ceps
      case(M1_14)
         yt = yt*cthLsq*(two*ceps**2-one)/ceps
         ytp = ytp*sthLsq*(two*ceps**2-one)/ceps
      case(M4_5)
         yt=yt*ceps*(cthRsq-seps**2/(one+ceps**2)*(cthLsq-cthRsq))
         ytp=ytp*ceps*(sthRsq-seps**2/(one+ceps**2)*(sthLsq-sthRsq))
      case(M4_14)
         yt=yt*(cthRsq*(two*ceps**2-one)/ceps-&
              &seps**2*ceps/(four*ceps**4-three*ceps**2+one)*&
              &(8._dp*ceps**2-three)*(cthLsq-cthRsq))
         ytp=ytp*(sthRsq*(two*ceps**2-one)/ceps-&
              &seps**2*ceps/(four*ceps**4-three*ceps**2+one)*&
              &(8._dp*ceps**2-three)*(sthLsq-sthRsq))
      case default
         call wae_error('set_mass_parameters','unrecognised model: ',&
              &intval=model)
      end select
```

```
  end if
```

In the statement above, `invfscale` is used to represent the value of f^{-1}. If this parameter takes the value of zero, the analytical limit $f \to \infty$ is implemented, as can be seen from the arguments in the first `if` statement above, i.e. `if (invfscale == zero)`. If `invfscale` is not set to zero, then the Yukawa couplings of the fermions are taken to be those listed in Eq. (3.68). `model` is used to determined which of the models herwig-jet must perform the computation with, which is done via `select case(model)`. The variables `yt` and `ytp` are used to denote the Yukawa couplings for the top quark and top partner in the theory respectively. In the computation of the Yukawa couplings, `seps` is used for the value of s_ϵ defined in Eq. (2.68) as can be seen from

```
seps = vev*invfscale
ceps = sqrt(one-seps**2)
```

where `vev` take the value of the EW scale v, and c_ϵ is defined in the second line of this part of the code. The variables `sthLsq`, `cthLsq`, `sthRsq` and `cthRsq` are introduced for storing the value of the $\sin^2\theta_L$, $\cos^2\theta_L$, $\sin^2\theta_R$ and $\cos^2\theta_R$ used in the bi-unitary transformation respectively. The relationship defined in Eq. (3.20) between between θ_L and θ_R is included in the code via

```
tanthLsq = (mtp/mt)**2*sthRsq/cthRsq
```

and this relation is linked to the definition of the $\cos^2\theta_L$ via

```
cthLsq = one/(one+tanthLsq)
```

For the case where there is more than one top partner multiplet in the theory, the program is modified in such a way that it could create arrays of masses and Yukawa couplings to perform the calculation out of some input files that user feeds to it. For this task, we created the following basic subroutine

```
subroutine read_top_partners(indev,nqmax)
  integer, intent(in) :: indev, nqmax
  !---------------------------
  integer :: i



  allocate(mass_array(nqmax),yukawa(nqmax))
```

```
  do i=1,nqmax
     read(indev, *) mass_array(i), yukawa(i)
  end do

  close(indev)

end subroutine read_top_partners
```

This subroutine is then called via a simple `if` statement as follows

```
  if (log_val_opt('-in')) then
     indev = idev_open_opt('-in',status="old")

     read(indev,*,iostat=ios) nqmax_eq, nqmax

     ! maximum number of quarks, including bottom and top
     nqmax = min(int_val_opt('-nqmax', nqmax),nqmax)

     call read_top_partners(indev, nqmax)
  else if (mb == zero) then
     allocate(mass_array(1),yukawa(1))
     mass_array = (/mt/)
     yukawa = (/yt/)
  else if (mtp == zero) then
     allocate(mass_array(2),yukawa(2))
     mass_array = (/mt,mb/)
     yukawa = (/yt,yb/)
  else
     allocate(mass_array(3),yukawa(3))
     mass_array = (/mt,mb,mtp/)

     ! The inverse of fscale
     if (log_val_opt('-fscale')) then
        invfscale = one/dble_val_opt('-fscale',zero)
     else
```

```
        invfscale = zero
     end if
     model = int_val_opt('-model',1)

     call set_top_yukawa(model,mt, mtp, invfscale, yt,ytp)
     yukawa = (/yt,yb,ytp/)
  end if
```

In this subroutine, the main `if` statement allows a user to open an input file containing numbers, masses, and Yukawa couplings of quarks via `-in` command-line option. It then calls the subroutine `read_top_partners` to create arrays of mass and top Yukawa couplings that herwigjet will use in the calculation for the case with more than one top partner multiplet. If we want to perform the calculation in the case where there is one top partner in the model, instead of feeding an input file to the programme, we can provide the value of f, $\sin^2\theta_R$, mass of the top partner and the model name. We can input to the programme, f scale via `-fscale` which the programme will automatically convert to `invfscale` as can be seen from

```
if (log_val_opt('-fscale')) then
        invfscale = one/dble_val_opt('-fscale',zero)
     else
        invfscale = zero
```

From this part of the code, if `-fscale` is not provided, `invfscale` will be set to zero, i.e. the limit $f \to \infty$ will be computed. The value $\sin^2\theta_R$ can be input by the user via the command-line option `-sthsq`. The part

```
call set_top_yukawa(model,mt, mtp, invfscale, yt,ytp)
```

is used to call subroutine `set_top_yukawa` which will contain the if statement for determining the form of the Yukawa couplings and the limit of the calculation for one top partner case we describe above. This subroutine `set_top_yukawa` would also contain the code to calculate the value of $\sin^2\theta_L$ and the relevant trigonometric functions described using Eq. (3.20). Notice that if a user does not specify the model to calculate and the value of `-fscale` is not set, herwigjet will perform the computation for the SM.

The HERWIG code modified for our work can be exploited as described below. If the code is obtained and properly set up on a machine, the user need to compile it by executing

```
$ make
```

At the directory where HERWIG is installed, the program can be simply run by

```
$ ./h1jet
```

By executing this command the program will compute the transverse momentum distribution $d\sigma/dp_T$ and the cross section $\sigma\left(p_T > p_T^{\rm cut}\right)$ of the $pp \to h + j$ process, in a given bin of the transverse momentum of a jet or Higgs p_T for the SM. Each of the bins is specified by the minimum, medium value and maximum p_T. The default units of $d\sigma/dp_T$ and $\epsilon(p_T > p_T^{\rm cut})$ are nb/GeV and nb respectively. In the version of HERWIG used in our work, this command is the most simple one, and there exist several options to specify how the program generates the simulations. The simplest option to the modify the command above is the choice of the maximum transverse momentum which can be achieved, for example, with the command

```
$ ./h1jet -ptmax 4000
```

where `-ptmax` is the syntax used to denote the maximum value of the transverse momentum, which is 4000 GeV in the example above. The c.m. energy used in the simulation can be controlled by adding the syntax `-roots`, e.g.

```
$ ./h1jet -roots 14000
```

would result in the SM simulation with 14000 GeV. If this option is not specified, the default value of the c.m. energy is 8000 GeV in our code. The output file can be generated with the option `-out`. For example, if the user wants to produce an output file named `LHC14-SM.res` for the SM computation with c.m. energy of 14 TeV, this could be done with the command

```
$ ./h1jet -roots 14000 -out LHC14-SM.res
```

For the models discussed in our work, the user may be able to generate result files for these models in two ways as outlined above. The first option is to input the values of the physical parameters used in the models directly to the Herwigjet. The user can generate the result files in this way only if they are restricted themself to models

with one top partner. As mentioned above, the parameters that can be input are the mixing angle $\sin^2\theta_R$, the compositeness scale f and mass of the top partner m_T. Before specifying these parameters, the user must indicate which of the composite Higgs models the program will compute the result files for, via the number assigned for each of the models considered in our work. The model selection can be done via the option `-model`, and the numbers used to identify the models are `1,2,3` and `4` corresponding to models $\mathbf{M1_5}$, $\mathbf{M1_{14}}$, $\mathbf{M4_5}$ and $\mathbf{M4_{14}}$ respectively. If the user does not specify the model, then the default one is the SM. The mixing angle can be specified via the option `-sthsq`. The scale f can be input into the computation via the option `-fscale`. The value of m_T can be specified in the computation via `-mtp` option. As an example of how to use the options described above, the command to simulate $pp \to h + j$ in $\mathbf{M4_5}$ with $\sin^2\theta_R = 0.1$, $f = 600\,\text{GeV}$, $m_T = 1250\,\text{GeV}$ at LHC with 14 TeV c.m. energy is

```
$ ./h1jet -roots 14000 -sthsq 0.1 -fscale 600 -mtp 1250 -model 3
-out LHC14-sth2_0.1-f_600-mtp1_1250.res
```

where `LHC14-sth2_0.1-f_600-mtp1_250.res` is the input file in this example. During the writing of this thesis, CP-odd contributions have been also implemented, according to the calculation in ref. [52]. The user then has also the option of taking into account only the CP-odd Yukawa couplings given in Eq. (3.69) for generating the result files, by adding the option `-cpodd`. Since the analytical forms of the CP-odd Yukawa couplings in Eq. (3.69) also depend on the value of $\text{Im}\,(c_1)$, the value of the imaginary part of the c_1 parameter must also be provided via `-imc1` after adding the option `-cpodd`. For illustrative proposes, if the user wants to repeat the computation in the previous example, with only the CP-odd Yukawa couplings taking into account, this can be done with the command

```
$ ./h1jet -roots 14000 -sthsq 0.1 -fscale 600 -mtp 1250 -model 3
-out LHC14-sth2_0.1-f_600-mtp1_1250_cpodd.res -cpodd -imc1 0.2
```

where now `LHC14-sth2_0.1-f_600-mtp1_1250_cpodd.res` is the name of the output file.

The second method for running the code is via an input file, a `.txt` file containing the mass and Yukawa couplings of the particles that would be considered in the computation. The advantage of running the code with this option is that the user can now perform the simulation in either cases with a single top partner multiplet or cases of more than one top partner multiplet. For an example of the input file that can be used

to run the program with this option, suppose the user wants to run the simulation for two top partners in any of the models discussed in chapter 3, the input file would be similar to the following:

```
nqmax: 4
4.65 0.951459791218233 0
173.74257800960504 0.9639943661520481 -0.015766977146788846
1246.0955797523338 -0.00009836393686296971 0.00027684138704548936
1679.545946828568 -0.012347921454152677 0.015490135759743444
```

Above, the first line is the total number of the particles that the program will take into account in the simulation. The information in the second line and the rest of the file will be the masses of the particles in the first column following by the CP-even Yukawa couplings and the CP-odd Yukawa couplings in the second and third columns respectively. Each column is separated from the other one by the blank space. The input file can be provided to the program via the option `-in`. If `-in` is used alone, the computation would be carried out with the CP-even coupling, i.e. the second column of the input file. The command that can be used to run the code will be, for instance,

```
./h1jet -roots 14000 -in M452tp_y1_M1200_f800.txt -out
pth-LHC14-HT_M452tp_y1_M1200_f800.res
```

where above `M452tp_y1_M1200_f800.txt` is an input file, and the name of the output file is `pth-LHC14-HT_M452tp_y1_M1200_f800.res`. Note that in the example above, the computation was performed with the CP-even Yukawa couplings and the c.m. energy is also specified. In fact, the user can perform the simulation with the CP-odd couplings, the third column of the input file, by adding the option `-cpodd`. Here is an example: If one wanted to perform the computation with CP-odd Yukawa coupling instead, the command will be

```
./h1jet -roots 14000 -in M452tp_y1_M1200_f800.txt -out
pth-LHC14-HT_M452tp_y1_M1200_f800_cpodd.res -cpodd
```

where `pth-LHC14-HT_M452tp_y1_M1200_f800_cpodd.res` is the name of the output file.

B.2 PERL

We used a PERL script to calculate the $\frac{\epsilon_{\rm BSM}(p_T>p_T^{\rm cut})}{\epsilon_{\rm SM}(p_T>p_T^{\rm cut})}$ for the case where there is one top partner in each of the four models studied in our work. Before using this script, data files must be produced for varying values of the scale f, the top partner M_T, $\sin^2\theta_R$ ($\sin^2\theta_L$) for the fourplet (singlet) models, along with the SM data file from herwigjet. The script starts with the variable corresponding to $p_T^{\rm cut}$, which we defined here as `$ptmin`. Then, we open the SM file, and store the value of $\sigma\left(p_T > p_T^{\rm cut}\right)$ defined in Eq. (4.22) for the corresponding value of $p_T^{\rm cut}$ with

```
$smfile = 'pth-LHC14-HT-SM.res';
open (IN,"<$smfile");
while ($line = <IN>) {
    if ($line =~ /^\s+$ptmin/) {
@sm = split(' ',$line);
    }
}
close(IN);
```

Here, we first search for the line in data file where the value of $\sigma\left(p_T > p_T^{\rm cut}\right)$ corresponding to $p_T^{\rm cut}$ is located. We then split that line with space, and store the data in the array `@sm`. We then used a similar code to search for the total cross section of the production σ

```
open (IN,"<$smfile");
while ($line = <IN>) {
      if ($line=~ /sigma0/){
            @smn= split(' ',$line);
     }
}
close(IN);
```

We can then use this style of code to store the values of σ and $\sigma\left(p_T > p_T^{\rm cut}\right)$ for the four composite Higgs model. Then, from the variable `@sm`, `@smn`, `@bsm` and `@bsmn`, we compute the ratio $\frac{\epsilon_{\rm BSM}(p_T>p_T^{\rm cut})}{\epsilon_{\rm SM}(p_T>p_T^{\rm cut})}$ for a data file. We can then define arrays to store this value for a specific set of parameters: f, M_T, $\sin^2\theta_{L,R}$ and the name of the models, which we can then loop over any pair of these arrays to generate the "table" of the

ratio for each of the specific values of the other two parameters. In our work, we loop over the compositeness scale f and M_T for each of the $\sin^2\theta_{L,R}$ and models.

B.3 Mathematica

We used a Mathematica code to make plots that illustrate the different in Higgs plus jet production between the SM and our models.

Contour plots for $\delta(p_T^{\rm cut})$

One way to present $\delta(p_T^{\rm cut})$ defined in Eq. (4.24) is to make a contour plots of this variable for each of the models for a value of $\sin^2\theta_R$ with a value of $p_T^{\rm cut}$. The Mathematica code that we used to plot the deviation $\delta(p_T^{\rm cut})$ works as follow. Suppose the ratio $\frac{\epsilon_{\rm BSM}(p_T>p_T^{\rm cut})}{\epsilon_{\rm SM}(p_T>p_T^{\rm cut})}$ is calculated for each of the models over ranges of f scale and top partner mass M_T, and this set of data is tabulated in a file for specific values of $\sin^2\theta_R$ and $p_T^{\rm cut}$. We can then import this file with the command

```
delta = Import["C:\\file.res", "Table"];
```

Here, the `delta` is used to store the table of the ratio of efficiency values. We then create a set of coordinates for the contour plot of the data in this table. In our work, we will define the coordinates as f in the range 600 GeV $< f <$ 1200 GeV and M_T in 1200 GeV $< M_T <$ 2200 GeV. This coordinate can be created by

```
coordinates =
 CoordinateBoundsArray[{{600, 1200}, {1200, 2200}}, {50, 50}];
```

weher `coordinates` is used to store the coordinates. In the code above, we created both coordinates with 50 increments. Then, we create the contour of $\delta(p_T^{\rm cut})$ by

```
dat = Table[0, {j, 13}, {k, 21}];
For[i = 1, i <= 13, i++,
     For[j = 1, j <= 21, j++,
  dat[[i, j]] = Flatten[{coordinates[[i, j]], (delta[[i, j]] - 1) 100}]
  ]
 ]
```

Then, we flatten the result with

```
datt = Flatten[dat, 1]
```

so that it could be included in the argument of `ListContourPlot`. We then make the contour plot using `ListContourPlot` directly out of `datt`.

Patches of Mathematica code have also been used to compute the masses and Yukawa couplings in the case with two top partners.

Bibliography

[1] S. L. Glashow, Nucl. Phys. **10** (1959) 107. doi:10.1016/0029-5582(59)90196-8

[2] S. Weinberg, Phys. Rev. Lett. **19** (1967) 1264. doi:10.1103/PhysRevLett.19.1264

[3] A. Salam, Conf. Proc. C **680519** (1968) 367.

[4] P. W. Higgs, Phys. Rev. Lett. **13** (1964) 508. doi:10.1103/PhysRevLett.13.508

[5] Y. Nambu, Phys. Rev. **117** (1960) 648. doi:10.1103/PhysRev.117.648

[6] J. Goldstone, Nuovo Cim. **19** (1961) 154. doi:10.1007/BF02812722

[7] J. Goldstone, A. Salam and S. Weinberg, Phys. Rev. **127** (1962) 965. doi:10.1103/PhysRev.127.965

[8] S. Weinberg, Phys. Rev. Lett. **27** (1971) 1688. doi:10.1103/PhysRevLett.27.1688

[9] S. Weinberg, Phys. Rev. D **7** (1973) 1068. doi:10.1103/PhysRevD.7.1068

[10] G. Aad *et al.* [ATLAS Collaboration], Phys. Lett. B **716** (2012) 1 doi:10.1016/j.physletb.2012.08.020 [arXiv:1207.7214 [hep-ex]].

[11] S. Chatrchyan *et al.* [CMS Collaboration], Phys. Lett. B **716** (2012) 30 doi:10.1016/j.physletb.2012.08.021 [arXiv:1207.7235 [hep-ex]].

[12] L. Susskind, Phys. Rev. D **20** (1979) 2619. doi:10.1103/PhysRevD.20.2619

[13] J. L. Gervais and B. Sakita, Nucl. Phys. B **34** (1971) 632. doi:10.1016/0550-3213(71)90351-8

[14] Y. A. Golfand and E. P. Likhtman, JETP Lett. **13** (1971) 323 [Pisma Zh. Eksp. Teor. Fiz. **13** (1971) 452].

[15] J. Wess and B. Zumino, Phys. Lett. **49B** (1974) 52. doi:10.1016/0370-2693(74)90578-4

[16] M. J. Dugan, H. Georgi and D. B. Kaplan, Nucl. Phys. B **254** (1985) 299. doi:10.1016/0550-3213(85)90221-4

[17] R. Contino, doi:10.1142/9789814327183_0005 arXiv:1005.4269 [hep-ph].

[18] R. Contino, Y. Nomura and A. Pomarol, Nucl. Phys. B **671** (2003) 148 doi:10.1016/j.nuclphysb.2003.08.027 [hep-ph/0306259]. K. Agashe, R. Contino and A. Pomarol, Nucl. Phys. B **719** (2005) 165 doi:10.1016/j.nuclphysb.2005.04.035 [hep-ph/0412089]. R. Contino, L. Da Rold and A. Pomarol, Phys. Rev. D **75** (2007) 055014 doi:10.1103/PhysRevD.75.055014 [hep-ph/0612048]. A. Pomarol and F. Riva, JHEP **1208** (2012) 135 doi:10.1007/JHEP08(2012)135 [arXiv:1205.6434 [hep-ph]].

[19] H. Georgi and A. Pais, Phys. Rev. D **10** (1974) 539. doi:10.1103/PhysRevD.10.539

[20] J. Kearney, A. Pierce and J. Thaler, JHEP **1310** (2013) 230 doi:10.1007/JHEP10(2013)230 [arXiv:1306.4314 [hep-ph]].

[21] J. Kearney, A. Pierce and J. Thaler, JHEP **1308** (2013) 130 doi:10.1007/JHEP08(2013)130 [arXiv:1304.4233 [hep-ph]].

[22] A. Azatov and J. Galloway, Phys. Rev. D **85** (2012) 055013 doi:10.1103/PhysRevD.85.055013 [arXiv:1110.5646 [hep-ph]].

[23] A. Banfi, A. Martin and V. Sanz, JHEP **1408** (2014) 053 doi:10.1007/JHEP08(2014)053 [arXiv:1308.4771 [hep-ph]].

[24] A. De Simone, O. Matsedonskyi, R. Rattazzi and A. Wulzer, JHEP **1304** (2013) 004 doi:10.1007/JHEP04(2013)004 [arXiv:1211.5663 [hep-ph]].

[25] G. Panico, M. Riembau and T. Vantalon, JHEP **1806** (2018) 056 doi:10.1007/JHEP06(2018)056 [arXiv:1712.06337 [hep-ph]].

[26] G. Panico and A. Wulzer, Lect. Notes Phys. **913** (2016) pp.1 doi:10.1007/978-3-319-22617-0 [arXiv:1506.01961 [hep-ph]].

[27] D. B. Kaplan and H. Georgi, Phys. Lett. **136B** (1984) 183. doi:10.1016/0370-2693(84)91177-8

[28] D. B. Kaplan, H. Georgi and S. Dimopoulos, Phys. Lett. **136B** (1984) 187. doi:10.1016/0370-2693(84)91178-X

[29] T. Plehn, Lect. Notes Phys. **844** (2012) 1 doi:10.1007/978-3-642-24040-9 [arXiv:0910.4182 [hep-ph]].

[30] P. W. Higgs, Phys. Lett. **12** (1964) 132. doi:10.1016/0031-9163(64)91136-9

[31] S. R. Coleman, J. Wess and B. Zumino, Phys. Rev. **177** (1969) 2239. doi:10.1103/PhysRev.177.2239

[32] C. G. Callan, Jr., S. R. Coleman, J. Wess and B. Zumino, Phys. Rev. **177** (1969) 2247. doi:10.1103/PhysRev.177.2247

[33] D. Marzocca, M. Serone and J. Shu, JHEP **1208** (2012) 013 doi:10.1007/JHEP08(2012)013 [arXiv:1205.0770 [hep-ph]].

[34] D. B. Kaplan, Nucl. Phys. B **365** (1991) 259. doi:10.1016/S0550-3213(05)80021-5

[35] G. F. Giudice, C. Grojean, A. Pomarol and R. Rattazzi, JHEP **0706** (2007) 045 doi:10.1088/1126-6708/2007/06/045 [hep-ph/0703164].

[36] C. Grojean, E. Salvioni, M. Schlaffer and A. Weiler, JHEP **1405** (2014) 022 doi:10.1007/JHEP05(2014)022 [arXiv:1312.3317 [hep-ph]].

[37] M. Schlaffer, M. Spannowsky, M. Takeuchi, A. Weiler and C. Wymant, Eur. Phys. J. C **74** (2014) no.10, 3120 doi:10.1140/epjc/s10052-014-3120-z [arXiv:1405.4295 [hep-ph]].

[38] M. E. Peskin and D. V. Schroeder, *An introduction to Quantum Field Theory*, Reading, USA: Addison-Wesley (1995) ISBN: 9780201503975, 0201503972

[39] M. Aaboud *et al.* [ATLAS Collaboration], Phys. Lett. B **784** (2018) 173 doi:10.1016/j.physletb.2018.07.035 [arXiv:1806.00425 [hep-ex]].

[40] I. Low and A. Vichi, Phys. Rev. D **84** (2011) 045019 doi:10.1103/PhysRevD.84.045019 [arXiv:1010.2753 [hep-ph]].

[41] A. D. Martin, W. J. Stirling, R. S. Thorne and G. Watt, Eur. Phys. J. C **63** (2009) 189 doi:10.1140/epjc/s10052-009-1072-5 [arXiv:0901.0002 [hep-ph]].

[42] U. Baur and E. W. N. Glover, Nucl. Phys. B **339** (1990) 38. doi:10.1016/0550-3213(90)90532-I

[43] G. Corcella, I. G. Knowles, G. Marchesini, S. Moretti, K. Odagiri, P. Richardson, M. H. Seymour and B. R. Webber, hep-ph/0210213.

[44] D. Bourilkov, R. C. Group and M. R. Whalley, hep-ph/0605240.

[45] A. Buckley, J. Ferrando, S. Lloyd, K. Nordstrm, B. Page, M. Rfenacht, M. Schnherr and G. Watt, Eur. Phys. J. C **75** (2015) 132 doi:10.1140/epjc/s10052-015-3318-8 [arXiv:1412.7420 [hep-ph]].

[46] G. P. Salam and J. Rojo, Comput. Phys. Commun. **180** (2009) 120 doi:10.1016/j.cpc.2008.08.010 [arXiv:0804.3755 [hep-ph]].

[47] R. V. Harlander, S. Liebler and H. Mantler, Comput. Phys. Commun. **184** (2013) 1605 doi:10.1016/j.cpc.2013.02.006 [arXiv:1212.3249 [hep-ph]].

[48] The ATLAS collaboration [ATLAS Collaboration], ATLAS-CONF-2018-018.

[49] The ATLAS collaboration [ATLAS Collaboration], ATLAS-CONF-2018-028.

[50] O. Matsedonskyi, G. Panico and A. Wulzer, JHEP **1412** (2014) 097 doi:10.1007/JHEP12(2014)097 [arXiv:1409.0100 [hep-ph]].

[51] M. Tanabashi *et al.* [Particle Data Group], Phys. Rev. D **98** (2018) no.3, 030001. doi:10.1103/PhysRevD.98.030001

[52] A. Banfi, B. M. Dillon, W. Ketaiam and S. Kvedaraitė, arXiv:1905.12747 [hep-ph].

[53] M. Aaboud *et al.* [ATLAS Collaboration], JHEP **1710** (2017) 141 doi:10.1007/JHEP10(2017)141 [arXiv:1707.03347 [hep-ex]]; M. Aaboud *et al.* [ATLAS Collaboration], JHEP **1708** (2017) 052 doi:10.1007/JHEP08(2017)052 [arXiv:1705.10751 [hep-ex]].

[54] S. Chatrchyan *et al.* [CMS Collaboration], Phys. Lett. B **729** (2014) 149 doi:10.1016/j.physletb.2014.01.006 [arXiv:1311.7667 [hep-ex]]; G. Aad *et al.* [ATLAS Collaboration], JHEP **1508** (2015) 105 doi:10.1007/JHEP08(2015)105 [arXiv:1505.04306 [hep-ex]].

[55] S. P. Jones, M. Kerner and G. Luisoni, Phys. Rev. Lett. **120** (2018) no.16, 162001 doi:10.1103/PhysRevLett.120.162001 [arXiv:1802.00349 [hep-ph]].